A STUDY OF THE APPLICATION OF REDUCTION GAS ANALYSIS IN DETERMINING THE RELATIONSHIP BETWEEN CARBOXYHAEMOGLOBIN AND TISSUE CO LEVELS IN BRAIN, HEART, AND SKELETAL MUSCLE AFTER EXTREME EXPOSURE TO CO POISONING IN RATS

BY

FRANS JOHANNES CRONJÉ, MBCHB(Pretoria), BSc(Hons) Aerospace Medicine

Promotor:

Chris le Roux, MBChB, MSc; Univ. Pretoria, Faculty of Health Sciences; School of Medicine –Aerospace Medicine

Co-Promotors:

Claude A. Piantadosi, MD; Duke University Center for Hyperbaric Medicine and Environmental Physiology; Duke University Medical Center; Durham; North Carolina: USA,

and

Hendrik J. Vreman, PhD; Senior Research Scientist; Neonatal & Developmental Medicine; Department of Pediatrics; Stanford University Medical Center; Stanford, California; USA

Study Site:

Laboratory / Experimental component: Duke University Medical Center; Center for Hyperbaric Medicine & Environmental Physiology; Durham; North Carolina; 27710

Administrative / Biostatistical component: Univ. Pretoria, Faculty of Health Sciences; School of Medicine – Department of Aerospace Medicine

SUBMITTED IN FULFILLMENT OF THE REQUIREMENTS FOR THE DEGREE OF MAGISTER SCIENTIAE IN AEROSPACE MEDICINE IN THE FACULTY OF HEALTH SCIENCES, UNIVERSITY OF PRETORIA.

ACKNOWLEDGEMENTS

As a novice researcher, this was a rather daunting project. It required mastering a number of unfamiliar laboratory techniques and embracing biochemistry and molecular biology at a differentiated level all within a relatively short period of time. Nevertheless, it was most gratifying to unveil a small part of the complex biochemical liaisons of CO within the body at this level of resolution. The subject has enormous research potential and profound clinical relevance.

This journey would not have been possible without the assistance of several tutors, mentors and assistants. Grateful thanks are hereby extended to:

- Chris Le Roux, MBChB, MSc of the University of Pretoria, Faculty of Health Sciences, School of Medicine - Aerospace Medicine, for supporting the project on behalf of the University of Pretoria;

- Claude Piantadosi, MD of Duke University: This study would not have been realized had it not been for his inspiration and mentorship;

- Hendrik J. Vreman, PhD of Department of Pediatrics at Stanford University, the pioneer in the application of the RGA technique to biology and biochemistry, for sharing the intricacies of accurately measuring CO using this technology and quantitating [CO] in tissues; for his mentorship and for the meticulous revision of the manuscript;

- Piet Becker, PhD of the South African Medical Research Council for his dedicated assistance with the biostatistical analyses and helpful means of displaying the data for the purposes of clarity;

- John J. Freiberger, MD, MPH, of Duke University for assistance in preparing the Institute for Animal Care and Use Committee protocol and preliminary biostatistical support; and

- Albert (Sonny) Boso, BS; Owen Doar, BS; and Craig Marshall, BS; for their tireless, technical assistance.

It has been, and remains, an enormous privilege to be associated with your respective laboratories and your generous assistance and mentorship is greatly appreciated.

INDEX

LIST OF TABLES

LIST OF GRAPHIC ILLUSTRATIONS

LIST OF EQUATIONS & CALCULATIONS

A STUDY OF THE APPLICATION OF REDUCTION GAS ANALYSIS IN DETERMINING THE RELATIONSHIP BETWEEN CARBOXYHAEMOGLOBIN AND TISSUE CO LEVELS IN BRAIN, HEART, AND SKELETAL MUSCLE AFTER EXTREME EXPOSURE TO CO POISONING IN RATS

BY

FRANS JOHANNES CRONJÉ, MBCHB(Pretoria), BSc(Hons) Aerospace Medicine

Promotor:

Chris le Roux, MBChB, MSc; Univ. Pretoria, Faculty of Health Sciences; School of Medicine – Department of Aerospace Medicine

Co-Promotors:

Claude A. Piantadosi, MD; Duke University Center for Hyperbaric Medicine and Environmental Physiology; Duke University Medical Center; Durham; North Carolina: USA

Hendrik J. Vreman, PhD; Senior Research Scientist; Neonatal & Developmental Medicine; Department of Pediatrics; Stanford University Medical Center; Stanford, California; USA

SUBMITTED FOR THE DEGREE OF MAGISTER SCIENTIAE IN AEROSPACE MEDICINE

SUMMARY

Little is known of tissue carbon monoxide (CO) changes after acute exposure because tissue levels are in the order of picomoles per milligram and the technology to measure such low concentrations has only become available relatively recently. This study tested three hypotheses: That tissue CO levels (1) vary among tissues after acute poisoning; (2) change over time; but (3) cannot be predicted by measuring carboxyhaemoglobin (COHb) levels.

Twenty four healthy male Sprague-Dawley rats were exposed to 2500 ppm CO in air for 45 min. This non-lethal exposure achieved reproducible COHb values of 66 to 72%. Animals were allowed to recover breathing air and were sacrificed at 30 minute intervals for 150 minutes. An additional nine male animals served as unexposed controls. Accurate measurements of tissue CO levels were made in blood, brain, heart, and skeletal muscle samples. All samples were prepared using the validated technique described by Vreman *et al.*[1], and Reduction Gas Analysis was used to determine the pmol CO per wet weight tissue. Co-oximetry and gas chromatography were performed on all blood samples.

Predictably, blood CO content dropped following exposure, but tissue CO content did not follow the same trend in all tissues.

This study supports the hypothesis of (1) tissue and (2) time-related variability of CO concentration in three body tissues after exposure and (3) documents lack of utility of COHb for predicting tissue CO tissue values.

Keywords: — CO toxicity; free radicals; reduction gas analysis.

'N STUDIE OOR DIE GEBRUIK VAN REDUKSIE GAS ANALISE VIR DIE BEPALING VAN DIE VERHOUDING TUSSEN KARBOKSIEHEMOGLOBIEN EN WEEFSEL KOOLSTOFMONOKSIED VLAKKE IN BREIN, HART, EN SKELETSPIER NA UITERSTE BLOOTSTELLING AAN KOOLSTOFMONOKSIED VERGIFTIGING IN ROTTE

DEUR

FRANS JOHANNES CRONJÉ, MBCHB(Pretoria), BSc(Hons) Lugvaart- en Ruimtegeneeskunde

Promotor:

Chris le Roux, MBChB, MSc; MBChB, MSc; Univ. Pretoria, Fakulteit vir Gesondheidswetenskappe, Mediese Skool – Departement van Lugvaart - en Ruimtegeneeskunde

Mede-Promotors:

Claude A. Piantadosi, MD; Duke Universiteit Sentrum vir Hyperbariese Medisyne en Omgewings Fisiology; Duke Universiteit Mediese Sentrum; Durham; North Carolina: VSA

Hendrik J. Vreman, PhD; Senior Navorsings Wetenskaplike; Neonatale & Ontwikkelings Medisyne; Department van Pediatrie; Stanford Universiteit Mediese Sentrum; Stanford, California; VSA

INGEDIEN TER VERKRYGING VAN DIE GRAAD VAN MAGISTER SCIENTIAE IN LUGVAARTGENEESKUNDE

OPSOMMING

Daar is min inligting bekend oor die veranderlikheid van koolstofmonoksied (CO) weefselvlakke na akute blootstelling. Sodanige vlakke is in die orde van pikomol per milligram en tegnieke om dié te kan meet het eers onlangs beskikbaar geword. Hierdie studie het drie hipoteses ondersoek: Dat CO vlakke (1) wissel tussen verskillende weefsels na vergiftiging; (2) dat hulle verander met verloop van tyd; maar (3) dat hulle nie voorspel kan word d.m.v. karboksiehemoglobien (COHb) vlakke nie.

Vier en twintig gesonde manlike Sprague-Dawley rotte is aan 2500 dele per miljoen (dpm) CO in lug blootgestel vir 'n tydperk van 45 min. Die nie-noodlottige blootstelling het tot herhaalbare COHb waardes van tussen 66 en 72% gelei. Die diere is toegelaat om na die blootstelling op CO-vrye lug te herstel. Die diere is as volg opgeoffer: direk na blootstelling en met 30 min intervalle tot en met 150 minute. 'n Verdere nege manlike diere het as kontroles gedien sonder CO blootstelling. Akkurate CO metings is gemaak in bloed, brein-, hart- en skeletspier-weefsel. Alle monsters is voorberei op die bewese tegniek beskryf deur Vreman *et al.*[1], en reduksie gas analise is gebruik om die hoeveelheid pikomol CO in vars weefsel te bepaal. CO-oksimetrie en reduksie gas analise is op alle bloedmonsters uitgevoer.

Bloed CO inhoud het voorspelbaar vinnig gedaal na die blootstelling. Hierdie tendens was egter nie die geval met alle weefselwaardes nie.

Hierdie studie ondersteun die hipotese dat daar (1) weefsel en (2) tyd-verwante veranderlikheid in CO konsentrasie in drie weefsels na vergiftiging is, en (3) dit dokumenteer die onvermoë om weefsel CO konsentrasies te voorspel d.m.v. COHb waardebepalings.

Sleutelwoorde: koolstofmonoksied toksisiteit; vry radikale; reduksie gas analise.

CHAPTER 1. INTRODUCTION & BACKGROUND

1.1 CO – THE COMPOUND & ITS DETECTION

Carbon monoxide (CO) – an ubiquitous asphyxiant gas – is colorless and odorless to the human senses [2]. It can be formed whenever carbonaceous fuel is burned in a large range of industrial and domestic circumstances [3]. Significant quantities are generated when burning occurs where the amount of available oxygen is limited relative to the amount of fuel.

Important global sources of CO include automobile exhaust fumes (76.6%), industrial processes (6.9%), fuel combustion (5.5%) and miscellaneous sources – including biomass burning (10.9%) [4,5].

Acute human toxicity is primarily due to accidental, occupational or intentional exposure to automobile exhaust fumes, domestic gas burning installations, coal stoves and fires [6]. However, there are also concerns about the effects of chronic exposure to CO due to environmental, occupational or social means (i.e., smoking) [5,7-12].

Because CO is undetectable to humans, deliberate safety precautions must be strictly observed whenever there is potential for CO accumulation, particularly in unventilated areas. The use of CO detector systems has significantly reduced accidental domestic exposure to CO [13]. This is likely to have ever increasing impact as installation becomes mandated and the monitoring devices become more robust, reliable and less expensive. Current sensor systems for CO detection include colorimetric; metal oxide semiconductor; electrochemical; and non dispersive infrared (NDIR) sensors[13].

Fundamental chemical characteristics of CO, which apply to the equations used in the manuscript and explain part of its biological behavior, are listed in Table 1.

Further detailed chemical characteristics are listed in Appendix D-4 for reference purposes.

Table 1. Properties of CO [14,15]

Formula		CO
Molecular Weight		28.01
Solubility in Water:	0°C	3.3 mL/100 mL H_2O/ATA
	20°C	2.3 mL /100 mL H_2O/ATA
	37°C	1.83 mL /100 mL H_2O/ATA
Ostwald coefficient (0°C)		0.0354

Most households in the colder states of North America are now familiar with CO detection devices and in several states CO sensors are now a statutory requirement[16]. Fortunately manufacturers of domestic appliances are also becoming proactive by introducing better gas burning systems that achieve complete combustion and therefore produce less CO. In accordance with the provisions of the 1990 Clean Air Act, the U.S. Environmental Protection Agency limits the maximum CO concentrations for short duration (1-hour) and average daily (8-hour) exposure to 35 parts per million (ppm) and 9 ppm CO respectively [4,16].

As far as biological systems go, there are an equally large number of ways to measure CO [1,17-23]. Its unique chemical, photometric and spectroscopic characteristics allow for the use of the following methods [24]:

- Radioactive Carbon (^{14}C) isotope

- Spectrophotometry

- Infrared Absorption Spectroscopy

- Gas Chromatography, including:

    - Flame ionization Detection

    - Mass Spectroscopy

    - Reduction Gas Analysis

- 16 -

There are many good references on these techniques. For the purposes of brief overview, they are summarized below:

1.1.1 Radioactive Carbon Isotope [25-27]

Radioactive carbon (^{14}C), having an extremely long half life, can be incorporated into molecules associated with the subsequent production of CO – such as hemeproteins. This may permit the determination of endogenously derived CO over long periods of time (e.g., during erythrocyte turnover).

1.1.2 Spectrophotometry [18,23,28-33]

Hemeproteins display optical characteristics: They absorb and reflect different wavelengths of red and near infrared light depending on their state of reduction and oxidation and their chemical associations with oxygen and CO. This is the basis of CO-oximetry. However, this only offers an indirect measure of CO (i.e., as part of hemoglobin or cytochromes) and was unsuitable for the purposes of this study.

1.1.3 Infrared Absorption Spectroscopy [34-36]

CO can be measured with infrared absorption spectroscopy. A tunable (4.61 µM) laser diode can be employed to measure CO in exhaled breath. While the instrument has great sensitivity (in the parts per billion range), the equipment's size and the need for large sample volumes render it impractical for the intended application.

1.1.4 Gas Chromatography [1]

Chromatography – in a generic sense – implies separation for the purpose of measurement. It is a method of separating and identifying various components of a complex mixture by differential movement through a two-

phase system: Movement is effected by flow of a liquid or gas (mobile phase) which then percolates through an adsorbent (stationary phase) or second liquid phase. Following separation and/or chemical modification, the constituents are detected sequentially and portray characteristics based on their respective interactions with the detector. The way in which compounds "follow" one another through the percolation or separation process and their subsequent interactions with the detector form the basis of their identification and quantification.

In the context of CO detection, there are at least three combinations of separation and detection that may be employed, i.e., gas chromatographic options: (1) Flame Ionization Detection; (2) Mass Spectroscopy ; (3) and Reduction Gas Analysis.

1.1.4.1 *Flame Ionization Detection (FID)* [37-40]

Flame ionization converts CO to CH4 which is subsequently quantified by an FID detector. It requires pre-separation from other hydrocarbons (particularly CH4) and other volatile organic (i.e., carbonaceous) compounds. The system has a sensitivity approaching 20 ppb, but requires an experienced operator for accuracy. This is still the primary method for determining CO in blood below the threshold of sensitivity for CO-oximetry (i.e. <2.5% COHb).

1.1.4.2 *Mass Spectroscopy (MS)* [41-43]

Mass spectroscopy is a useful alternative in CO measurement when it is contained within a complex mixture of volatile organic compounds. By submitting organic vapors to high-energy electron bombardment, as they leave the analytical column, some become ionized and are subsequently accelerated within a magnetic field. Based on their respective mass and electrical charges, these can then be measured as individual compounds by a detector. Based on comparison to known characteristics, compounds can subsequently be identified. The carrier gas needs to be carefully selected so

as not to interfere with the identity of the compound being detected. Nitrogen, for example, has similar characteristics to CO and cannot be used.

1.1.4.3 Reduction Gas Analysis (RGA) [1]

RGA is a type of gas chromatography that uses a heated molecular sieve to separate gases, based on their respective molecular sizes. It then brings the gases in contact with a heated mercuric oxide chemical bed where reducing gases e.g., CO and hydrogen, are oxidized to carbon dioxide and water respectively, in exchange for a proportional reduction in the mercuric oxide to mercury vapor. The latter is measured spectrophotometrically in an optical cell. The sensitivity of the technique associated with the choice of mercuric oxide lies in the property of high ultra-violet absorptivity of mercury vapor. The key to the identity of each gas is its unique retention time in the column, whereas its concentration is determined indirectly through the measurement of the amount of released mercury vapor (see section 4.3. for more details).

1.2 CO TOXICITY

CO poisoning is one of the most common and important forms of accidental poisoning in adults and children in the United States [44]. Internationally, it ranks third amongst adult poisonings, following drugs and alcohol [6]. Fire, faulty central heating systems and the exhaust fumes from internal combustion engines are all significant exogenous sources of CO [45].

Endogenous CO is produced during the physiological breakdown of heme [46,47]. It is also a byproduct of the detoxification of methylene chloride – common in paint removers – and other dihalomethane compounds [48-50].

CO resembles closely the chemical structure of molecular oxygen and it accordingly competes for the same hemeprotein binding sites. Potential targets include hemoglobin, myoglobin, cytochrome p450 and cytochrome oxidase [51-58].

CO combines more than 220 times as readily with hemoglobin (Hb) than oxygen, making COHb a useful assessment to confirm exposure [50,59]. Due to endogenous production, there is a physiological level of 1 to 3% COHb and an exhaled breath [CO] of around 2 parts per million (ppm) in non-smokers[44,60,61]. Smokers may have between 4 and 9% COHb and produce between 6 and 13 ppm exhaled [CO] [60,62,63].

Our limited ability the measure cellular and sub-cellular CO makes it difficult to determine precisely the threshold at which elevated levels of CO levels become biologically harmful. We do know that when air or breathing gas is contaminated by approximately 20 ppm of CO, COHb levels become elevated above normal baseline physiological values [64,65]. Vascular and rheological effects have been described at very low exposures to CO and these are believed to be of clinical importance [66]. On the other side of the spectrum there are also gaps in our understanding of overt CO intoxication. Several mechanisms are known to be involved, including toxic anemia due to COHb formation; histotoxicity via cytochrome oxidase blockade; nitrosative and oxidative injury; lipid peroxidation; vasodilatation, and rhabdomyolysis [44,67-69]. Nevertheless, the full pathophysiological impact of CO toxicity remains a source of ongoing research.

Early mortality due to acute CO poisoning is associated with cardiac injury and dysrhythmias. Delayed mortality is usually related to cerebral edema, rhabdomyolysis and renal failure [45,70-72]. Long-term morbidity in survivors, however, is related to neurological injury. In addition to the acute hypoxic encephalopathy, a syndrome of delayed neurological sequelae (DNS) may arise in 15% of severely poisoned patients [73]. DNS develops within 2-28 days following exposure and runs a variable clinical course [44,69]. Unfortunately the correlation of COHb level, clinical presentation, and prognosis are notoriously poor, suggesting that tissue toxicity – rather than COHb – is the determining factor in prognosis [45,70-72,74,75].

To date CO elimination studies have focused on changes in COHb and exhaled CO quantities. CO elimination appears to be biphasic or even triphasic, suggesting distribution to and from vascular and extravascular compartments [65,76,77]. However, to date no studies have been performed that have actually measured CO elimination from tissues over time.

Total elimination time depends on the duration and level of CO exposure. Although various mathematical models have been proposed, these have found little clinical applicability [76,78]. Elimination half-times vary greatly and may exceed 3 to 6.5 hours while breathing air. This may be reduced to 23 minutes breathing oxygen at three times atmospheric pressure (i.e. hyperbaric oxygen) [79,80]. In spite of this profound difference in elimination, complications of CO poisoning are not proportionally reduced by breathing oxygen or even hyperbaric oxygen [68,73,81,82]. This has prompted the author to determine the dynamics of [CO] within tissues. Even small amounts of cellular CO may be highly significant [83].

COHb elimination, which occurs relatively quickly following exposure, may not mirror changes in tissue CO. Indeed few studies have successfully evaluated elimination of CO from tissue. Sokal et al measured blood, heart, skeletal muscle and brain CO levels in rats after CO intoxication at different exposures. However, they were unable to determine brain CO levels beyond those obtained immediately following the exposure. In addition, they did not specifically remove all blood, i.e., COHb from the samples prior to measurement, thereby introducing an important source of CO contamination [84].

Therefore, for the past 150 years, the prevailing assumption has been that COHb and tissue CO levels are in some form of equilibrium [78,85-87]. If so, COHb values would provide a useful measure of whole body CO toxicity. However, clinicians have known for many years that COHb values are not prognostic for morbidity or mortality in CO poisoning [88-90]. Goldbaum *et al* were able to show in a dog model that neither COHb itself, nor the resulting functional anemia, is the primary cause of CO toxicity and mortality; they suggested that pCO was a

principal factor in CO toxicity and that this led to additional toxic mechanisms unrelated to COHb concentration [91].

Further advances in our understanding of CO toxicity have been delayed by technical limitations related to measuring cellular and tissue CO concentrations. Although several authors have performed simultaneous measurements of blood and tissue CO under physiological or post mortem conditions [92], only two experimental publications have specifically measured blood and tissue CO following hyperacute, non-lethal poisoning [84,93]. Both groups were only able to document blood and tissue CO concentrations immediately following exposure and either did not, or were unable to, track CO tissue levels over time. Importantly, neither irrigated their tissue samples so that these were probably contaminated by blood (COHb). Predictably, both studies suggested a correlation between blood and tissue CO values in orders of magnitude consistent with their intravascular spaces: spleen > liver > kidney. The lungs had relatively high values, possibly due to direct CO absorption, but paradoxically the most metabolically active organs – the heart and brain – had the lowest concentrations. This relative distribution is at odds with the clinical features of CO toxicity that primarily affect the latter organs.

1.3 CO PATHOPHYSIOLOGY & PHYSIOLOGY

The toxic properties of carbon monoxide have been known for thousands of years. Even though the exact mechanism for its toxicity was unknown, Aristotle in the 3rd century BC already suggested that "coal fumes lead to heavy head and death" and Cicero actually killed people using CO some two hundred years later. However, the association of CO with hemoglobin as a proposed mechanism for its biological and toxicological effects, dates back to the original work of Claude Bernard in 1857 [94]. Several years later, John Scott Haldane – perhaps most famous for his work in the prevention of decompression sickness – examined the effects of CO (or carbonic oxide as it was known then) on arterial oxygen levels [85,86].

His work yielded the relationship between oxygen- and CO binding to Hb as is defined in his first law:

$$([COHb]/[HbO_2]) = M \ (PCO/PO_2)$$

Equation 1. Haldane Equation for the relationship between CO and O_2 binding to Hb

Where M, the Haldane coefficient or equilibrium constant for the reaction of CO and HbO_2, varies between 200 and 230 for human Hb [95,96].

Since then physiological and pathophysiological studies on CO have revolved around six interrelated areas: (1) its affinity to hemoglobin and its effects on oxyhemoglobin (HbO_2) dissociation [97-99]; (2) its affinity to other hemeproteins and its effects on aerobic metabolism [100,101]; (3) its endogenous synthesis during the breakdown of heme [102,103]; (4) its vasoregulatory effects [104]; (5) its biochemical properties and interactions with reactive oxygen species and nitric oxide [105]; and (6) its neurophysiologic role [106].

All these areas of research add relevance and justification to refining methods for tissue CO detection. This study, however, was only aimed at questioning the relationship between blood and tissue CO levels following acute exposure to determine its relative distribution and, in so doing, contribute towards our understanding of CO toxicity. As such, only the following considerations are relevant:

➢ COHb and CO concentration
➢ Dissolved CO Concentrations in Plasma
➢ CO Content In Whole Blood
➢ CO Concentrations in Tissue
➢ Physiological and Pathophysiological effects of CO

1.3.1 COHb & CO concentration

The concentration of CO in blood is reflected by the following equation (units modified from the original) [107]:

$$COHb \ (\%tHb) = \frac{mL.CO_{RBC} \ / \ dL}{(g)tHb \ / \ dLx1.39}$$

therefore

$$mL \ CO_{RBC} = COHb \ (\%tHb) \ x \ (g)tHb/dL \ x \ 1.39$$

Equation 2. Relationship between %COHb and CO content of red blood cells (RBC). COHb(%tHb) is the fraction of COHb relative to total Hb (tHb); (gtHb) is the amount of total Hb and is measured per 100mL blood (dL); and 1.39 is Hüfner's factor that describes the molar amount of CO to bind to 1 g of Hb expressed as volume of CO at standard temperature and pressure (STP) where 22.4 L would represent 1 mole [108].

This formula does not consider the small amounts of dissolved CO in blood at usual low inspired CO concentrations.

1.3.2 Dissolved CO Concentrations in Plasma

At levels of 2500 ppm CO in air, breathed at 1 atmosphere of pressure (i.e., the exposure used in this study), dissolved CO quantities become more significant. It also accounts for the portion of CO entering the body which is not "captured" or buffered by Hb and is therefore able to diffuse directly into tissues according to perfusion, metabolic activity (reduced pO_2) and the presence of tissues CO 'sinks' (e.g., myoglobin and cytochromes).

To calculate the dissolved CO content as a function of inspired partial pressure of CO (p_iCO) , the following calculation can be used:

$$\textbf{mL CO}_{\textbf{plasma}} = (\textbf{p}_i\textbf{CO x S) x AD}$$

Equation 3. Dissolved CO in plasma. CO content   (molar amount) – expressed as volume of CO gas at standard temperature and pressure (STP) – is equal to the partial pressure of inspired CO (p_iCO) multiplied by the solubility factor for CO in plasma at 37°C (S) expressed as mLCO per unit pressure. Due to the addition of water vapor and CO_2 to inspired air in the alveolar space, there is an inherent dilution effect (AD) on all inspired gas concentrations. At 1 atmosphere (1ATA) this is approximately 0.89.

1.3.3 CO Content In Whole Blood

By implication, the total blood CO content can be predicted by means of the following consolidated equation:

$$\textbf{[CO]}_{\textbf{Blood}} = \textbf{[COHb(\%tHb) x (g)tHb/dL x 1.39]x[(p}_i\textbf{CO x S)x AD]}$$

Equation 4. Total blood CO content. This is made up of mL CO_{RBC} (Equation 2) and CO_{plasma} (Equation 3).

Predicted blood CO values, where listed in this manuscript, refer to the results of Equation 4.

As in the case of oxygen, there is equilibrium between COHb and a small amount of dissolved CO in plasma. Increased oxygen tensions in the lung favor the release of CO from hemoglobin which explains its eventual elimination from blood by the lungs as well as the increase in COHb elimination by raising inspired pO_2. What is less clear is the transfer of CO from COHb and plasma to tissues and cells as a function of perfusion, pO_2 and CO 'sinks' (i.e., heme concentration). This was the focal point of our study.

1.3.4 CO Concentrations in Tissue

CO concentrations in tissue are ultimately the result of contributions from exogenous and endogenous sources [52].

Exogenous CO reaches tissue almost exclusively by perfusion in the form of COHb and dissolved plasma CO [109]. In organs such as the lung, direct absorption from the environment may also be relevant [110].

In 1952, Sjostrand published the important discovery that decomposition of hemoglobin, following hemolysis, led to the endogenous production of CO [111]. This discovery ultimately led to the finding of a multitude of endogenous sources of CO including lipid peroxidation and photo-oxidation reactions [107]. Since then, much has been written on the endogenous sources of CO. In fact, it was this avenue of research – rather than the pursuit of understanding the toxicological effects of CO – that rendered the RGA methodology used in this study [1]: In an effort to measure endogenous CO production as a surrogate for [heme] released in neonatal hemolysis, Vreman *et al* adapted an industrial CO RGA detection system to accurately detect CO in tissue [1].

It should be apparent by now that there might be difficulties in predicting tissue CO values from blood CO values alone – both in homeostasis and following poisoning. Moreover, studies evaluating the concentrations of CO following perturbations of these various interrelated factors emphasizes the need to control for these. Already, following this study, there has been progress in this direction using the same methodology [110,112]. The latter have not only illustrated the value of the technique, but its immediate utility beyond the study of CO toxicity alone. Specifically the effects of variations in pO2 [112] and heme concentrations [110] have been considered. This study, however, has only considered gross changes in blood and tissue CO following poisoning.

Much of the important data relating to the distribution and uptake of CO in the body from exogenous sources comes from the University of Pennsylvania

through the physiological studies of Coburn et al [52,78,103,113-124]. Similarly, a model to predict transplacental CO transfer was introduced by Hill *et al* in 1977 [125]. However, these models have not been validated so that to date there is still no universally accepted formula to derive or predict tissue CO levels. The most recent attempt was by Shinomiya *et al* who measured immediate post poisoning tissue CO levels in an effort to correlate these to COHb and derive regression data [93]. However they did not examine subsequent tissue CO changes over time during CO elimination. Also, their lowest COHb value was in the order of 12% which means that the relationship between COHb and tissue CO was not determined within the physiological ranges. By all accounts, the quantity of unbound CO in tissue remains unknown although, due to its low concentrations and high affinity to hemeproteins, it is not unreasonable to assume that most of it is in bound form.

Once CO is delivered to tissues, it associates with hemeproteins. Our understanding of this association is credited to the work of Otto Warburg. In 1926, together with David Keilin *et al*, he discovered a CO-sensitive iron porphyrin enzyme that catalyzed cell respiration – cytochrome oxidase. This discovery underpinned the importance of CO as a cellular asphyxiant [57,58,87,126]. Importantly, Warburg published the well known partition coefficient for CO that defines its affinity to various heme compounds, e.g., myoglobin, cytochrome P450 and cytochrome oxidase (Equation 5):

$$K=(n/n-1)(CO/O_2)$$

Equation 5. Warburg equation for the partition coefficient of CO that reflects its relative affinity for a binding site relative to oxygen. Where n, the fraction of a compound bound to CO, is equal to 0.5. K is therefore the ratio of CO to O_2 required to saturate a CO binding site by 50%.

The Warburg equation serves as a means of illustrating the relative affinity of binding sites to CO and defines the competitive relationship between O_2 and CO. Warburg coefficients range between 0.025 to 0.04 for myoglobin , 0.045 for hemoglobin, and 5 to 15 for cytochrome c [50,127].

- 27 -

Once CO has been absorbed by the lungs and distributed to tissues, the effects of metabolism and elimination of CO should also be considered. These variables affect tissue [CO] as well as its potential physiological and pathophysiological impact. Interestingly, cells seem capable of metabolizing CO. Fenn and Cobb described the oxidation of CO to CO_2 in living tissue in the 1930's [128], but it took a further 50 years before this was attributed to mitochondria by Young et al [129-132]. This introduces yet another variable in tissue CO concentrations. Finally it must be assumed that following non-lethal exposure, tissue CO levels eventually return to baseline as a function of CO gradients favoring elimination and a gradual decrease in COHb levels providing a vehicle for it.

1.3.5 Physiological and Pathophysiological effects of CO

Depending on particular tissue [CO], various physiological and pathophysiological effects may be anticipated. Over the past twenty years they have included effects on vasoregulation [133]; platelet aggregation [134]; inflammation and leukocyte adherence [135-137]; oxidative and nitrosative stress [138-141]; intracellular signaling [142-145]; apoptosis [146]; and cell proliferation[147]. Indeed, ever since Robert Furchgott *et al* discovered the role of nitric oxide (NO) as an important regulator of the cardiovascular system [148], the role of biological gases as signaling molecules has received ever-increasing attention [140,149-157]. CO is now known to be an important cell signaling molecule [158]; it is closely associated with normal cellular physiology. Recently CO has been implicated as an important vasoactive gas and as a neuronal transmitter [106,159,160]. There also appears to be an interactive relationship between NO and CO [46,47,140,149-157,161].

Thus the relevance and importance of measuring tissue and cellular CO levels clearly extends beyond issues of toxicity towards unraveling complex physiological processes. Importantly, with the exception of four scientific articles, in which the actual removal of COHb was not specified, the inter-relationship and exchange between blood and tissue CO remains elusive [84,92,93,162].

As far as toxicity is concerned, our current understanding is that CO toxicity is a product of the interrelated consequences of hypoxemia and tissue hypoxia leading to reduced blood oxygen carrying capacity (toxic reduction of HbO_2 carrying capacity), reduced oxygen delivery to tissue (left-shifting of HBO_2 dissociation curve), and interference with intracellular heme compounds (myoglobin and cytochrome binding).

CHAPTER 2.   LITERATURE SURVEY

2.1 METHODS EMPLOYED FOR LITERATURE SURVEY

An exhaustive search of the literature was performed in preparation for this study. The search included a comprehensive Medline and PubMed search from 1965 to 2004, as well as a review of more than 500 articles in textbooks, symposia proceedings, conferences, and manuscripts. Important references predating Medline were also included.

A total of 14732 articles and texts were screened for relevance after collating these in an Endnote® reference library. The latter is appended to this thesis on a CD-Rom for reference purposes. A reduced database of 3591 was ultimately used as the primary reference source for this manuscript. Of these, 3402 related to historic and background information that were not deemed necessary for inclusion. The balance of 189 cited references were studied in greater detail: 124 of these were reviewed according to their relevance to this paper. Sixty four references that applied directly to the physiology, toxicology and methodological aspects of this study were studied in detail.

2.2 RELEVANCE OF LITERATURE SURVEY TO THIS STUDY

While much is known about the production and toxicity of CO, relatively little is known about its uptake and distribution within tissues. Variables in absorption, distribution, metabolism and elimination as well as endogenous production and varying affinities to heme compounds, pO_2 ranges make this a complex issue as delineated in sections 1.3.4 and 1.3.5. Therefore, even though various models and predictions for CO distribution from blood to tissue have been proposed, none have been elaborated from actual tissue measurements [163-165]. Accordingly, in the absence of such experimental or clinical verification, their value and reliability cannot be determined.

There are many excellent monographs and texts on CO, its toxicity and environmental and biological impact. For those unfamiliar with the topic, however, the definitive report by the World Health Organization in 1999 [166] provides an invaluable introductory overview, whereas the current trends in CO research and medicine are synthesized in a recent review article on the biological chemistry of CO [50].

Our limited understanding of CO is most evident in observing the known discrepancies between quantitative CO measurements in blood (COHb) and the associated range of clinical findings and complications related to CO poisoning.

With the technology now available to measure CO levels in picomoles per milligram, it has become possible and important to determine the distribution of CO in COHb-free tissue, relative to blood, following acute CO poisoning. Equally important is following the movement of CO from tissue after such exposures.

2.3 OVERALL SIGNIFICANCE OF THIS STUDY

Both the physiology and toxicology of CO have far reaching implications (see section 1.3). Accordingly, refining the technology able to evaluate the dynamics of CO flux at tissue level has great potential.

In South Africa, in particular, CO poisoning is a silent epidemic, particularly amongst the previously disadvantaged portions of the population and those in certain occupations. Examples include: informal housing with unsafe heating systems (e.g., kerosene stoves or open fires); prolonged transport in unventilated vehicles or where exhaust fumes are entrained; and working in unventilated areas where combustion engines are used.

The management of CO exposure and toxicity has depended largely on a determination of elevated COHb levels to confirm exposure and subsequent evaluation of metabolic, cardiac and neurological status to determine the associated risks of mortality and morbidity. At this level of scrutiny and understanding we are unlikely to delineate the value of avoiding exposure and the need for, and impact of, actively treating the consequences of such exposure.

The effects of chronic exposure are also unknown, again due to deficiencies in our knowledge on CO tissue uptake and pathophysiology.

It is the hope of the author that this work will contribute in no small way towards better understanding the need for this.

CHAPTER 3. OBJECTIVE & RESEARCH QUESTION

3.1 INTRODUCTION

Until 1984, when Vreman *et al* first applied a very sensitive, proprietary measuring technique to study CO in biological systems by using mercuric oxide reduction gas analysis (RGA), there was no practical way to determine tissue CO levels in tissue within the picomoles per milligram range [1]. Their primary application was to accurately determine CO production as a function of heme breakdown in neonates suffering from hemolysis and jaundice [107,167-170]. More recently their technique has been extended towards measuring physiological CO tissue levels and variability in response to biological manipulation of heme oxygenase [170,171].

Only two studies were found in which blood and tissue CO levels were specifically measured following acute, non-lethal exposure, and the tissue samples were not specifically cleared of COHb – the largest CO reservoir – that would possibly have overshadowed true tissue CO levels immediately and for some time following exposure [84,93].

Various techniques for tissue and blood CO detection have been described in section 1.1. and following sections. However, based on all the factors listed including practicability, the availability of equipment and recommendations by the co-promoters – based on their own extensive experience – the RGA methodology was chosen.

During a clinical fellowship in Diving and Hyperbaric Medicine at Duke University, Durham, North Carolina, USA, from September 2002 to August 2003, the author had the opportunity to study the use of RGA under the tutelage of Henk Vreman – pioneer of this application of the RGA technique in

biological systems – at Stanford University, San Hose, California, USA. Equipped with this knowledge the author then set up and configured a resident RGA5 analyzer and acquired the supporting equipment to allow the methodology to be replicated at Duke University. Although assisted by the laboratory technologists, acknowledged previously, the author was primarily responsible for developing competence in the application of the techniques and establishing them at the Centre for Hyperbaric Medicine and Environmental Medicine at Duke University Medical Centre: This involved adapting the previously published technique within a new laboratory environment and applying it for the purpose of simultaneously assessing blood and tissue CO in brain, heart muscle and skeletal muscle following exceptional exposure to CO and following it over time. In response to a specific request, this thesis addressed the specific technical aspects of the technique in great detail.[♥] While others have measured post exposure tissue CO levels in tissues [162,172], the removal of tissue COHb by irrigation and the evaluation of CO concentration in blood and tissues over time are unique. Further study on the most effective means of eliminating COHb from tissue samples is recommended and this should also be considered carefully when reviewing literature on tissue CO.

This study provided an opportunity to validate this analytical technique [1]; it also provided an important opportunity to examine blood and tissue [CO] simultaneously, both immediately following extreme CO exposure and also over a 150 minute recovery period.

The purpose of this study was to examine the variable relationship between COHb and clinical CO toxicity by simultaneously measuring COHb and tissue CO levels in the brain, heart and skeletal muscle following extreme exposure to CO; to see if a statistical relationship (interaction) existed between blood and

---

[♥] It has been the author's intention to facilitate the development of similar capabilities within the University of Pretoria and this manuscript therefore serves this purpose also. In addition – as the study was performed off site and away from the direct oversight of the University awarding the qualification – the technical descriptions are intentionally specific, detailed and may appear repetitive. To the reader familiar with reduction gas analysis, this approach may seem redundant. However, to the uninitiated it is hoped that it will offer greater clarity and facilitate replication of the methodology in pursuit of better understanding.

tissue CO; and to determine to what extent [CO] varied between tissues, over time, following such exposure. The practical research question was whether or not tissue CO values could be predicted from COHb values following CO exposure and during recovery on air. An expanded part of this study has since investigated the effect of varying pO_2 [112].

3.2 HYPOTHESIS

Due to the large number of variables potentially affecting tissue CO concentrations, this study did not presume the ability to model CO tissue distribution from blood. It merely endeavored to measure [CO] in blood and three tissue compartments simultaneously and examine their statistical relationship. For the purposes of questioning the utility of COHb in predicting tissue CO levels this approach proved sufficient. Apart from the central hypothesis, the study addressed the time- and tissue-related variability of tissue [CO] in an effort to explore variables of CO distribution relevant to individual tissues.

3.2.1   Null hypothesis (H_o):

Following exposure to CO, changes in blood and tissue [CO] do not differ over time.

3.2.2   Alternative Hypothesis (H_1)

Following exposure to CO, changes in blood [CO] are different to those in tissue over time.

Testing of this hypothesis was done for CO values using a logarithmic scale in order to use linear regression in the case of exponential elimination. A p-value less than 0.05 was considered statistically significant. If this were achieved, it would support the clinical finding that COHb levels are unable to predict tissue CO values at any given time following CO exposure.

3.3 STUDY DESIGN

3.3.1   Outline of the Study

The study involved measuring blood and tissue (brain, heart and skeletal muscle) CO levels in twenty four rats, harvested sequentially in groups of 4, following a 45 minute sub-lethal exposure to 2500 ppm CO in air. Nine animals served as unexposed controls. The CO levels in blood and tissue were measured using CO-oximetry and RGA respectively. Measurements were made immediately following exposure and thereafter in 30 minute increments up to 150 minutes to track changes in tissue and blood [CO] (see Table 2). The objective was to ultimately determine whether changes in blood and tissue [CO] were similar or not and to determine whether there were statistical interactions between the [CO] of the three tissues over time.

Table 2. Study outline indicating numerical assignments for control and exposed animals and respective label assignments for tissue samples with the extraction (harvesting) time point allocations

CONTROL ANIMAL GROUP ASSIGNMENTS						
	TISSUE SAMPLES		BRAIN	HEART	MUSCLE	BLOOD
C1			C1-B	C1-H	C1-M	C1-BL
C2			C2-B	C2-H	C2-M	C2-BL
C3			C3-B	C3-H	C3-M	C3-BL
C4			C4-B	C4-H	C4-M	C4-BL
C5	Unexposed Controls		C5-B	C5-H	C5-M	C5-BL
C6			C6-B	C6-H	C6-M	C6-BL
C7			C7-B	C7-H	C7-M	C7-BL
C8			C8-B	C8-H	C8-M	C8-BL
C9			C9-B	C9-H	C9-M	C9-BL

EXPERIMENTAL AIR RECOVERY GROUP ASSIGNMENTS											
TIME ALLOCATIONS		0	30	60	90	120	150	BRAIN	HEART	MUSCLE	BLOOD
A1		X						A1-B	A1-H	A1-M	A1-BL
A2			X					A2-B	A2-H	A2-M	A2-BL
A3				X				A3-B	A3-H	A3-M	A3-BL
A4					X			A4-B	A4-H	A4-M	A4-BL
A5						X		A5-B	A5-H	A5-M	A5-BL
A6							X	A6-B	A6-H	A6-M	A6-BL
A7		X						A7-B	A7-H	A7-M	A7-BL
A8			X					A8-B	A8-H	A8-M	A8-BL
A9				X				A9-B	A9-H	A9-M	A9-BL
A10	2500 ppm				X			A10-B	A10-H	A10-M	A10-BL
A11	CO					X		A11-B	A11-H	A11-M	A11-BL
A12	in Air						X	A12-B	A12-H	A12-M	A12-BL
A13	x 45 min	X						A13-B	A13-H	A13-M	A13-BL
A14			X					A14-B	A14-H	A14-M	A14-BL
A15				X				A15-B	A15-H	A15-M	A15-BL
A16					X			A16-B	A16-H	A16-M	A16-BL
A17						X		A17-B	A17-H	A17-M	A17-BL
A18							X	A18-B	A18-H	A18-M	A18-BL
A19		X						A19-B	A19-H	A19-M	A19-BL
A20			X					A20-B	A20-H	A20-M	A20-BL
A21				X				A21-B	A21-H	A21M	A21-BL
A22					X			A22-B	A22-H	A22-M	A22-BL
A23						X		A23-B	A23-H	A23-M	A23-BL
A24							X	A24-B	A24-H	A24-M	A24-BL

Preparation for the study included:

- obtaining approval from the Institute for Animal Care and Use Committee at Duke University, Durham, NC and the University of Pretoria, Onderstepoort to perform the study (Appendix C-1 and C-2)
- obtaining and configuring the necessary equipment to perform the RGA measurements
- developing a calibration sequence to derive a RGA detector or R value prior to each experimental and control session
- obtaining and configuring the equipment for the animal exposures, recovery, euthanasia and dissection
- developing techniques to permit consistent processing and preparation of tissue samples including:
  - ➢ euthanizing animals in Halothane and weighing them
  - ➢ applying an appropriate technique to ensure the removal of Hb (blood) from tissue to avoid COHb as a contaminant
  - ➢ dissecting the rats and harvesting & weighing appropriate quantities and consistent amounts of tissue
  - ➢ performing CO-oximetry of blood samples (calibrated for rat blood)
  - ➢ adding de-ionized-distilled water (dd-H_2O) with a micro-pipette to harvested tissue samples according to weight to produce a standardized homogenate
  - ➢ dicing and homogenizing tissue samples with instruments and an ultrasonic sonicator
  - ➢ centrifuging samples briefly with a micro centrifuge to ensure that all solvent (water) and solute (tissue) were admixed
- preparing reaction vials for the RGA including:
  - ➢ purging reaction vials with CO-free nitrogen prior to measurement
  - ➢ Inserting dd-H_2O and 2 µL of 60% sulfosalicylic acid in each vial
  - ➢ Inserting appropriate amounts and concentrations of tissue homogenate to permit measurements within the range of the standard calibration curve

- Recording of all measurements (triplicate samples of each of the four tissues types at each of the 6 time points). Excluding calibration, a total of 432 individual measurements were made.
- Determining tissue [CO] by back extrapolating RGA measured CO values in the headspace of the reaction vials based on the quantity (volume) and dilution factor (concentration) of the respective tissue homogenates added to the vial from which detected CO had been released.
- Analyzing CO values and the changes in [CO] over time to determine whether the statistical relationship between tissue and blood [CO].

Although assisted in some aspects of the study – such as the rat dissection and blood CO-oximetry – the author personally prepared all reaction vials and tissue samples; performed all RGA measurements; programmed the RGA measurement sequence; developed competence to perform all aspects of the study without assistance; and produced a descriptive technique manual that the Duke Laboratory continues to use.

3.3.2 Study Design

This was an experimental study designed to measure and statistically compare the change in [CO] over time in blood and three tissues (brain, heart and skeletal muscle) following sub-lethal exposure using a linear regression of [CO] on a logarithmic scale. Thirty three animals were used as follows: nine were used as controls (unexposed; baseline) and the remaining 24 provided four sets of measurements (i.e., four animals per time point) post exposure (0; 30; 60; 90; 120; 150 minutes respectively) from the moment of ending the exposure to 150 minutes and thereafter while breathing CO-free air. This permitted the regression and cross-sectional time-series analyses that would allow assessment of differences in the change of [CO] in blood and three tissues (brain; heart & skeletal muscle) and a determination of whether these tissues behaved differently over time, i.e., whether these tissues statistically interacted with time.

3.4 METHODOLOGY & TECHNIQUE

The methods are detailed in Chapter 4 and separated into the following methodological categories:

- Reduction Gas Analysis
- Calibration and derivation of a Standard Curve
- Reaction Vial Preparation
- Animal Exposure, Tissue Harvesting and Preparation
- RGA Measurement
- Recording of results
- Calculation of CO Concentration
- Analysis of Results:
    - Comparison of Exposed to Unexposed Tissues.
    - Comparison of Exposed Blood and Tissue CO Values over Time
    - Comparison of CO Tissue Concentrations between Tissues over Time

3.5 ETHICAL CONSIDERATIONS

The study protocol was approved by the Institute for Animal Care and Use Committee (IACUC) at Duke University as well as the University of Pretoria Animal Ethics Committee - Onderstepoort. Its justification and acceptability are considered below:

The study was *ethically justified* for the following reasons:

- CO poisoning is one of the most common causes of adult poisoning in the world. As this study contributes towards understanding the way in which CO is eliminated, not only from the blood but – importantly -- also from the three target organs of the body (i.e., the brain, heart and skeletal muscle) it is fundamental to our understanding of this form of poisoning and the development of effective treatment strategies in humans.

- A human study would neither be possible nor ethically acceptable. A rodent study was also considered an important precursor to larger animal studies.

- No computer models exist to accurately predict elimination of CO from the body tissue. There is multi compartment transfer, both in accumulation and elimination. All previous studies have evaluated elimination from blood only.

The study was *ethically acceptable* for the following reasons:

- The selected animal model had been used previously by this laboratory in several other studies so that wastage could be minimized.

- CO exposure is not painful. The gas itself is colorless and odorless (this is why it is so deadly and its exposure so insidious). Based on previous experience, animals do not appear distressed during exposure. Feeding and nesting behavior continued during the exposure.

- The number of animals exposed to CO was reduced to the absolute minimum that would permit valid results and statistical analysis.

All specimens collected for the analysis were used and consumed. Specimens were only collected from animals after they had been sacrificed. All remaining animal material was discarded in the way designated by the IACUC.

CHAPTER 4. MATERIALS & METHODS

4.1 OVERVIEW

This study compared levels and changes in blood, brain, heart and skeletal muscle CO levels following sub-lethal exposure. These tissues are clinically associated with the morbidity and mortality in CO poisoning.

The materials and methods involved the following key elements:

- Reduction Gas Analysis (RGA) or Reduction Gas Detection (RGD) setup
- Calibration and derivation of a Standard Curve
- Reaction Vial Preparation
- Animal Selection, Sample Size, Exposure, Tissue Harvesting and Preparation
- RGA Measurement
- Recording of results
- Calculation of CO Concentration in blood and tissues
- Analysis of Results:
  - ➢ Comparison of Exposed to Unexposed Tissues.
  - ➢ Comparison of Exposed Blood and Tissue CO Values over Time
  - ➢ Comparison of CO Tissue Concentrations between Tissues over Time

4.2 TERMINOLOGY

The following terms are relevant to the materials and methods section and are used repetitively. Most are also explained in context, but those relating to reduction gas analysis (RGA) technique in particular are in need of prior definition and are provided here:

Analytical Column:

The portion of the RGA where the gaseous components contents of the sample are separated before detection. *Synonyms*: Column; Retention Column; Molecular Sieve; Chromatograph Column (see section 4.3.).

Blanks

Reaction vials not containing tissue or CO for the purposes of determining a zero value on the RGA. Apart from standardizing the zero set point for the technique, the silicon septa used for the experiment actually generate CO. By performing blank measurements before and after an *experimental session*, it could be verified that CO production was minimal and this provided a CO quantity average that was subtracted from all samples to account for this spontaneous production by the septum (see section 4.5.).

Bunch: (see Sense and Forcebase)

A RGA chromatograph parameter that defines the approximate width of the peak to be detected. Widths can vary significantly with gas concentration and are set between minimum and maximum amounts. Maximum amounts prevent merging of gas identities while minimum amounts improve correct identification of small peaks. For this study an appropriate bunch setting of 4 was selected to ensure both accurate identification and avoiding merging with other gases -- particularly hydrogen (see section 4.3.).

Calvarium:

The upper domelike portion of the skull without the lower jaw or the lower jaw and the facial parts (see section 4.5.2.).

COHb:

The compound that is formed when inhaled CO combines with hemoglobin, binding more tightly than oxygen and rendering the hemoglobin incapable of transporting oxygen.

Carrier Gas:

An inert or non-reactive gas – usually nitrogen or air – used to transport gas samples into and through a gas chromatograph. In this RGA, the carrier gas carries the contents of the reaction vial headspace into the detector (see section 4.3.).

Chromatogram:

RGA measurement concludes with the production of a chromatogram. It contains the following parameters of the detection including – but not limited to – date; time; Retention Time (RT); Column Temperature; Detector Temperature; Carrier Gas Flow Rate; Detection curve; Peak Area; R-value; and ppm CO (calculated).

Control Session:

A complete subset of this experiment for the purpose of determining unexposed baseline (control) values by euthanizing 4 and 5 unexposed animals in respective sessions (total: 9 control animals); harvesting tissue; preparing tissue homogenate; calibrating and setting up the RGA; preparing reaction vials; introducing appropriate quantities of tissue homogenate into the vials; measuring the CO content in the consequent 54 and 66 vials respectively (total: 120) with a 107-second programmed cyclical detection sequence on the RGA; recording the results; providing quality control of the results; and repeating any anomalous samples. Animals exposed to CO were examined during so-called *experimental sessions* (see Experimental Session).

CO-Oximetry:

A hemoglobin profile monitor that typically measures the respective percentages of oxyhemoglobin, methemoglobin, and COHb as well as hemoglobin concentration and oxygen saturation. Modern CO-Oximeters can be calibrated for animal blood, including rat hemoglobin – as was done for this experiment.

De-ionized, Distilled Water:

Very pure, non-reactive form of water used in sensitive chemical experiments where charged particles or impurities that may effect measurement or reactions are minimized.

Detector Response

In the context of RGA it refers to the electrical signal generated by the spectrophotometric measurement of mercury vapor in the optical cell of the detector assembly. The released mercury vapor is proportional to the reagent gas thus providing linearity to the device and a sensitive means of measurement (also see *Reduction Gas Analysis*). The term detector response is usually used in relation to sensitivity of the device (see section 4.3.).

Dicing:

The snipping up of tissue with sharp scissors for the purpose of simplifying sonication or homogenization (see section 4.5.3.).

Dihalomethane:

A compound – usually used as an industrial solvent (e.g., paint stripper or a dry cleaning agent such as methylene chloride) or a volatile anesthetic (e.g., halothane) – with the characteristic of being metabolized by the body to CO (see section 4.5.1. and 4.5.2.). However although Halothane was used for the purpose of euthanasia in this experiment, its metabolism is not instantaneous (within 5 minutes of exposure), has never been deemed to be of clinical importance, and there is no reason to believe that within the very short duration of exposure (which was less than 60 seconds) any significant metabolism would have occurred to introduce any appreciable amounts of CO into tissue.

Dissection:

The examination of tissues by incision, and / or excision (see section 4.5.2.).

Experimental Session

A complete subset of this experiment involving the exposure of 6 experimental animals to 2500 ppm CO in air for 45 minutes; euthanizing the animals; harvesting tissue; preparing tissue homogenate; calibrating and setting up the RGA; preparing reaction vials; introducing appropriate quantities of tissue homogenate into the vials; measuring the CO content in the consequent 78 reaction vials with a 107 second cyclical detection sequence on the RGA; recording the results; providing quality control of the results; and repeating any anomalous samples. There were four experimental sessions in this study. In addition nine control animals were processed in a similar fashion, but excluding the CO exposure (i.e., control session). The total number or Reaction Vials measured in all experimental sessions was 312.

Euthanasia:

The act of ending the life of an experimental animal by the least painful, most expedient method while minimizing the effect of or interfering with the objective of the experiment (see section 4.5.1.).

Forcebase: (see Sense and Bunch)

In RGA, the forcebase command is used to avoid calculating incorrect peak areas that result from excessively long peak baselines. The latter may be due to detector noise or drift. Baseline errors are not noticeable when peaks are large but may become significant as one approaches the limits of detection. An appropriate force base was chosen but did not significantly affect measurements due to our appropriate manipulations of homogenate volumes (tissue concentrations in the reaction vial) to maintain readily detectible CO peaks (see section 4.3).

Gas Chromatography:

A form of chromatography (actually completely unrelated to color as suggested by the name) in which the gaseous substances are transferred by a carrier gas and separated by differential absorption in a liquid or solid adsorbent or filter (also see *Reduction Gas Analysis* and section 4.3.).

Getter:

A material added in small amounts during a chemical or metallurgical process to absorb impurities such as CO (see section 4.3.).

Hamilton Syringe:

Gas-tight syringe permitting the accurate dispensing of gases, liquids and tissue homogenate (see section 4.5.3.).

Harvesting:

Removing tissue from animals after euthanasia (see section 4.5.2.).

Head space:

The portion of the reaction vial not filled with liquid or wet samples (see section 4.5).

Homogenization:

The act of making something homogeneous or uniform in composition. In this case a blending of tissue with solvent (water) to create a standardized tissue suspension for the determination of average CO levels in tissue (see section 4.5.3). For this study sonication was used for homogenization and therefore the terms *homogenate* and *sonicate* may be used interchangeably in this particular study.

Irrigation:

In the context of this document, irrigation implies the experimental method of passing a large quantity of normal saline (60 mL) through the circulatory system of the experimental animal for the purpose of flushing out blood and – specifically – hemoglobin from tissues to avoid contamination with COHb while

performing tissue CO measurements. It is achieved by obtaining needle puncture access to the left ventricle and flushing the circulation through all tissues towards the pulmonary artery which is transected to allow drainage of blood and fluid (see section 4.5.2.).

Parts Per Million:

Concentration of a given substance expressed in quantities per million parts of solvent or diluent. One part per million is equivalent to 0.0001 %. Accordingly 2500 ppm is equivalent to 0.25% CO.

Parts Per Billion:

Concentration of a given substance expressed in quantities per billion parts of solvent or diluent. One part per billion is equivalent to 0.000,000,1 %.

Peak Area (PA): (also see Sense, Bunch and Forcebase)

The area under each chromatogram peak.. PA is proportional to the concentration of the compound being detected. During sample analysis, the RGA 5 automatically measures peak areas according to the control settings that are set by the operator by using a calibration gas. *Sense*, *Bunch* and *Forcebase* are related controls that affect the way the peak is measured (see *Chromatogram*).

Purging:

The process of flushing a reaction vial with CO-free gas for the purpose of achieving a near- zero CO baseline (see section 4.3.). In this experiment reaction vials were flushed at 300 mL per minute for a period of 6 seconds (i.e., allowing 30 mL to flow through the vial) to remove any residual CO. Typical concentrations of CO in air are 0.5 or 0.3 ppm. Considering the RGA was calibrated using only 50 to 550 μL of 4.89 ppm CO in the reaction vial, the importance of purging is obvious.

R-Value:

The R-value or detector value represents the responsiveness of the detector to CO. It is the ratio between peak area (PA) and the associated quantity of CO and

– in this experiment – was expressed in pmol CO/mV.sec. It was determined by introducing known quantities of CO into the reaction vial; determining the PA in the chromatogram; and deriving a standard curve. In RGA the relationship between PA and CO concentration is linear; therefore in the algebraic equation for linearity: $Y = MX + C$, with Y representing PA; and X representing CO concentration; the R value is M.

Reaction Vial:

A 2 mL glass (borosilicate) vial with a perforated cap and silicon septum used in gas analysis where a reaction precipitates release of the reagent gas – in this case CO.

Reduction Gas Analysis (RGA):

A specific type of gas chromatography that uses heated molecular sieve or column to separate gases based on their respective molecular sizes (i.e., varying retention times); then brings them in contact with a heated mercuric oxide chemical bed where the gases e.g., CO and H_2, are oxidized to CO_2 and water respectively, in exchange for a proportional reduction in the mercuric oxide to mercury vapor. The latter is measured spectrophotometrically in an optical cell at 238 nm. The sensitivity of the technique lies in the property of high ultra-violet absorptivity of mercury vapor. The key to the identity of each gas is its unique retention time in the column, whereas its concentration is determined indirectly through the measurement of the amount of released mercury vapor (see section 4.3.).

Retention Time (RT):

This is the length of time required for a particular gas species, or compound, to pass through the separation column. In practical terms it is the delay from injecting the sample to its detection as a chromatogram "peak". It is unique for each gas species and is therefore used to identify the type of gas detected. Carrier gas flow rate, column composition and temperature control the retention time. To determine the appropriate identity of a particular compound, the parameters

of each gas' unique column retention time is determined in advance by means of a calibration gas (see section 4.3.).

RGA Column:

A stainless steel column, packed with a 5 A or 13X molecular sieve heated to 140°C through which CO-free carrier gas is circulated at a flow rate of 30 to 50 mL per minute (see section 4.3.).

Sense: (also see Bunch and Forcebase)

This setting in the RGA controls the sensitivity of peak detection and can be set to coarse, medium or fine. It is performed only once the 'bunch' settings have been performed. In simple terms, the sense setting affects the threshold at which a peak will be identified. A setting of fine may result in erroneous identifications. For the purpose of this study a setting of medium was used and as CO values were always relatively high through manipulation of the amount of homogenate added to the reaction vials, this never presented practical problems (see section 4.3.).

Sonication:

The process of dispersing, disrupting, or inactivating biological materials by use of sound-wave energy (see section 4.5.3.). For this study sonication was used to achieve tissue homogenization and therefore the terms *homogenate* and *sonicate* may be used interchangeably in this particular study.

Zeolite

Any one of a family of hydrous aluminum silicate minerals, whose molecules enclose cations of sodium, potassium, calcium, strontium, or barium, or a corresponding synthetic compound, used chiefly as molecular filters and ion-exchange agents (see section 4.3.).

4.3 REDUCTION GAS ANALYSIS

There are various laboratory methods for detecting CO (see Chapter 1). The most sensitive method for quantitating CO in biological systems, however, is by means of a gas chromatograph (GC) with a mercury vapor reduction gas analyzer (RGA) or detector (RGD).

The RGA system was originally developed by the Stanford Research Institute after which it was commercially manufactured by Trace Analytical; Menlo Park, CA in the 1970's based on reduction of mercuric oxide to mercury vapor [℘]. They produced various models of which the RGA5 was used in this experiment (see Figure.2).

Figure 1. RGA5 manufactured by Trace Analytical; Menlopark; CA

The principles of reduction gas analysis are relatively simple: Gas samples are injected into a flow loop attached to the sample injection valve. Upon activation the sample is injected into the separation column. Upon separation, the gases

---

[℘] Trace Analytical is no longer in business, but similar equipment and services can be obtained from Peak Laboratories, Mountainview; CA

continue in tandem to a 260 – 270 °C heated mercuric oxide chemical bed where the 'oxidizable' gases e.g., CO and hydrogen, are oxidized to carbon dioxide and water respectively. In exchange a reduction occurs as mercuric oxide is reduced to mercury vapor. The latter is measured spectrophotometrically in an optical cell. The sensitivity of the technique and choice of mercuric oxide lies in the property of high ultra-violet absorptivity of mercury vapor. The key to the identity of each gas is its unique retention time in the column, whereas its concentration is determined indirectly through the measurement of the amount of released mercury vapor. A basic overview of the system is provided in Figure 2.
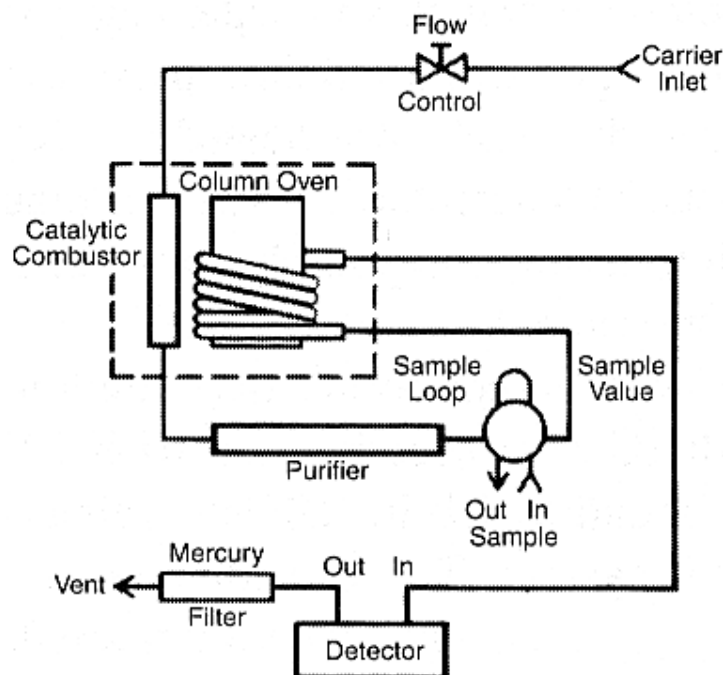
Figure 2. Overview of the Reduction Gas Analyzer. This flow diagram illustrates the path of carrier gas: It enters the circuit (top right) at a set flow rate (usually 30 to 50 mL per min). A catalytic combustor removes any traces of CO in the carrier gas after which it is purified. Gas then passes through a valve assembly that is activated to inject the sample into the circuit. The carrier gas (with or without the entrained sample) is then passed to the heated column where any injected components are retained depending on their respective molecular size; the temperature of the column; and the carrier gas flow rate. After leaving the column, the carrier gas (with the various sample gases now separated by their respective retention times in the column), passes to the detector where any oxidizable component gases are oxidized in exchange for a proportional reduction of mercuric oxide to mercury vapor. The latter is measured in an optical cell after which it is filtered out. The carrier gas – unchanged throughout – is then discharged to the environment. (*Courtesy of Trace Analytical, Inc. Copyright 1996.*)

The principle elements in this RGA are the heated column (separator); heated RGD detector; sample valve; carrier gas; and reaction vial double needle assembly.

4.3.1 Heated Column

This RGA 5 system utilizes a stainless steel column, heated between 100 to 140°C (105°C for this study) packed with a 5 A molecular sieve (see Figure 3). The molecular sieve temporarily traps gases – based on their respective molecular sizes – and then delivers them sequentially to the next principal element, the RGD detector. The delay (or trapping) of reagent gas in the heated Column is called the retention time (RT). In addition to molecular size, the latter is also dependent on the temperature of the column and the flow rate of the carrier gas through it. This is all accounted for during the calibration process (see section 4.4.).
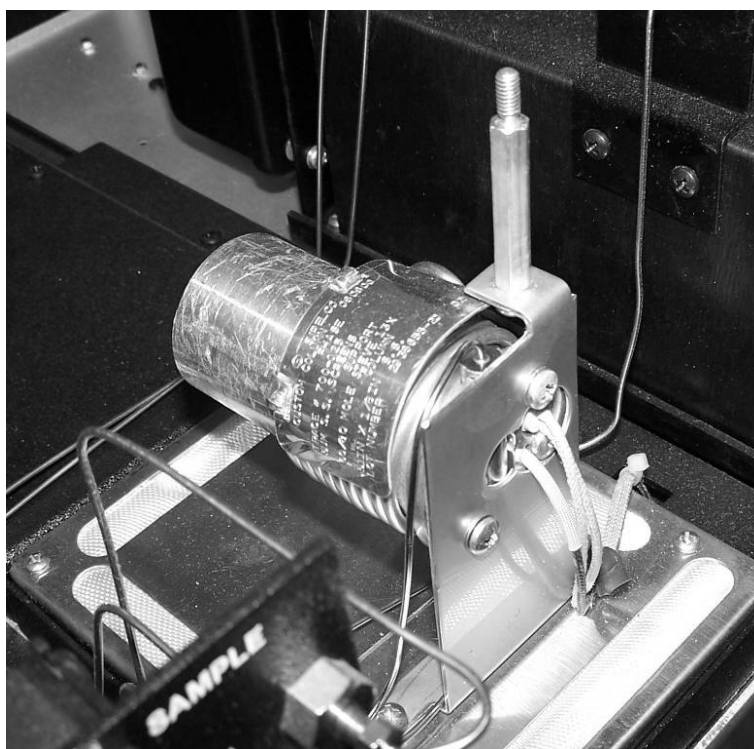
Figure 3. RGA Column containing a heated molecular sieve.

4.3.2 Reduction Gas Detector (RGD)

The RGD contains a 5 mg solid mercuric oxide (HgO) bed heated to 260°C. Upon oxidizing CO to carbon dioxide and H_2 to water, an equivalent amount of mercuric oxide is reduced to mercury vapor. The latter is measured spectrophotometrically in a 10 cm optical cell (see Fig. 4 and Fig 5B).
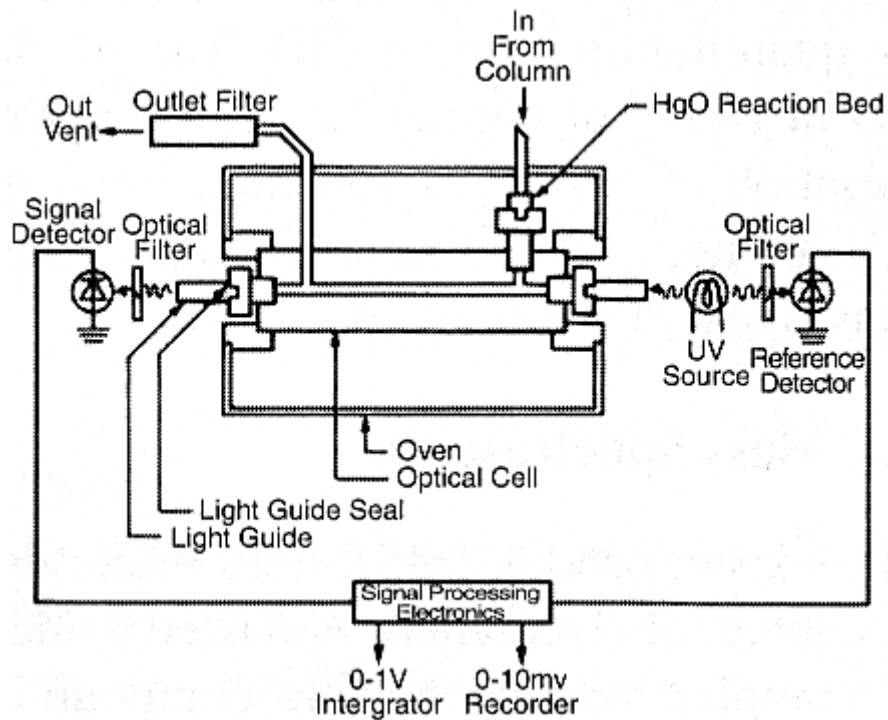
Figure 4. The RGD Circuit Diagram. This is a close-up circuit diagram showing carrier gas (previously circulated through the column) entering the oven containing the detector. It passes into the heated mercuric oxide reaction bed. Once the mercury vapor is released the latter is measured by an optical cell after which the mercury vapor and carrier gas passes through an outlet filter to remove the toxic mercury after which it is discharged to the atmosphere. (*Courtesy of Trace Analytical, Inc. Copyright 1996.*)

Mercury has very high ultraviolet light absorptivity – in the 254 nm range – which is the basis for the high sensitivity of the technique: The RGA/RGD/GC has a sensitivity of 1 pmol of CO with linearity up to 120 pmols (see Fig. 5.).
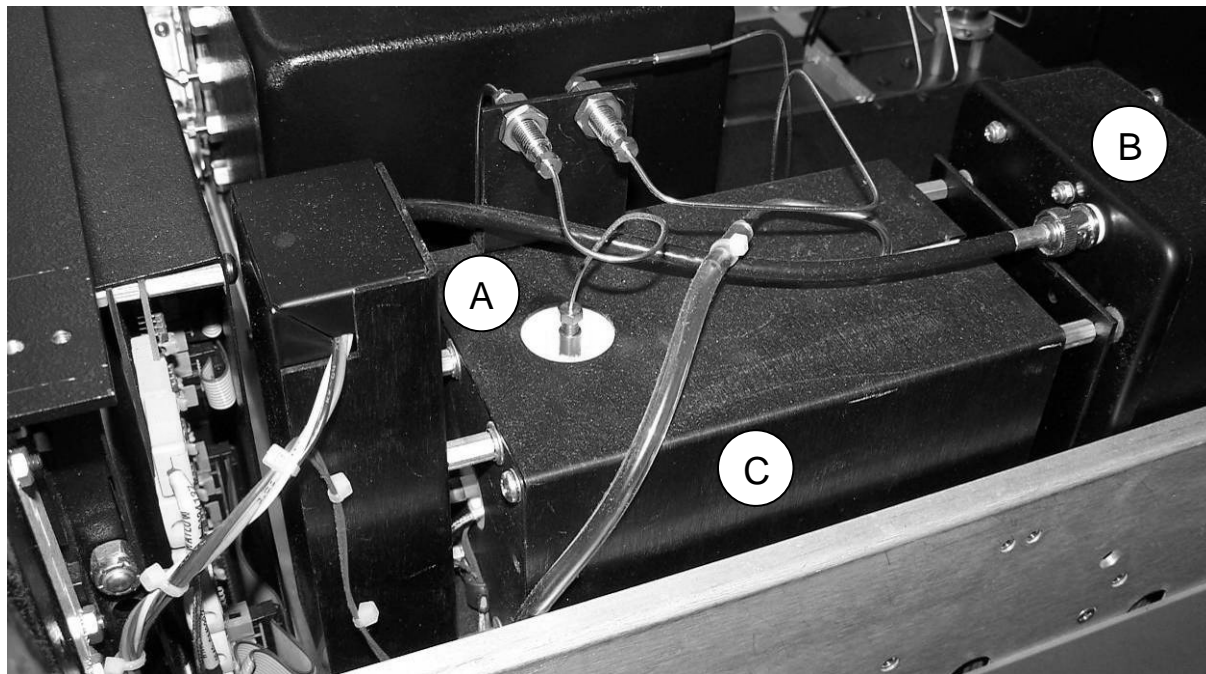
Figure 5. The RGD. (A) Shows the entry point to the mercuric oxide bed; (B) is the UV light detector housing and electronic circuit board and; (C) is the oven cover.

For safety reasons, the mercury vapor is absorbed by a mercury trap before the carrier gas is discharged to the environment (see Fig. 5).

4.3.3 Sample Valve

The sample is injected into the RGA circuit by means of a pneumatically activated sample valve (see Figure 6.).
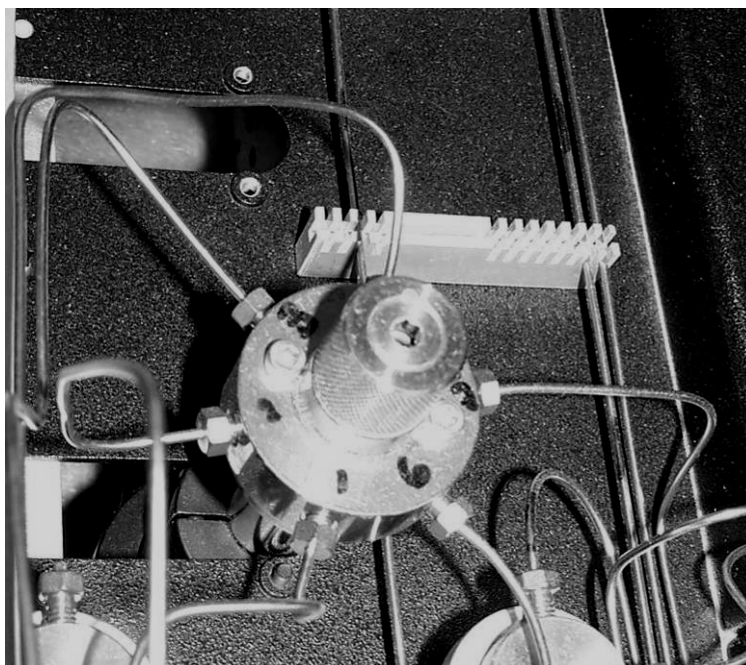
Figure 6. The Sample Valve showing various connections that direct carrier gas through the RGA or through the reaction vial (i.e., sample injection).

Timed activation of the valve is by means of a programmed detection sequence. The specific sequence for this study, using the RGA5, is shown in Figure 7.

```
                      ------  ---  -------
P2=NEW30CC                              02-09-04 10:25
     0000    PKDET     · OFF       A   0
     0001    SENSE       MEDIUM    A   1
     0002    BUNCH       4         A   2
     0003    VALVE1      CW            3
     0023    VALVE1      CCW           4
     0049    FORCEB                A   5
     0051    PKDET        ON       A   6
     0088    PKDET       OFF       A   7
     0090    FORCEB                A   8
     0091    ANEND                     9
     0092    ZSET                  A  10
     0107    END                      11
```

```
  * END REPORT   06/01/05   11:39:17   RUN 0   SERIAL NO. 315
```

Figure 7. RGA Sampling and Detection Sequence. This manually programmed sequence – filed as New30CC under Programme 2 (P2) ran as follows (note that the left column indicates the run time for each sampling sequence). During a sample sequence of 107 seconds, the following events were programmed: Peak detect turned off initially to avoid misidentification due to the presence of other gases. *Sense* set to medium; Bunch to 4. The sample valve opened at 3 seconds and remained open for 20 seconds allowing 10 mL (based on a carrier gas flow rate of 30 mL per minute) through the vial. This removed 99% CO from the headspace and entrained it into the 2.4 mL sample loop. Force base command ensured that the baseline detection was zeroed before the arrival of the sample. Based on a retention time of 59 seconds (see figure 5) from activation of the valve, the peak detect was activated for a period between 51 (i.e., 48 seconds from injection) to 88 (i.e., 85 seconds from injection). A force base command followed at 90 seconds to ensure a cutoff in case of any long tailing peaks beyond the probable retention time of any CO after which the analysis was ended at 91 seconds. The print command followed and the sequence ended after which the cycle was automatically repeated until manually stopped.

The valve should be opened long enough to permit entry of the complete sample (reaction vial headspace gas) into the separation and detection loop circuit; this is based on three factors: (1) the volume of the reaction vial – 2 mL; (2) the volume of the sample loop connections – 0.4 mL; and (3) the flow rate of the carrier gas – 30 mL per minute for this study.

Based on exponential elimination principles, a 20 second delay was selected to deliver a predicted volume of 10 mL through the sample loop. This represented five-times the internal volume of the reaction vial. By performing a series of sequential tests with increasing amounts of CO calibration gas added to the

reaction vial, we confirmed 95 to 99% removal of CO from the reaction vial headspace with these settings.

Table 3. Effect of 20-second Sample Valve opening with a 30 mL per minute carrier gas flow rate (i.e., 10 ml)on CO elimination from the Reaction Vial Headspace. Calibration gas contained 4.89 ppm CO in N_2.

Calibration Gas Volume	pmol CO	Peak Area		% Retained
		1st Pass	2nd Pass	
50	9.7	481	21	4.4
50	9.7	493	5	1
50	9.7	472	15	3.2
100	19.4	994	30	3
100	19.4	982	49	5
100	19.4	991	35	3.5
200	38.8	1979	25	1.3
200	38.8	1984	20	1
200	38.8	1999	65	3.3
400	77.6	3923	105	2.7
400	77.6	3947	175	4.4
400	77.6	3932	66	1.7

4.3.4 Carrier Gas

The carrier gas serves three purposes: (1) it provides continuous convection through the system to keep it clear of contaminants with a stable baseline; (2) it delivers the sample to be analyzed into the detector loop upon activation of the sample loop valve; (3) and it removes mercury vapor and oxidized products from the heated mercuric vapor bed and detector.

To be reliable, a carrier gas needs to be free of any oxidizable components. Nitrogen and air provide suitable carriers. However CO is a ubiquitous gas and is invariably present as a contaminant. Because of this, all carrier gases used in CO studies must be chemically or catalytically filtered. For the purpose of the

experiment, CO-free carrier gas for the vial purging and for the RGA circuit was obtained by chemically filtering nitrogen through SAES Getter (PS11-MC1 Ambient Temperature Gas Purifier – Getter Stabilized Zeolite – SAES Getters USA Inc; Colorado Springs, CO) see Figure 8. The complete configuration is illustrated in Figure 9. In addition, the RGA has its own built-in catalytic combustor (see Fig. 2).

Figure 8. SAES Getter. Used to filter gas for purging reaction vials prior to instillation of tissue homogenate to ensure a zero CO baseline.
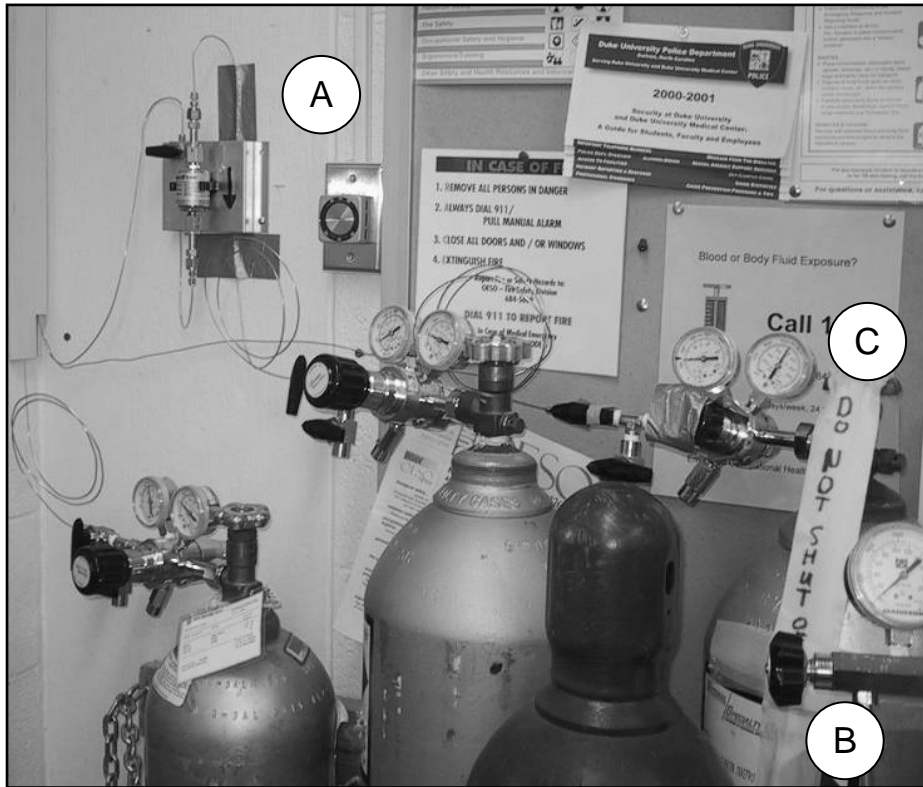
Figure 9. Configuration of CO-free gas supply. A SAES Getter (A) as shown in Fig. 8. Reliable source of compressed pure nitrogen with minimal quantities of CO (B). As the carrier gas also purges mercury vapor from the system into a mercury trap it should not be discontinued (C).

4.3.5 Double Needle Assembly

To provide carrier gas flow through the reaction vial, a double needle assembly was used for sampling and purging reaction vial contents. This is illustrated in Figure 10.
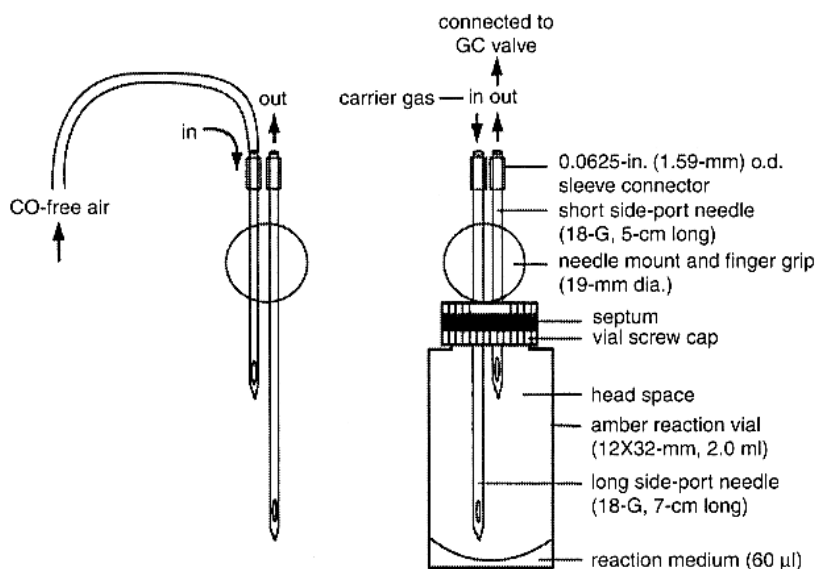
Figure 10. The double needle assembly used to purge (left) and sample (right) the headspace of the reaction vial. The dissimilar length of the double needle assembly serves a dual purpose: (1) For purging, flow is from the short to the long needle so that – upon removal – the flow into the vial is discontinued first allowing it to depressurize to ambient pressure via the long needle end while avoiding any seepage from atmospheric air. (2) During sampling, flow is from the long to the short needle to maximize convection over the gas-liquid interface and to prevent accidental admission of liquid into the RGA as the short needle stays well away from the liquid content of the reaction vial. (*Reprinted with permission from Vreman H.J. et al., in Current Protocols in Toxicology, p. 9.2.1. John Wiley & Sons, Inc. Copyright 1999*)

The needles were of different length to allow for maximal convection of the reaction vial headspace during the injection of gas through the sample loop. Simultaneously this avoids accidentally entraining fluid into the RGA as carrier gas is circulated from the long to the short needle. When purging the vials with CO-free air during the vial preparation, however, the direction of flow was reversed from the short to the long needle so that the carrier gas supply was

discontinued when extracting the needle assembly – thereby preventing inadvertent pressurization and preventing seepage from atmospheric air into the vial during such depressurization because the exhaust loop still contained CO-free gas if retro flow were to occur (see Figure 11.).
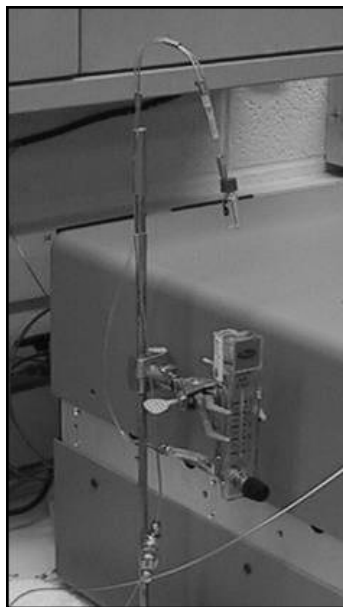
Figure 11. Vial purge assembly. Using a CO free gas at a flow rate of 300 mL per minute, the vials were purged twice before the addition of tissue homogenate: Once immediately after the dd-H_2O and sulfosalicylic acid was added and the vial sealed, and again just before the homogenate was added.

The needles were manually inserted through the gas-tight silicon septum. Care was taken not to bend the needles, blunt them by scraping them on the vial cap, or inserting them into the liquid or tissue homogenate.

In spite of obvious theoretical concerns regarding repetitive use of the septa (i.e., multiple punctures due to repeated measurements), there was no effect on precision irrespective of the number of times the septa were used. Once visible cracks appeared in the septa, they were discarded. Importantly, even though the reaction vials were transiently pressurized during the injection of carrier gas, no bubbles appeared when the membrane was covered with water. This was repeated sufficiently to be confident and the use of three reaction vials for each tissue sample also overcame any concerns about incidental leakages.

4.3.6 Chromatogram

The RGA process ended with the production of a detection chromatogram. This contained all parameters of the detection including – but not limited to -- date; time; Retention Time (RT); Column Temperature; Detector Temperature; Carrier Gas Flow Rate; Detection curve; Gas identity assignment; Peak Area (PA); R-value; and ppm CO (calculated) – see Figure 12.

```
                    FILE:  P2  = NEW30CC
                    GENERATED BY: CYCLE
         CHROMATOGRAM:    DETECTOR A    START- 09:56:07   RUN 10
           START VIEW = 0 sec     VIEW = 70 sec    SPAN = 512 mv
```

Sample Volume: 150uL   Bunch: 4

CO Concentration 4.89 ppm   Sense: Medium

CO Content: 29.1 pmol   Forcebase: On

RT: 59 sec   Detection Cycle length: 107 sec

Column Temp: 105 °C

RGD Temp: 265 °C

Flow Rate: 30mL per minute

μV

Time (sec)

0   11   22   33   43   54   65   76   87   98   109

```
         DATA    START- 09:56:07   RUN 10
          Name:   PPB:    Rt:    Area:   Rfact: Det:
          ------  ------  ----  -------- ------ ----
          CO      382.5    59   1443965  3775.5  A00
```

Area rounded from μV.sec to mV.sec

```
******* END REPORT  09/19/03   09:57:34  RUN 10   SERIAL NO. 315
```

Figure 12. RGA Chromatogram. This shows the results of 150 μL of 4.89 ppm CO in N_2 injected into a 2 mL CO-free reaction vial to calibrate the RGA. Note that the Peak Area (PA) of 1443965 μV.sec was rounded to 1444 mV.sec. Using the calculations described in detail in section 4.4, the CO content of 150 μL is 29.1 pmols. Accordingly the R value for the detector is: 29.1 / 1444 = 0.0202 pmols/mV.sec.
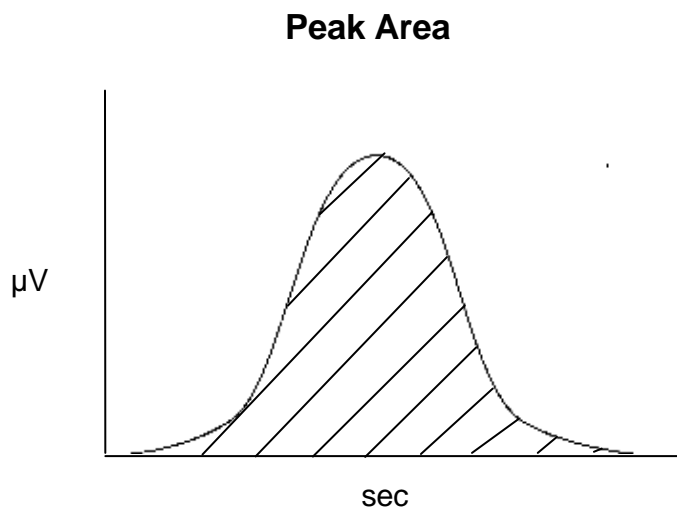
Peak Area

Figure 13. Peak Area. The PA of the chromatogram is the result of integration of the µV vs. time curve. It is expressed as µV.sec. Peak areas were subsequently converted to mV.sec without any impact on precision.

4.4 CALIBRATION

4.4.1   Gas measurements and calculations

Gas measurements are by nature more prone to error and require careful preparation and execution: being invisible and subject to large variability with changes in pressure, temperature and volume, gas analysis relies on standardization of, or compensation for, ambient conditions and comparison to a known standard: a calibration gas concentration. As the concentrations of gas to be measured become smaller, the possibility for error increases proportionally, as does the potential analytical impact of any inaccuracy. In this, this study was no exception.

For the purposes of this study the reduction gas analyzer was calibrated using a given volume of a known concentration of CO in nitrogen. Scott Specialty Gases provided our laboratory with a cylinder of gas certified as containing 4.89 ppm CO in Nitrogen. This gas was used throughout the experiment as the calibration gas. Accordingly there remains the inevitable possibility that the baseline determination of CO concentration could have been in error. If so, this would have resulted in a systematic error for all calculations on CO quantity. Importantly, however, this study had a relational premise whereby accurate quantification of CO, while important, was not a prerequisite. The hypothesis of this study and a subsequent scientific paper [112] was based on the observation of relative changes in tissue CO concentrations.

While every effort was made to ensure precision, the accuracy of the quantitative gas analyses were therefore dependent on the prior precision and accuracy in the determining the concentration of the calibration gas. Accordingly, while it is not possible to guarantee the actual numerical quantities of CO in tissue beyond reasonable scientific certainty, the technique was reproducible to the extent that we are confident that the relative changes are precise.

4.4.2   Factors determining CO quantity in the Calibration Gas

To calculate the quantity of CO within a given volume of 4.89 ppm CO in Nitrogen (N_2) for the purposes of calibrating the reduction gas analyzer, the following calculations and deductions were made based on verified gas physics and chemistry:

Avogadro [§] determined that one mole of an element or compound contained *6.0221367 x 1023 atoms or molecules* [108]. In the case of an ideal gas, 1 mole occupies 22.4 L at Standard Temperature and Pressure (STP = 0°C; 1 atmosphere or 101.3 Bar). Conversely, 22.4 L of pure, <u>ideal gas</u> at STP contains 1 mole of a given compound or element.

[§] Amedeo Avogadro theorized in 1811 that "equal volumes of all gases at the same temperature and pressure contain the same number of molecules." Today, this is known as Avogadro's Law. Later experiments led to the calculation of the number of molecules in one cubic centimeter of gas: roughly 6.02 x 10²³. This was eponymned "Avogadro's number." One mole of any substance contains Avogadro's number of molecules or atoms.

4.4.3   Calculations for the Determination of CO quantity based on Standard Conditions and Ideal Gas Behavior:

Available equipment, the need for accuracy, convenience and a need to calibrate within a range representative of predicted tissue CO concentrations determined that the Standard Curve was derived on multiples of 50 µL.

Based on the theoretically fixed 22.4 L per mole relationship, the following could be determined:

50 µL CO gas contains 0.050 mL/22,4 mL x 1 mole = **2.2 x 10⁻⁶** moles CO

therefore

50 µL of 4.89 ppm CO contains 2.2 x10⁻⁶/(1/4.89 x 10⁻⁶) = **1.076 x 10⁻¹¹** moles

Equation 6. Determination of CO quantity in the calibration gas based on the molar volume of an ideal gas: 22.4 L/mole @ STP

4.4.4   Correction Factors due to deviations from STP Conditions:

All real gases are imperfect in that they deviate slightly from the behavior of an ideal gas primarily due to two factors: (1) the size of the respective atoms or molecules which affects the minimum compressible volume of the gas and (2) the strength of the attractive forces between atoms or molecules of the gas. In addition there are variations due to differences between actual ambient and STP conditions to consider.

The latter can be accounted for approximately by calculating the proportional effect of changes in absolute pressure and temperature, whereas the Van der Waals equation (see section 4.3.4.2) can be applied to determine to what extent

CO will deviate from ideal gas behavior [f]. The net result can then be accounted for by a single correction factor [Ω].

4.4.4.1 *Deviation due to Temperature & Pressure:*

Deviations in temperature (T) and pressure (P) from STP conditions will affect the number of moles (n) per unit volume of gas (V) in the following way:

$$\mathbf{PV = nRT} \qquad \textit{therefore} \qquad \mathbf{n = PV/RT}$$

Equation 7. Ideal Gas Law. (P) absolute pressure; (V) volume; (T) absolute Temperature; (n) the number of moles of gas; and (R) the universal gas constant: 8.315 $J.mol^{-1}.K^{-1}$. On the right the formula is solved for *n*.

Therefore either a decrease in pressure (P) or an increase in temperature (T) will reduce the number of moles (i.e., any given number of moles will occupy a larger volume, so that any given volume of gas will contain fewer molecules than predicted by the ideal molar volume relationship under standard conditions).

---

[f] Joseph van der Waals received a Nobel prize in 1910 for his studies on liquids and gases, including the derivation of this equation.

[Ω] This relatively complicated calculation is only relevant to the calibration of the analyzer. Once the ratio between CO and GC reactivity has been determined, actual measurement is performed on a dimensionless quantity of CO released into the reaction vial headspace (the volume containing the CO is irrelevant at this point as the calibrated RGA response is based only on the number of molecules in the vial, not on the volume containing them). The entire headspace is measured and the CO contained within it is tied only to the weight of tissue from which it was released; this ultimately allowed the calculation of CO concentration in pmols/mg.

Temperature

The ambient temperature during the experiment was a near-constant 22°C. This represents an absolute temperature of:

$$273.15 + 22 = 295.15 \text{ Kelvin (K)}$$

Equation 8. Determination of absolute temperature in the ambient conditions of the study.

The standard temperature at which the molar volume of gas was determined is 0°C. This represents an absolute temperature of:

$$273.15 + 0 = 273.15 \text{ K}$$

Equation 9. Determination of the absolute temperature at 0°C (i.e., Standard Temperature)

This change in the absolute temperature will result in a proportional volume increase of:

$$295.15 / 273.15 = 1.0805$$

Equation 10. Determination of the relative impact of variance between STP and ambient conditions of measurement on the basis of absolute temperature.

This means that due to the change in temperature, the volume of gas containing 1 mole will increase by 1.0805 or that the number of moles in a volume of 22.4 L will decrease by the inverted factor of:

$$273.15 / 295.15 = \underline{0.9318}$$

Equation 11. Determination of the factor for reduction in molar contents of a given volume of gas at ambient (rather than at STP) conditions on the basis of the difference in temperature.

Pressure:

The ambient pressure during the experiment was a near-constant 754 mmHg. The standard pressure at which the molar volume of gas is determined is 760 mmHg. Accordingly the difference between ambient and STP would represents a proportional volume increase of:

$$760/754 = 1.008$$

Equation 12. Determination of the relative impact of the difference between STP and ambient conditions of measurement on the basis of absolute pressure.

This means that the volume of gas containing 1 mole will increase by 1.008 or that the number of moles within a volume of 22.4 L will decrease by a factor of:

$$754 / 760 = 0.9921$$

Equation 13. Determination of the factor for reduction in molar contents of a volume of gas at ambient (rather than STP) conditions on the basis of pressure.

Thus the correction factor to account for the difference between STP and ambient conditions is:

$$0.9318 \text{ x } 0.9921 = 0.9244$$

Equation 14. Correction factor accounting for difference between Standard Temperature and Pressure and Ambient Temperature and Pressure. It is made up of both temperature and pressure correction factors. Effectively the combined effect results in a 7.6% reduction in molecular content relative to STP conditions.

4.4.4.2   Deviation due to Imperfect Gas Behavior:

The behavior of real gases (i.e., beyond their critical temperature) falls within $\pm$ 5% of the ideal gas law for most temperatures and pressures. However, at extremely low temperatures or very high pressures, real gases deviate significantly from ideal gas behavior. Dutch physicist Johannes van der Waals developed an explanation for these deviations and in 1873 developed an equation that was able to fit the behavior of real gases over a wide range of pressures and temperatures. His equation is as follows:

$$\left[P + \frac{an^2}{V^2} \right] (V - nb) = nRT$$

Equation 15. Van der Waals Equation. This accounts for deviation by real gases from the molar volume relationship of real gases by including the relative gas particle size (a) and the attractive forces between molecules (b) in addition to the factors of absolute pressure (P), volume (V) and absolute temperature (T)

Van der Waals was able to account for the deviation using two gas-specific variables respectively for gas particle size (a) and the attractive force between molecules (b). The respective van der Waals Factors *a* and *b* for a variety of gases are listed in Table 4.

Table 4. The Van der Waals Constants for Various Gases

Compound	a (L^2-atm/mol^2)	b (L/mol)
He	0.03412	0.02370
H_2	0.2444	0.02661
Ar	1.345	0.03219
O_2	1.360	0.03803
N_2	1.390	0.03913
CO	**1.485**	**0.03985**
CH_4	2.253	0.04278
CO_2	3.592	0.04267
NH_3	4.170	0.03707

As can be seen CO has midrange values similar to the inert gas argon and diatomic gases N_2 and O_2 with minimal intermolecular interactions.

Applying the van der Waals equation to CO would result in a correction factor of:

0.9989

Equation 16. Van der Waals correction factor. Using STP conditions while performing the Van der Waals equation for 1 mole of CO gas generates a predicted volume of 22.42 rather than 22.4L. Thus the correction factor is a relative increase in molar volume by a factor of 1.0011 or effectively a reduction in the number of moles contained in 22.4L by a factor of 1/ 1.0011 or 0.9989

4.4.4.3 General Correction Factor

The impact of ambient and intrinsic factors can be summarized in a consolidated correction factor of:

$$0.9244 \ \textbf{x} \ 0.9989 = \textbf{0.9234}$$

Equation 17. Consolidated correction. This consolidated factor is made up of (1) the factor accounting for deviation from STP (Equation 11) and (2) the Van der Waals correction factor to account for deviation from the ideal gas laws to allow calculation the quantity of CO in a sample of calibration gas under ambient conditions (Equation 13.)

Accordingly, 50 µL of 4.89 ppm CO in Nitrogen is estimated to contain:

$$\textbf{1.076 x 10}^{-11} \textbf{ moles CO x 0.9234} = \textit{9.9 x 10}^{-12} \textit{ moles of CO or 9.9 pmol}$$

Equation 18. Correction to CO quantity in 50 µL of calibration gas (4.89 ppm CO in N_2) to account for ambient conditions and deviation from ideal gas behavior.

4.4.5   Standard Curve

The RGA was calibrated prior to each control and experimental session using gas certified by Scott Specialty Gases (Plumsteadville, PA) to contain **4.89 ppm** CO in nitrogen.

Volumes of 50, 150, 250, 350, 450 and 550 µL of calibration gas were added to a 2 mL reaction vial that was purged with CO free nitrogen immediately prior to the addition of the calibration gas (see section 4.3.5.); this produced a standard curve that spanned the anticipated range of CO tissue values.

Table 5 shows the data derived from the calibration sequence prior to one experimental session and Figure 14 is the associated graph. They illustrate the determination of the R-value.

Table 5. Calibration Data.

Volume	pmol CO	Peak Area	Average PA(μV.sec)	Average PA(mV.sec)	R-value
50μL	9.9	467830	474802	475	0.0209
		473828			
		483828			
		473721			
150μL	29.7	1435065	1436351	1436	0.0207
		1422454			
		1443918			
		1443965			
250μL	49.5	2571374	2562589	2563	0.0193
		2580910			
		2570008			
		2528062			
350μL	69.3	3661212	3672300	3672	0.0189
		3705207			
		3664347			
		3658435			
450μL	89.1	4715875	4657091	4657	0.0191
		4444637			
		4761143			
		4706707			
550μL	108.9	5767855	5864519	5865	0.0186
		5955539			
		5804771			
		5929909			
Average R-Value					**0.0192**

Linearity was maintained over the entire range of the calibration. Over a two month trial, using the RGA, the detector or R-values varied by 10% between 0.0208 and 0.0195 pmol/mV.sec [א].

Figure 14. Standard Curve. Data from calibration displayed as a Standard Curve. It shows remarkable linearity, providing confidence in the precision and reliability of the technique.
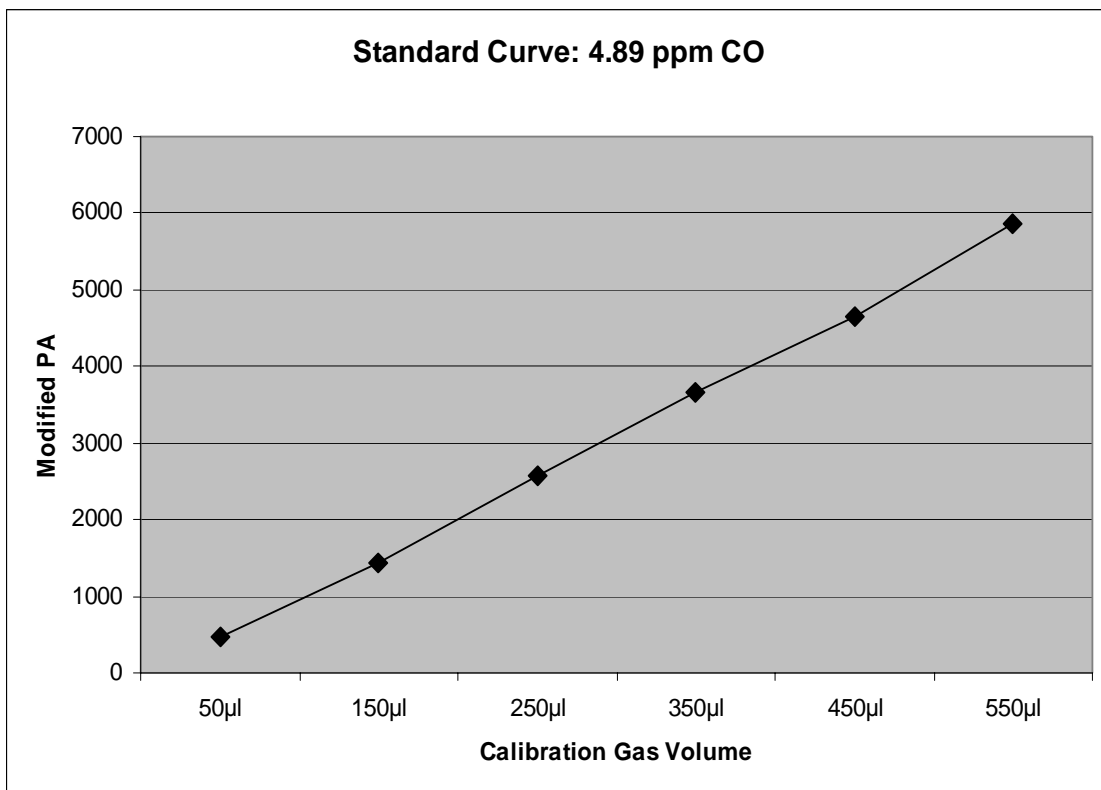
[א] The linearity does not change abruptly upon exceeding a sample amount of 120 pmols. However the R-value tends to gradually decrease. Nevertheless extrapolation is still possible within a 500 pmol per sample range.

4.5 REACTION VIAL PREPARATION

Gas chromatograph (GC) borosilicate reaction vials (2 cc vial; Alltech Associates, IncState College, PA) were prepared as follows:

Prior to use, batches of 80 GC vials were packed in a Test tube rack (VWR Scientific Products; Suwannee, GA). The spikes were sawn off at 2 cm length (as recommended by Vreman) to allow easy handling of the vials – Figure 15.

Figure 15. Reaction vial racks. Shown with pegs sawn off for easier handling of the reaction vials.

The vials were then pre-cleaned using PCC-54 Detergent Concentrate (Pierce Biotechnology Inc. Rockford, IL) – Figure 16. After instillation of the detergent with a spray dispenser, the vials were steamed for 15 minutes at 135 ºC (275 ºF) in a heated frying pan and then rinsed three times with tap water and twice with dd-H_2O.
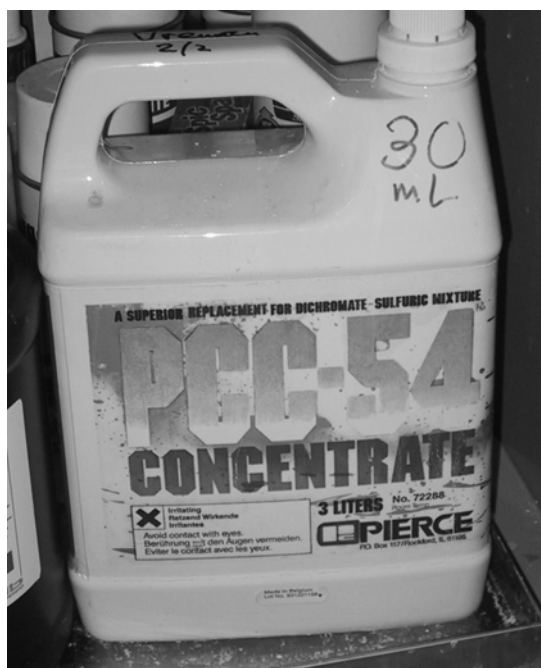
Figure 16. Vial cleaning concentrate: PCC-54.

Using a stainless steel 8 mm (¼ inch) wire mesh to retain the vials in the racks, all excess water was shaken out of the vials following each rinsing and finally the vials were left inverted on a paper towel to air dry.

Once dry, 2 μL of 60% w/v sulfosalicylic acid (SSA) was added to the vials with a 100μL, Hamilton®, gas tight syringe (Hamilton Company; Reno, NV) with a repeating mechanism (see Figure 17.).
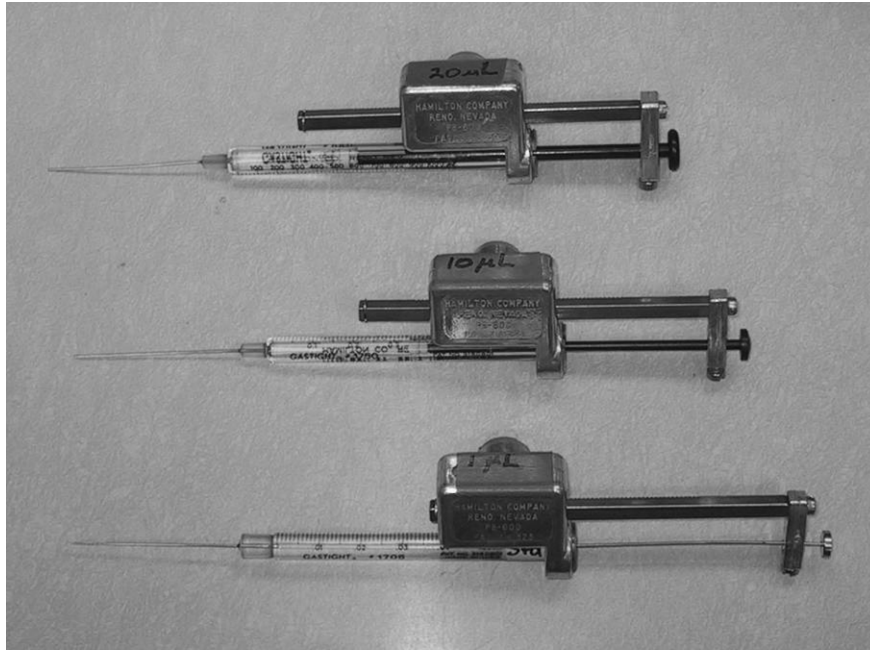
Figure 17. Various size Hamilton® gas-tight syringes with repeating mechanisms. The repeating mechanism discharges a 50th of the syringe volume (all syringe barrels are of the same length but different diameters). Accordingly the top syringe is a 1000 µL syringe that would deliver 20 µL per activation of the mechanism; the middle syringe is a 500 µL delivering 10µL; and the bottom a 50 µL syringe delivering 1 µL per activation.

This was followed by the addition of 20 µL of dd-H_2O via a 1,000 µL Hamilton® syringe with a repeating mechanism. Based on an ultimate vial volume of 62 µL (i.e., 2 µL SSA plus 20 µL dd-H_2O plus 1 to 40 µL of tissue homogenate) this provided a minimum SSA concentration range of 2/23 to 2/62 of 60%, i.e., 1.94 to 5.22% w/v. Vreman has confirmed the appropriateness of these concentrations in providing near-complete release of CO after more than 5 minutes on ice [110]. Also volumes of liquid up to 250µL do not appear to significantly affect release of CO – see Figure 18.

Figure 18. Effect of Reaction Vial Fluid Volume on quantity of released CO
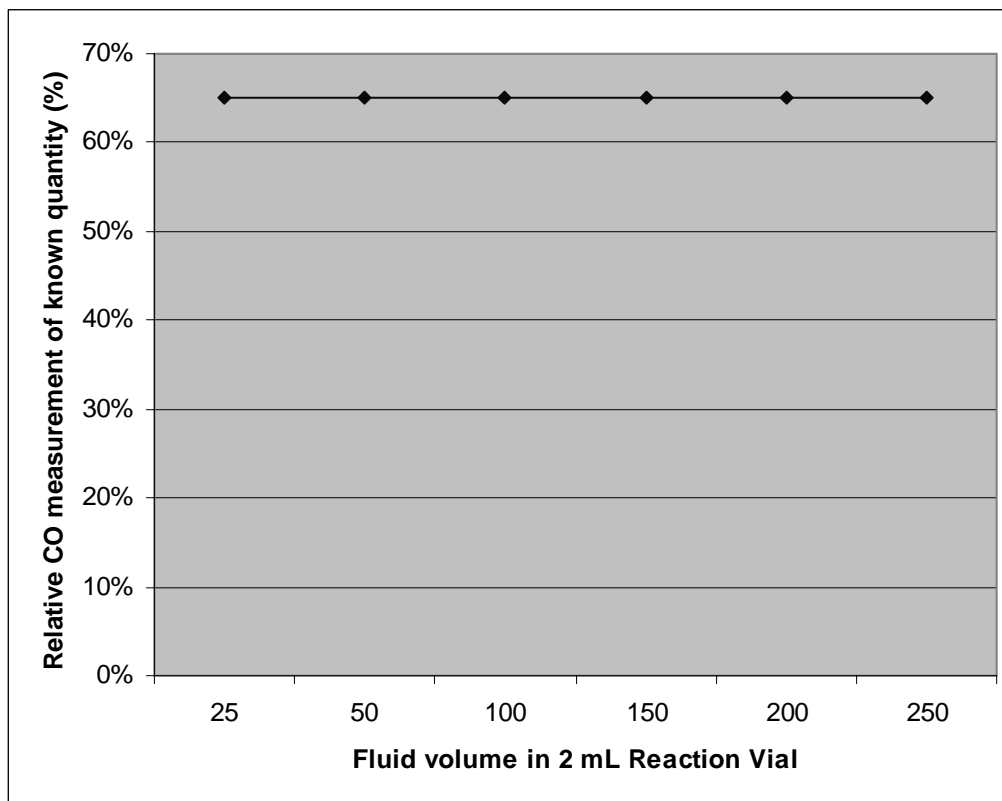
The sealed vials were purged with CO free nitrogen at a flow rate of 300 - 400 mL per minute for 3 seconds (also see section 4.3.5). This was repeated; the second purge being performed just prior to the addition of the tissue homogenate to ensure baseline reaction vial CO levels before releasing the CO from tissue.

4.6 ANIMAL SELECTION, SAMPLE SIZE, EXPOSURE, TISSUE COLLECTION AND PROCESSING

4.6.1 Animal Selection

Sprague Dawley rats were the animal model of choice due to the Duke Laboratory's extensive prior experience with these animals in other, unrelated studies, involving CO exposure [112,138,141,146,173-185]. These animals exhibit predictable uptake of CO and they demonstrate histological damage with these exposures.

Accordingly the laboratory had confidence in the reliability of the model; knew the appropriate exposure duration to achieve a clinically significant but sub-lethal exposure; was familiar with and had resident proficiency in the basic dissection and tissue harvesting techniques; and had housing facilities suitable for these animals.

4.6.2 Sample Size

The study outline and design are summarized in sections 3.3.1. and 3.3.2 as well as table 2:

Thirty three healthy, male Sprague Dawley rats weighing between 240 and 325 g were used for the study. Nine were used as controls (unexposed; baseline).

The remaining 24 provided four sets of measurements (i.e., four animals per time-point) post exposure:

- 4 animals were harvested at time **0** min (i.e., immediately after exposure)
- 4 animals were harvested at time **30** min post exposure
- 4 animals were harvested at time **60** min post exposure
- 4 animals were harvested at time **90** min post exposure
- 4 animals were harvested at time **120** min post exposure
- 4 animals were harvested at time **150** min post exposure

This allowed determination of a standard deviation for tissue CO values from the moment of ending the exposure until 150 minutes after the exposure with the animals breathing regular compressed air. The latter permitted mathematical and statistical correlation between blood and tissue CO values.

4.6.3 Animal Exposure

Nine male animals were used as controls without CO exposure to provide reliable baseline tissue CO values. Twenty-four animals were exposed in batches of six at a time to 2500 ppm (0.25%) CO in air for a total of 45 minutes. The exposures were performed by housing the rats in 10 by 35 cm (2 L internal volume) empty, Plexiglas CO_2 absorbent canisters (Fig. 19). The gas supply containing 2500 ppm CO in air was continuously vented through each of the six Plexiglas containers at a rate of 5-7 liters per minute for a total of 45 minutes (Fig. 19).
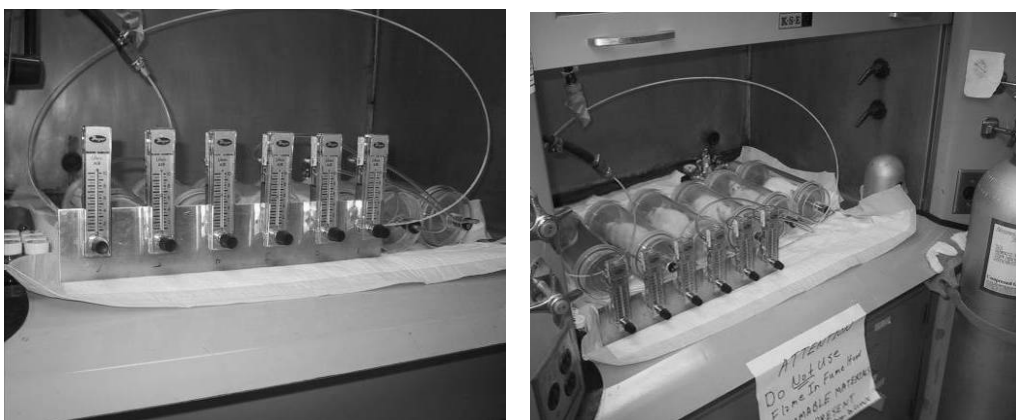
Figure 19. Animal Exposure Setup. Gas supply to six Plexiglas containers vented with 5-7 L.p.m. 2500 ppm CO in air within a fume hood.

The flow of gas was sufficient to exchange the internal canister volume more than three times per minute. Doing so ensured homogenous CO levels throughout the canister; removed any exhaled CO_2; but avoided any pressurization of the container (which would have increased the inspired pressure of CO). From previous experience this has been shown to be a sub-lethal exposure associated with cognitive deficits and histological damage – thus clinically relevant [146]. In this study, these exposures consistently achieved COHb levels between 66 and 72%.

Immediately upon termination of the exposure, the first animal of each experimental session was removed and euthanized with Halothane (Figure 20). This procedure lasted less than 1 minute. Although it is known that dihalomethanes (including Halothane) are metabolized to CO [186,187], the duration of exposure for euthanasia was less than 60 seconds and comparison to control animals asphyxiated with nitrogen did not show any variation in base-line tissue CO levels. However, the ultimate choice of Halothane was based, not only on the directive (i.e., the experimental protocol approved) by the Institute for Animal Care and Use Committee at Duke University, but also because of the need to reduce the delay post exposure to a minimum.

Figure 20. Euthanasia jar saturated with Halothane®

Decapitation was an option and has been used by Vreman *et al*, but this would have denied us the opportunity to irrigate the brain and other tissues.

The first animal served as a control for the exposure and provided the 'zero' point for the subsequent spontaneous elimination of CO during air breathing. The supply gas was changed from 2500 ppm CO in air to regular compressed air (i.e., a residual of 6-20 ppm CO), and the animals were sequentially removed from this air breathing environment at 30 minute intervals (i.e., 0; 30; 60; 90; 120; and 150 min) and sacrificed.

4.6.4 Tissue Harvesting

The dissection and tissue harvesting area was prepared in advance (see Figure 21).
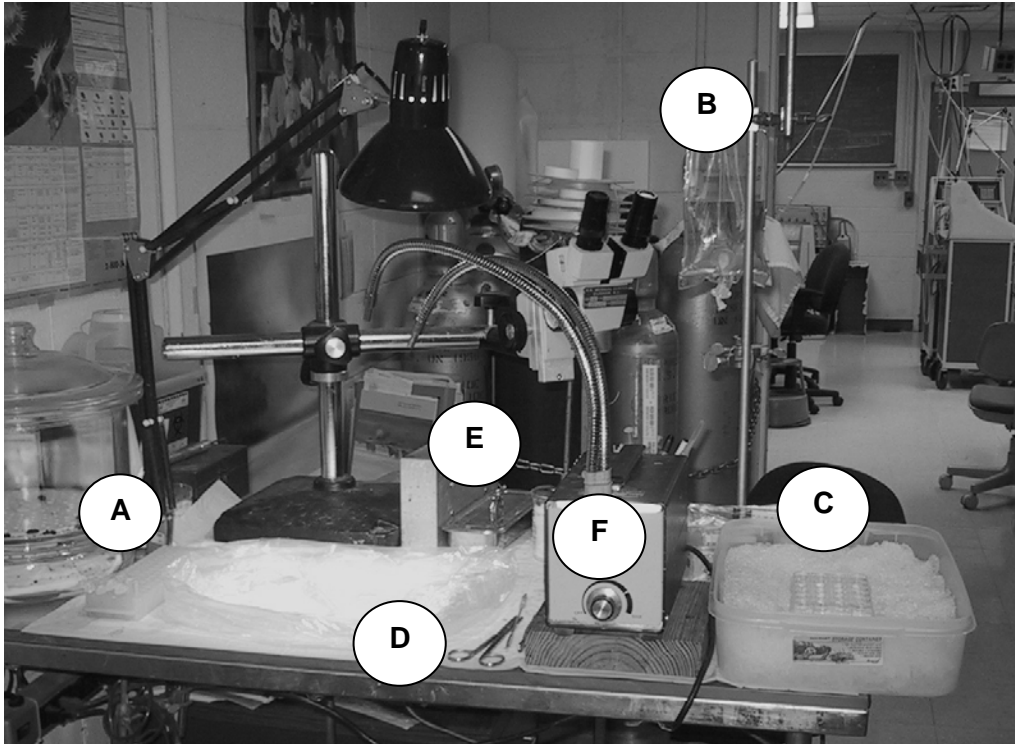
Figure 21. Prepared dissection and tissue harvesting area. In the graphic illustration are the micro centrifuge tubes for RGA analysis of blood (A); normal saline for irrigation (B); prepared tissue wells on ice filled with dd-H$_2$O for collection of tissue samples (C); instruments for dissection, irrigation and harvesting of tissue (D); blood gas syringes in a container for CO-Oximeter analysis (E); and a dissection light (F).

Immediately following Halothane euthanasia, the animals were weighed and then dissected: The specific dissection technique, developed by the author together with Craig Marshall, BSc, was as follows:

Using straight surgical scissors, the peritoneal cavity was opened and the anterior attachments of the diaphragm were resected to expose the thoracic cavity (Figure 22).

Figure 22. Rat dissection: Opening of the peritoneal cavity and resection of the diaphragm

A blood sample was taken from the inferior vena cava with a heparinized 2 mL syringe for CO-Oximetry and RGA (Figure 23).

Figure 23. Withdrawal of blood from the inferior vena cava by means of a 2 mL, heparinized syringe analysis by CO-oximetry and RGA.

To remove blood and specifically COHb from the tissues, the animals were perfused with 60 mL 0.9% saline. Vascular access was obtained by puncturing the left ventricle with a large bore hypodermic needle (Figure 24).
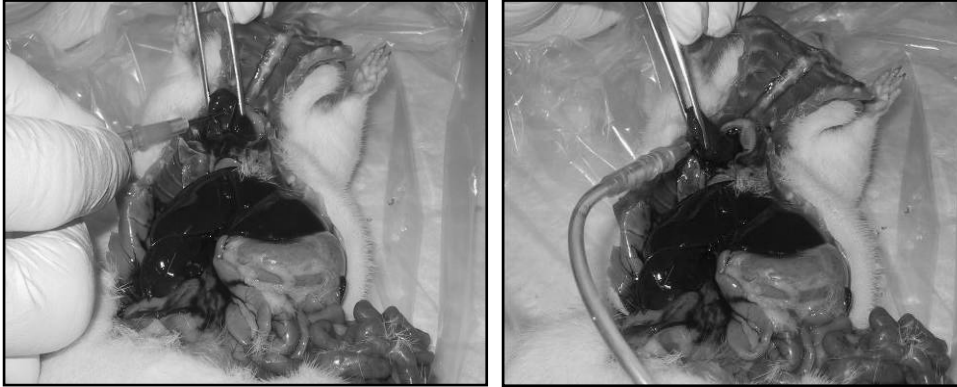
Figure 24. Puncturing of the left ventricle with a hypodermic needle in preparation for tissue irrigation (left). Securing the needle in the left ventricle (right).

The pulmonary artery was then transected with scissors to permit egress of blood and fluid during irrigation while perfusing all tissue beds except the lung (Figure 25).
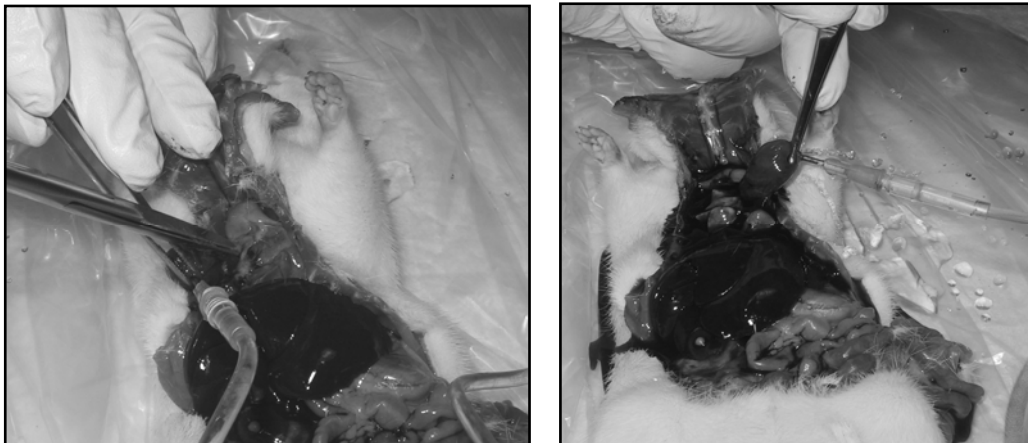
Figure 25. Transecting of the pulmonary artery (left). Irrigation of the circulation with 60 mL of normal saline to eliminate COHb by purging blood from the circulatory system.

This technique proved to be very effective and was able to remove >95% Hb in the brain and other organs. Upon completing irrigation, the heart was resected. The cranial cavity was then opened (see Figure 26) by decapitating the animals and cleaving the *calvarium*.
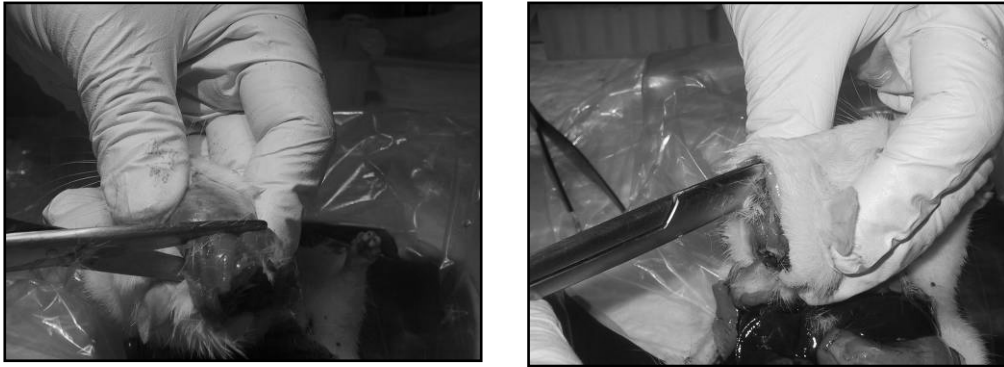
Figure 26. Opening of the calvarium prior to removal of the brain

This allowed atraumatic removal of the entire brain. Finally, the skin overlying the left *pectoralis* major muscle was resected and a mid-section of the muscle removed.

CO-Oximetry was performed within 10 minutes using an IL Model 482 CO-Oximeter (Instrumentation Laboratory; Lexington, MA) – Figure 27.

Figure 27. IL-482 CO-Oximeter

The analysis was repeated on every sample and the device was specifically calibrated for rat blood (see Appendix D-5) ♠.

Where variations in excess of 0.5% COHb were detected between measurements, a third measurement was performed; the average value of the two that were closest was then recorded.

♠ The absorbancy coefficients for COHb, HbO2 and Met-Hb differ in rat vs. human blood. Specific details and information on calibration are provided in Appendix D-5.

4.6.5 Tissue Processing

The brain, heart and muscle tissue was immediately immersed in separate saline-filled compartments of a 24 Well Cell Culture Cluster #3524 with flat bottom and lid (Corning Incorporated; Corning, NY) and cooled on a bed of crushed ice (see Figure 28).
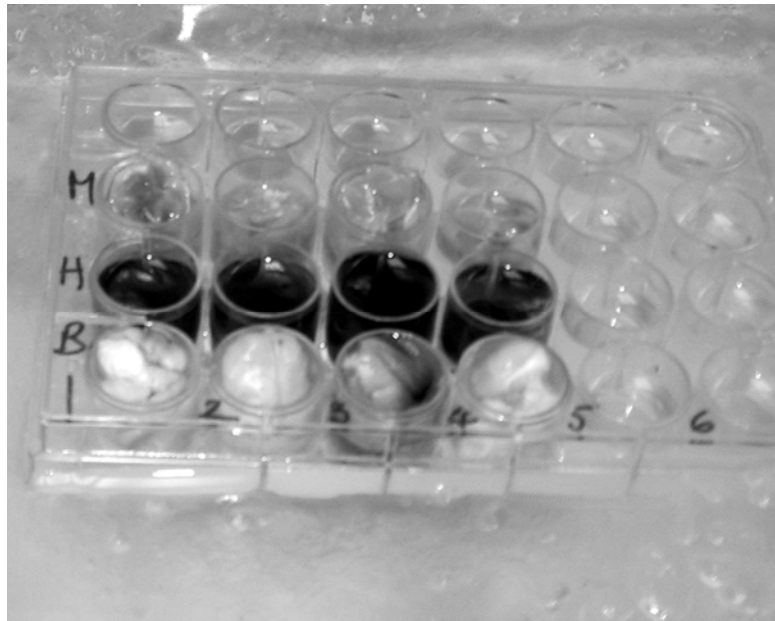
Figure 28. Cell Culture Cluster (24-Well). Shown here are tissue samples of the first 4 Control Animals showing muscle tissue (M); heart tissue (H); and brain (B)suspended in dd-H2O on a bed of crushed ice.

Between 0.060 and 0.12 g of tissue, and 0.001 g (1 mg ≈ 1 µL) in the case of blood, were added to a 2 mL Microcentrifuge tube (Fisherbrand®; Fisher Scientific; Pittsburg, PA).

The density of water is 1 kg / L (i.e., 1 g per mL). As a frame of reference and to simplify understanding of the various volume (weight) additions used in preparing the standardized 10% (tissue) and 0.5% (blood) w/w solutions (homogenates) the following table provides the volume to weight equivalence – Table 6:

Table 6. Weight to Volume Relationships for Tissue Homogenate based on an average density of 1 L/kg.

Volume	Weight
1 L	1,000 g
100 mL	100 g
1 mL	1 g
1 μL	1 mg

Distilled de-ionized water (dd-H_2O) was added according to weight using Pipetman P-20 and P-1000 pipets (Rainin Instrument Company, Woburn, MA) and a 500 μL Hamilton Syringe ® (Hamilton Company; Reno, NV) with a repeating mechanism (i.e., 10 μL – equivalent to 10 mg – added per activation); and a Mettler Balance (Model AE100; Mettler-Toledo, Inc.; Columbus, OH) to produce the desired 10% w/w tissue suspensions of heart, muscle and brain tissue and a 0.5% w/w suspension of blood. These dilutions were chosen on two principles: (1) to ensure that the tissue would not be too viscous for the Hamilton® syringes (Hamilton Company; Reno, NV) used to add homogenate to the RGA reaction vials; and (2) to reduce the amount of CO in the homogenate and blood to values that would fall within the linearity of the RGD upon addition of 1 to 40 μL of suspension to the reaction vials).

The tissue preparation area and components is shown in Figure 29.

Figure 29. Tissue Processing Area. Seen here are the various instruments and devices used in initial preparation of the 10% w/w tissue solution and 0.5% w/w blood solution prior to homogenization (sonication): The recording sheet (A); the dissection instruments (B); the micro centrifuge tubes (C); the Hamilton Syringe for the addition of 10 µL quantities of water to ensure accuracy (D); the Mettler Balance with a measuring cup and micro centrifuge tube in place set to zero before the addition of tissue (E); and a beaker of dd-H_2O (F).

To improve consistency, tissue sampling was performed at the same anatomical areas each time: the frontal lobes, left ventricle and midsection of the pectoralis major muscle. Heart and skeletal muscle tissue was diced with scissors to facilitate subsequent homogenization.

Homogenization was achieved by means of a Branson-Sonifier (Model 450; Branson Ultrasonics; Danbury, CT) – Figure 30.

Figure 30. Branson Sonifier.

The tubes with tissue suspensions were stored in crushed ice prior to, and during, sonication to prevent heating. Sonication was performed at a setting of 50% duty cycle, and an intensity of #4 (i.e., 40%) [ℜ]. The suspended tissue was sonicated for 1 minute. These intensity settings were selected to ensure complete homogenization without increasing the temperature of the sonicate. The duration was based on the finding that tissue CO levels increased between 30 and 90 seconds after which they dropped off (Figure 31).

Figure 31. The effect of homogenization time on tissue CO values.
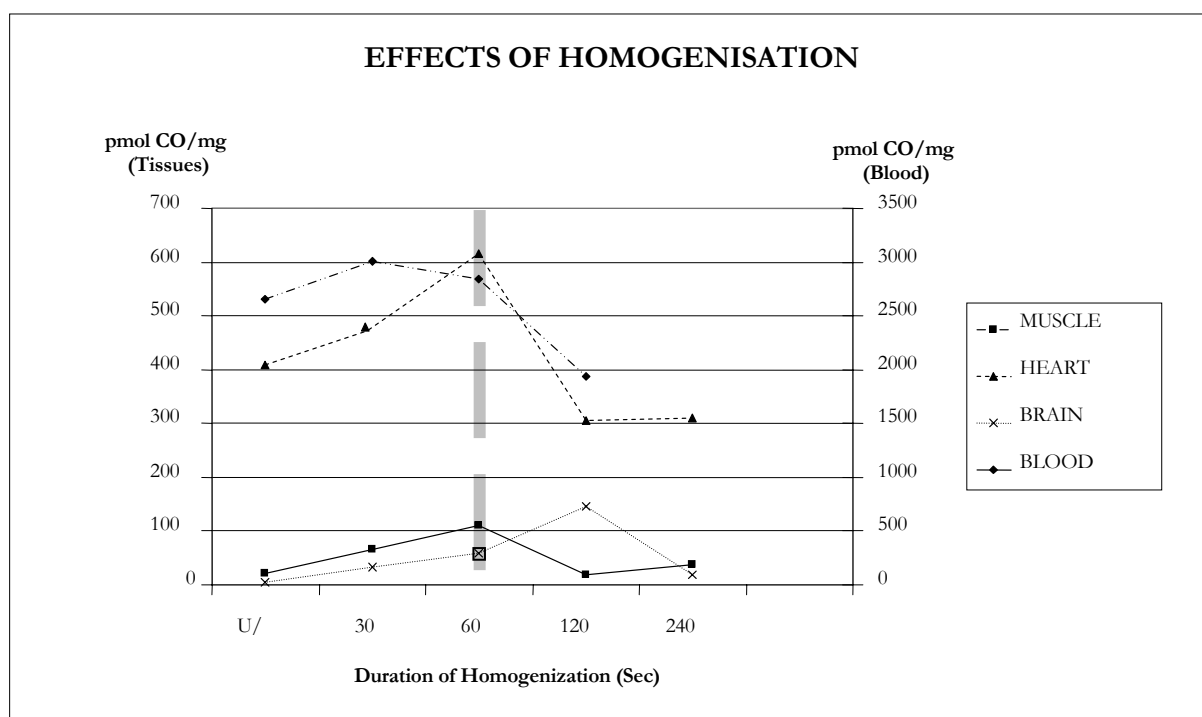
Peak or near-peak levels were consistently found in all tissues at 60 seconds with these sonicator settings. Immediately after sonication the Microcentrifuge tubes were closed and spun in a Microcentrifuge for less than 20 seconds at 1000 RPM to ensure complete admixture of all liquid and tissue homogenate. The tubes

---

[ℜ] In the technique described by Vreman *et al* [150], the sonication was performed for ≤ 15 seconds using a small Microson ultrasonic cell disruptor (Misonix, Farmingdale, NY). However, in our laboratory – specifically when monitoring the temperature in the microcentrifuge tube using different settings – it was found that when using the larger Branson-Sonifier (*Model 450; Branson Ultrasonics; CT*) on a 50% duty cycle at #4 (i.e., 40%) intensity setting, this yielded both the most reliable results, minimal increase in temperature and no spillage of homogenate due to the sonication process.

were left closed and the sonicate was stored on ice in preparation for RGA analysis. The time between harvesting and RGA analysis was between 20 min and 3 hours for all tissue samples with an average of 40 minutes. No significant changes were observed when determining CO levels in the same tissues after storage on ice for periods of up to 6 hours.

4.6.6 Tissue Homogenate and Measurement

Prior to withdrawing sonicate, the Microcentrifuge tubes were gently inverted several times to ensure that no tissue-fluid separation had occurred during the delay to measurement or due to the short Microcentrifugation.

Depending on the anticipated amount of CO in the tissue, between 1 and 40 μL of tissue homogenate was added to the prepared vials using a 50, 100 or 1000 μL Hamilton® repeating syringe, as needed. Upon injecting the homogenate into the reaction vials, they were shaken thoroughly to ensure contact between the SSA and the tissue sample. The vials were then returned to the bed of crushed ice for a minimum of 5 minutes (actual range: 15 to 120 minutes) to allow protein denaturation to occur and CO to be released from heme compounds into the headspace of the vial. Vreman has subsequently shown that periods in excess of 5 minutes are indeed adequate for CO release from tissues at 0° and that this release is complete when using more than 1% SSA[110]. The SSA concentration in this study ranged from *2 μL of 60% SSA in 22 μL homogenate* to *2 μL of 60% SSA in 62 μL homogenate*, i.e., 1.94 to 5.45% w/v . Accordingly, these parameters of the study are validated.

Gas analysis was performed by attaching the reaction vial to a double needle assembly connected to the sample valve. As described in section 4.3.3., a cyclical programmed event sequence actuated the valve at 107 second detection intervals for 20 seconds during which time approximately 10 mL of carrier gas was diverted through the reaction vial headspace to transfer the CO in the headspace towards the detector.

Six reaction vials with only SSA and dd-H_2O (i.e., blanks) were prepared simultaneously with those in which homogenate was dispensed. Three blanks were analyzed prior to the tissue samples and three at the end of the batch. The objective was to record and correct for any spontaneous CO generation by the silicon septa as described by Vreman *et al* [1]. The difference between the average CO content in the first and second series of blanks was subtracted from all tissue CO measurements. The three separate analyses were performed for each tissue sample and time point, and the average was used to determine the amount of CO in tissue (see section 4.7.1.).

A total of 78 individual analyses were performed for each subset of 6 animals: 3 pre-analysis baseline; 12 per animal (3 brain; 3 heart; 3 muscle; 3 blood); and 3 post-analysis baseline. Each measurement took 107 seconds and the measurements were run sequentially. A total of 432 individual measurements were made. The RGA measurements alone – if added up – involved more than 12 hours of continuous measurements.

CHAPTER 5. RESULTS

5.1 COLLECTION OF DATA

Each *experimental session* involved exposing, processing and measuring the tissue samples and blood of six animals. Each session generated batches of 6 blanks (three before and three after all samples to provide a baseline) plus 3 vials for each of the 4 tissue types (brain, heart, muscle and blood) and for each of the 6 exposed animals (i.e., 72 sample vials); thus 78 vials for each of the four experimental sessions: a total of 312 vials from all experimental sessions. In one animal – A 6 – the tissues that were inadequately irrigated and retained significant quantities of COHb. As a result the tissue measurements were discarded. The tissues of the latter were used to determine the effects of homogenization illustrated in Figure 31.

Each *control session* involved measuring baseline levels of a number of control animals. There were two control sessions with four and five animals respectively. Each animal required 3 reaction vials for each of the four tissue types (brain, heart, muscle and blood) and 6 blanks so that the total number of measured vials was 120 for all the control sessions.

A total of 432 individual reaction vial measurements were made. At varying intervals during measurements tissue samples were measured twice without removing them from the needle assembly. This was done to confirm complete removal of CO from the sample and to confirm that the baseline measurements fell within an acceptable range. This method confirmed both the 99% complete removal of CO from the samples as well as stability of the RGA throughout the experimental and control sessions.

Each individual measurement generated a printed report which recorded the date and time of the measurement; the retention time; chromatogram; integrated area under the curve; and parts per billion CO as determined by multiplying the integrated peak area under the curve with the 'R' value derived from the calibration process. Integration was performed by an integrating recorder built into the RGA 5 assembly, as determined by the respective predefined "peak

detect", "sense" , "bunch" and "force base" settings (see section 3.6 on Terminology).

As recommended by Vreman [188], CO peak area measurements were rounded from μV.sec to mV.sec. This did not affect precision or sensitivity appreciably, and was applied to the calibration data and subsequently to all sample measurements.

Three measurements were made of every tissue sample and a mean value was determined. The latter was used for the purposes of determining tissue [CO]. Where there was a discrepancy of more than 10% between one sample and the other two, that sample was omitted from calculation of the mean. Where all three samples were dissimilar, the measurement was repeated with three fresh samples. The latter only happened twice in 432 measurements. All values were entered into an MS Excel Spreadsheet, developed by the author and included in the resource CD (Appendix D). It contained the following:

- A calculator to determine the 'R' or detector value (see Table 7). After confirming linearity in response to CO content (i.e., for the range of calibration gas additions of 50 to 450 μL of the certified 4.89 ppm CO in nitrogen to the reaction vial) the 150 μL (29.1 pmol CO) calibration – which was consistently the most reliable – was used to determine the average "R" value: The calculator divided the molar amount in the reaction vial by the determined peak area (PA) to determine the detector value (R) in *pmol per mV.sec*. This value was then be used for that particular experimental session.

Table 7. R-value Calculator

CO	54.58	PA	2639	R	0.0207

- Blank CO calculator: By entering data from the 3 blank vials (labeled 1 A, B and C) prior to and another 3 blank vials (labeled 2 A, B, and C)

following each experimental session a Mean Blank value would be calculated, i.e., [(1A+1B+1C)/3+(2A+2B+2C)/3]/2 – see Table 8.

Table 8. Mean Blank CO Calculator

BLANK 1A	10	BLANK1B	14	BLANK1 C	16	MEAN BLANK1	13	MEAN BLANK	36.83	
BLANK2 A	67	BLANK2B	57	BLANK2 C	57	MEAN BLANK2	60	MEAN C0		1

- The Mean Blank Peak Area value was determined by averaging the 6 blank reaction vials (three before and three after all sample measurements). This value was subsequently deducted from the average Mean Peak Area from each tissue type to account for baseline CO in the "CO-free" carrier gas; baseline drift of the detector during the experiment; and spontaneous CO production by the silicon septa. The pmol amount of CO was also calculated to ensure this value did not exceed the acceptable 1-5 pmol range.

The data from the respective control and experimental sessions were also entered onto the spreadsheet – see Table 9.

Table 9. Data collected on each control (top) and experimental animal (bottom) during the experiment. Not visible here is (1) the information on the weight of tissue sample and combined solution and (2) the complete CO-oximetry information contained in the cell with the COHb value.

ANALYSIS SPREADSHEET

WEIGHT	LABEL	R	V Sample	Sample 1	Sample 2	Sample 3	Mean	R	Mean Blank	CO-pmol	CO-pmol/mg
274	C1-B	0.0208	40	5279	4684	4473	4812	0.0208	37	99	24.83
	C1-H	MEAN BLANK	40	5247	4917	4936	5033	0.0208	37	104	25.98
	C1-M	36.500	40	132	152	144	143	0.0208	37	2	0.55
	C1-BG	CO-Hb	2	353	274	280	302	0.0208	37	6	276.47
	C1-BC	1.000									

WEIGHT	LABEL	R	V Sample	Sample 1	Sample 2	Sample 3	Mean	R	Mean Blank	CO-pmol	CO-pmol/mg
290	A1-B	0.0194	20	138	152	120	137	0.0194	16	2	1.17
TIME OFF CO	A1-H	MEAN BLANK	10	2354	2268	2300	2307	0.0194	16	44	44.46
0	A1-M	15.670	40	1719	1582	1626	1642	0.0194	16	32	7.89
	A1-BG	CO-Hb	10	12349	10161	9696	10735	0.0194	16	208	2079.61
	A1-BC	40.700									

The following information was specifically captured for each experimental and control animal:

- The weight of the experimental animal: *Weight*

- The time from ending the exposure until the animal was sacrificed in 30 minute increments (experimental sessions only): *Time Off CO* (range: 0 to 150 minutes)

- The tissue label assignment: [א]

  - *Session Assignment*: "A" for air recovery or "C" for controls

  - *Sequential Number Assignment*: 1 to 9 (Control Animals) or 1-24 (Experimental Animals)

  - *Tissue Type Assignment*: "B" – brain tissue; "H" – heart ; "M" – muscle; "BG" – blood by Gas Chromatograph (RGA); "BC" – blood analysis by CO-oximetry.

- The R-value for that particular control or experimental session: *R*

- The average Mean Peak Area for the six blank reaction vials as described above: *Mean Blank*

- The amount of COHb as determined by CO-oximetry using the IL-482 pre-calibrated for Rat blood : *COHb* [φ]

- The volume of homogenate in µL that was added to the reaction vial based on estimated CO content to remain close to the standard curve range: *V sample*

- The Peak Area (PA) values for the three measurements: *Samples 1,2 and 3,* rounded to mV.sec as described above (i.e., the Modified PA or MPA).

- The Average MPA Value for the three Samples: i.e., [(Sample1+Sample2+Sample3)/3]: *Mean*

[א] The complete information on the amount of tissue and weight of dd-H_2O and tissue making up a 10% w/w homogenate (tissue suspension) and 1% homogenate (blood) was embedded in the tissue label assignment spreadsheet cells for record purposes. As these did not directly impact the experiment, this simplified the data presentation. However they are provided in the complete data tabulation in Appendix B.

[φ] The complete CO-Oximetry analysis was recorded as an embedded comment in the spreadsheet. This provided date-time stamping for each experiment and provided the Hb concentration to be used in subsequent calculations of predicted blood CO content for purposes of comparing blood and tissue [CO].

- The R-value again for the purposes of calculation of the mean CO concentration in the reaction vial: *R*

- The average Mean Peak Area value for the 6 blank Reaction Vial measurements – 3 before and 3 after the experimental or control session: *Mean Blank Value*

- The CO pmol value calculated by multiplying the *Mean* Peak Area for each tissue with the *R*-value

- CO tissue concentration as determined by dividing the RGA determined CO concentration of the sample with the diluent factor of the homogenate: *pmol/mg*

5.2 DATA SUMMARY

The consolidated data is listed in Table 10.

Table 10. Data List from Experimental and Control sessions. From left to right it shows the experimental and control animal assignments; the Experimental and Control Session Number; Animal number; time off CO (experimental sessions only); CO in respective tissues in pmol/mg; Blood CO Content as predicted by the COHb values; COHb values; Hb concentration in g/dL; and Weight of the animals

Session	Animal	Time (min)	Brain pmol/mg	Heart pmol/mg	Muscle pmol/mg	Pred. CO pmol/mg	COHb % of Hb	[Hb] g/dL	Weight g
					EXPERIMENTAL SESSION DATA				
1	A1		9	150	13	6787	71	15.40	295
2	A7	0	12	118	25	5979	69.3	13.90	323
3	A13		14	338	17	6292	72.4	14.00	308
4	A19		9	92	13	6498	72.2	14.50	271
Averages			*11*	*175*	*17*	*6389*	*71.2*	*14.45*	*299*
1	A2		8	14	4	2341	26.2	14.40	273
2	A8	30	15	94	14	3023	33.6	14.50	343
3	A14		8	179	14	2636	29.1	14.60	302
4	A20		18	141	17	2801	29.5	15.30	281
Averages			*12*	*107*	*12*	*2700*	*29.6*	*14.70*	*300*
1	A3		2	6	5	1387	16.2	13.80	307
2	A9	60	7	26	3	1416	16.3	14.00	350
3	A15		6	113	6	1665	18.5	14.50	294
4	A21		17	105	26	1620	17.4	15.00	292
Averages			*8*	*62*	*10*	*1522*	*17.1*	*14.33*	*311*
1	A4		2	14	4	1283	13.0	15.90	276
2	A10	90	18	94	28	1006	11.1	14.60	330
3	A16		18	91	4	1199	14.1	13.70	294
4	A22		4	54	31	1160	12.3	15.20	281
Averages			*11*	*63*	*17*	*1162*	*12.6*	*14.85*	*295*
1	A5		3	26	8	744	8.5	14.10	319
2	A11	120	9	91	2	565	6.6	13.80	339
3	A17		14	70	26	652	7.4	14.20	314
4	A23		31	28	18	642	7.5	13.80	274
Averages			*14*	*54*	*14*	*651*	*7.5*	*14*	*312*
1	A6		N/a	N/a	N/a	N/a	N/a	N/a	N/a
2	A12	150	24	21	6	417	4.8	14.00	347
3	A18		43	65	15	298	3.5	13.70	310
4	A24		12	9	39	373	4.2	14.30	283
Averages			*26*	*32*	*20*	*363*	*4.2*	*14.00*	*313*

Session	Animal	Brain pmol/mg	Heart pmol/mg	Muscle pmol/mg	Pred. CO pmol/mg	COHb % of Hb	[Hb] g/dL	Weight g
				CONTROL SESSION DATA				
1	C1	25	26	1	92	1.0	14.90	274
	C2	12	34	6	81	0.9	14.80	275
	C3	27	81	2	80	0.9	14.40	279
	C4	8	89	1	112	1.2	15.10	279
2	C5	24	26	4	77	0.8	15.50	274
	C6	2	40	9	95	1.0	15.30	282
	C7	3	50	19	45	0.5	14.60	*286*
	C8	3	60	26	35	0.4	14.10	286
	C9	3	25	6	27	0.3	14.50	298
Averages		*12*	*48*	*8*	*72*	*0.8*	*14.80*	*281*

5.3   CO-OXIMETRY DERIVED BLOOD CO CONTENT

The objective of the study was to measure and compare COHb to tissue [CO] over time following acute exposure. However, to ensure that the study would not be criticized for comparing unrelated units of measure, actual blood CO content was calculated from the COHb value as described in section 1.3.3. and Appendix D. This provided an equivalent measure of blood CO in pmol/mg for blood.

Although RGA was also used to measure blood CO, the blood homogenate dilution of 1% w/w was ultimately found to be too low. Even though the quantity of homogenate introduced into the reaction vial could be adjusted to compensate for the changing quantities of CO, the dilution factor itself introduced a possibility of random errors. Values remained proportional to the CO values calculated from CO-oximetry, but it was deemed more appropriate to use the latter as this was the parameter of interest for blood used in the hypothesis.

As a matter of reference, measured RGA values for blood differed from predicted blood CO content by an average factor of 4.47 – refer to Appendix B. This was maintained consistently throughout in spite of the high dilution factor. Table 11 shows the result after applying this correction factor to the RGA blood value; this demonstrates the close correlation between RGA and CO-oximetry determined CO values. Importantly, this study and its hypothesis is based on the relation between blood and tissue CO values. Therefore, although this finding may challenge quantitative aspects (accuracy) of the RGA measurements, it provides confirmation on the reliability (precision) of the technique and adds confidence that the relational analyses are correct. Specific recommendations are listed in Chapter 6 on how to address this discrepancy in future quantitative studies.

CO-oximetry is reported to be unreliable for values lower than 2.5% [21,22,107]. This is supported by the finding that the RGA-derived blood CO values showed much greater variability in the control animals where the COHb values were low.

However the COHb values in the exposed animals never dropped below the 2.5% threshold; the lowest value was 3.5% COHb. Thus here the relationship between blood RGA and CO-oximetry was close, supporting the use and reliability of CO-oximetry in the exposed animals where the COHb values were high. Therefore, as stated in the hypothesis, the relationship between COHb-derived blood CO values (i.e., so-called predicted CO values) and RGA tissue values could be used with confidence in the analysis.

The large discrepancy in the control animals is likely to be the result of a variable underestimation of CO by CO-oximetry in the 0.4 to 2% COHb range (Table 11). Importantly, if this study were to be replicated in a physiological model, the use of CO-oximetry would not be appropriate and RGA would have to be used for blood and tissue.

Table 11. Comparison of RGA vs. CO-oximetry blood CO values. Blood (M) values have been adjusted by a factor of 4.47 from measured values (as described above). The relationship was close where COHb values were high, but very poor where these were low. This supports the reported unreliability of CO-Hb measurement when values are ≤ 2.5% but is consistent with reliability when COHb values are high.

Session	Animal	Time	Blood (M)	Pred. CO	% Predicted
1	A1		6503	6787	104
2	A7	0	8048	5979	135
3	A13		5543	6292	88
4	A19		6025	6498	93
Averages			*6530*	*6389*	*105*
1	A2		2518	2341	108
2	A8	30	2837	3023	94
3	A14		2365	2636	90
4	A20		2841	2801	101
Averages			*2640*	*2700*	*98*
1	A3		1110	1387	80
2	A9	60	1425	1416	101
3	A15		1710	1665	103
4	A21		1987	1620	123
Averages			*1558*	*1522*	*101*
1	A4		973	1283	76
2	A10	90	904	1006	90
3	A16		1148	1199	96
4	A22		1248	1160	108
Averages			*1068*	*1162*	*92*
1	A5		267	744	36
2	A11	120	523	565	93
3	A17		1127	652	173
4	A23		715	642	111
Averages			*658*	*651*	*103*
1	A6		N/a	N/a	N/a
2	A12	150	351	417	84
3	A18		553	298	185
4	A24		355	373	95
Averages			*419*	*363*	*122*

Session	Animal	Blood (M)	Pred. CO	% Predicted
1	C1	276	92	301
	C2	195	81	241
	C3	162	80	202
	C4	260	112	232
2	C5	224	77	291
	C6	181	95	191
	C7	208	45	462
	C8	173	35	494
	C9	170	27	631
Averages		*183*	*51*	*444*

5.4 COMPARISON OF BLOOD TO TISSUE CO VALUES

Binding of CO to heme moieties in the presence of oxygen is described by the Warburg hypothesis and partition coefficients [189]. These predict that as pO_2 in tissue is increased the amount of CO binding to various heme proteins will be proportionally reduced and therefore the total amount of tissue CO may be expected to decline also.

To follow the Warburg hypothesis, tissue CO would be expected to rise with exposure to CO due to a combination of increased CO content in the blood and a concomitant reduction in tissue oxygen delivery; the latter being due to (1) the reduction in oxyhemoglobin and (2) a leftward shift of the oxyhemoglobin dissociation curve. Upon recovery (i.e., termination of CO exposure), a reduction in inspired pCO would favor a gradual elimination of CO in the presence of normalizing pO2 values. It is therefore somewhat surprising that for brain and muscle tissue in particular these predicted changes were not observed:

Firstly, when comparing the blood and tissue CO values of the control animals to those immediately following CO exposure, only the blood and heart CO values were statistically different (i.e., elevated) as determined by Mann-Whitney U-test [♣] (Table 12.).

Table 12. Comparison of control vs. exposed animal (at time = 0) blood and tissue CO values using Mann-Whitney U-Test

Compartment	Two-tailed p-value
Blood	0.007
Brain	0.59
Heart	0.007
Muscle	0.10

[♣] The Mann-Whitney U-test, a non parametric test, was chosen due to the small sample size.

This suggests that only blood and heart tissue absorbed significant amounts of CO during the exposure period.

Secondly, when comparing regression lines for blood vs. tissue CO over time, the respective tissue CO slopes were significantly different to that of blood (Table 13). Even heart tissue, which followed the decreasing COHb trend more closely, remained statistically different. The conclusion is therefore that the change in COHb (i.e., the change in blood [CO]) is statistically different from changes in tissue [CO] and H_o should be rejected in favor of H_1.

Table 13. Comparison: Slopes of Regression Lines for Blood and Tissue, $\log_e(CO)$ vs. time

Tissue	N	Slope ($\log_e$ scale)	Comparison of slopes: Tissue vs. Blood
Blood	23	-0.018	N/A
Brain	23	0.003	$P < 0.0001$
Heart	23	-0.01	$p < 0.049$
Muscle	23	-0.001	$P < 0.0001$

The slope (rate of change or change over time) for blood CO was -0.018 whereas for brain tissue it was slightly positive at 0.003; heart tissue was -0.01; and muscle tissue was -0.001. This suggests that as COHb values were decreasing, brain CO values were slowly increasing; heart CO values were decreasing, but at a slower rate; and muscle values were decreasing only slightly.

The following scatter plots show the variability of tissue CO in relation to COHb% over time (Fig. 32):
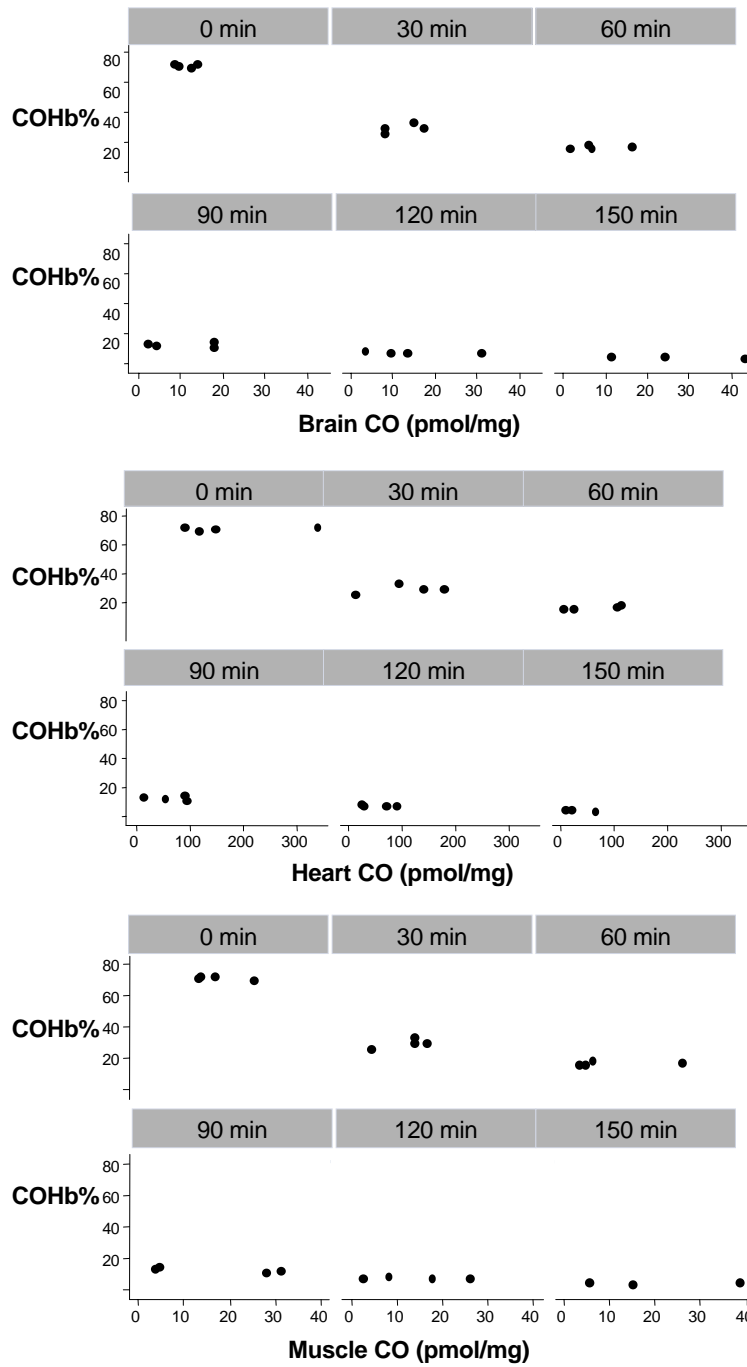
Figure 32. Scatter plots of COHb% vs. tissue CO in pmol/gm for each time point showing the tissue variability inside a narrow range of COHb; hence no relationship exists between COHb and tissue [CO] at any given point in time.

Although COHb changed significantly over time, the values were remarkably consistent between animals at any given time point. In contrast, the associated tissue values were highly variable. This illustrates how – for similar COHb value – tissue CO values vary widely.

5.5 TIME AND TISSUE-RELATED CHANGES IN CO

Compared to blood [CO] that dropped exponentially over time (Figure 33), the changes over time observed in tissue [CO] (Figure 34) were less distinct.

To assess the inter-tissue differences and interaction between tissue and time with respect to [CO], a cross sectional time-series regression analysis was employed. The analysis showed that heart CO values were significantly higher (p< 0.0001) than brain- and muscle CO values. Brain and muscle tissue on the other hand, did not differ significantly (p <0.86).

Heart tissue followed a decreasing yet statistically different trend to blood [CO] and the possible interpretations and reasons for this are discussed in Chapters 6 and 7.

There also existed a significant statistical interaction between tissue and time that can be attributed to the high CO levels in heart tissue immediately following exposure; these decreased over time to levels comparable to the other tissues (p<0.0001).

Importantly, however, brain [CO] appeared to gradually increase while muscle tissue remained largely unchanged in spite of the presence of intracellular myoglobin – an important CO 'sink'.
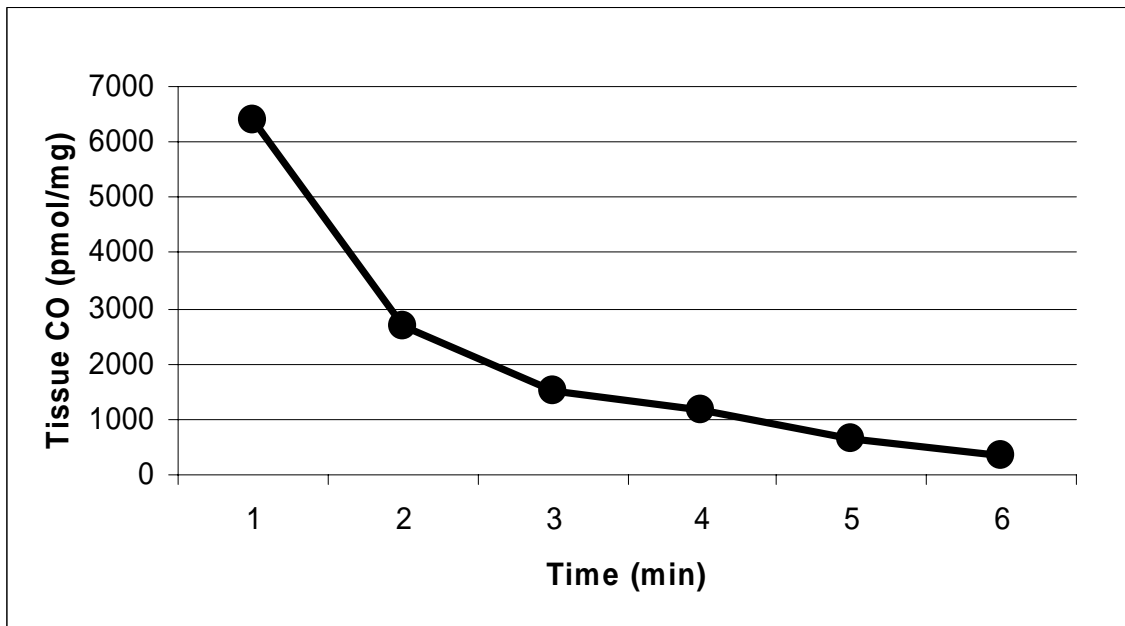
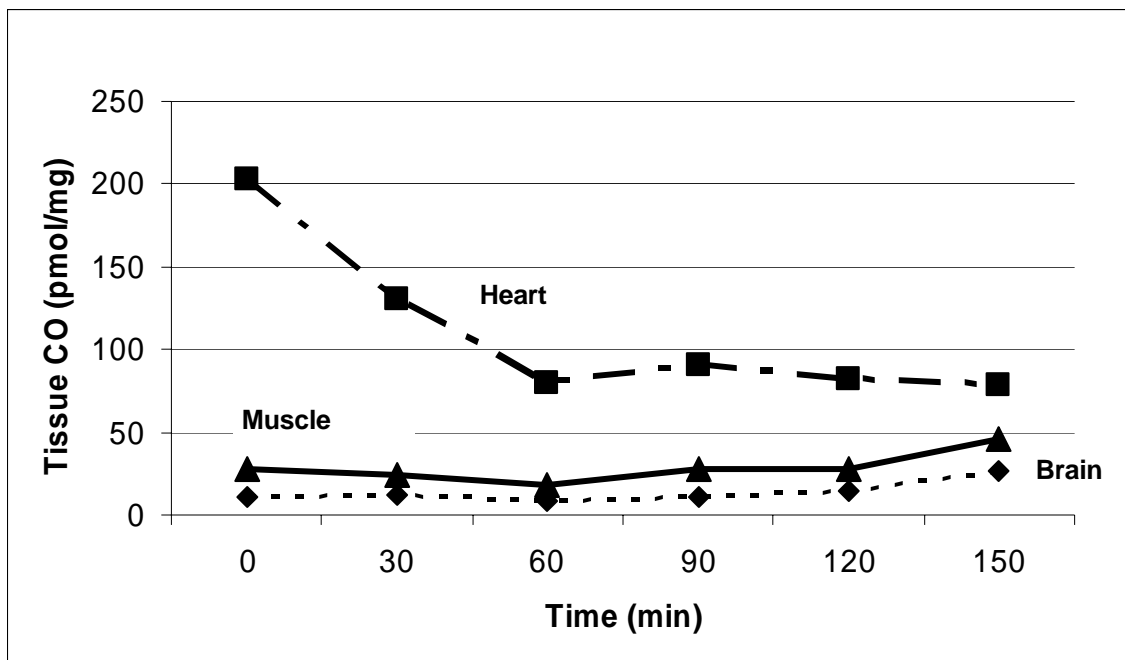**Figure 33**. Changes in Blood [CO] (pmol/mg) over time.

Figure 34. Tissue [CO] changes over time.

CHAPTER 6. DISCUSSION AND CONCLUSIONS

This study measured, and compared the changes in, blood and tissue CO levels following acute exposure to 2500 ppm CO. Predictably, blood [CO] dropped following exposure, but tissue [CO] did not.

The blood values – as measured by CO-oximetry and RGA – followed an exponential decline over time (see Fig. 33).   However tissue values did not follow the same trend (Fig. 34). For instance the initial CO values for brain tissue were not at their peak. They appeared to increase towards the later parts of the air-breathing recovery suggesting either a redistribution of CO or endogenous CO production. The latter is quite plausible as lipid peroxidation is well described in brain tissue, as is oxidative stress following CO poisoning. Elevations in free heme and concurrent induction of heme oxygenase (HO-1) by hypoxia-inducible factor might also explain the elevation in tissue CO values, in which case the trend would indeed be most apparent towards the end of the study period as was observed here. In fact a subsequent publication by the author has since supported the hypothesis that CO poisoning causes a release of heme and that this contributes significantly to CO increases in tissues rich in HO-1 [112]. Nevertheless, because current data supports the premise that at least some of the toxic effects of CO are attributed directly to an increase in tissue CO concentrations, these elevations – irrespective of their source (i.e., exogenous or endogenously derived) – are relevant as is the need to recognize this divergence between COHb and brain CO values; the latter has not previously been described. Ultimately it will be important to identify and respectively exclude various potential sources of CO in tissue before firm conclusions can be drawn. The use of tissue homogenate – an accordingly average tissue CO values – as well as the small quantities of CO involved caution against bold conclusions, but the paradoxical findings of this study should not be ignored or their importance underestimated.

Of particular clinical importance is that tissue values not only *did not* follow COHb changes – they were also misleading: (1) for a narrow range of COHb

values, the tissue CO values were highly variable and (2) only heart tissue followed the drop in COHb to some extent; the other tissues did not. Accordingly COHb values do not predict tissue CO values and – with the technology now being available – the former should no longer suffice as a measure of the latter [Σ].

A surprising finding was that muscle tissue appeared to absorb very little CO – in spite of the presence of myoglobin. This may be because the animals were resting during the exposure and accordingly the circulation and potential distribution of CO to muscle tissue was relatively low. One would therefore need to be cautious to extrapolate this type of CO exposure to industrials or occupational settings where the increase in muscular activity may not only increase the absorption of CO within muscle, but serve as an additional 'sink' for CO. This could possibly attenuate the potential for inflicting neuronal injury and partially explain why the morbidity in CO poisoning appears greater with longer exposures in resting individuals (e.g., suicide attempts and accidental home poisonings). This hypothesis is worth considering for future studies.

 Of all the tissues, heart tissue had the highest CO values and followed COHb most closely. It is attractive to hypothesize that this was the result of the combination of (1) increasing hypoxemia due to the formation of carboxyhemoglobin and left-ward shifting of the oxyhemoglobin dissociation curve; leading to (2) a reduction in available pO_2 in cardiac muscle and subsequent greater competitive blocking of myoglobin as Warburg partitioning favored CO as well as other heme moieties; and (3) greater perfusion due to the resulting acidosis delivering greater quantities of CO to the myocardium. However, from a technical point of view the heart was also the tissue most difficult to irrigate. Puncture of the left ventricle and transection of the

---

[Σ] A recent improvement has been the use of exhaled CO as an indication of CO exposure. However when this method is used, it should again be realized that the use of inspired oxygen will accelerate CO elimination so that this method may overestimate CO exposure if used in conjunction with oxygen therapy. This illustrates the importance of thinking in terms of tissue CO elimination rather than indirect measures.

pulmonary artery did ensure that the coronary arteries were perfused and the heart tissue did blanch. However, even though the section of cardiac muscle that was sampled was some distance away from the puncture site, the combination of disruption by cardiac puncture as well as the increased ventricular wall pressure during gentle irrigation, may have reduced homogenous perfusion and may thus inadvertently have led to retention of some COHb.

While every effort was made to ensure accuracy and precision, the following aspects of this technique may introduce variability or inadvertent errors of measurement:

- Choice and accuracy of CO concentration in the RGA calibration gas.

- The integrity of the gas-tight seal on the reaction vials.

- The choice of homogenate concentration: 0.5; 5 or 10% w/w: Higher concentrations are more reliable, but increased viscosity may affect transfer of tissue to the reaction vials.

- The concentration and effectiveness of the SSA in releasing tissue CO. Verified as reliable and consistent.

- The volume of tissue homogenate used in the reaction vials. Higher volumes of liquid may trap CO and reduce the quantity in the headspace.

- The CO concentration in the homogenate. Lower CO concentrations are subject to greater errors of measurement.

- The inter-animal variability in absorption of CO for a particular piCO due to differences in [Hb], cardiac output, and relative perfusion of respective tissue beds.

- The delay from removal of the animals from the exposure or recovery period until euthanasia has been completed. CO elimination in rats is rapid so that immediate post-exposure values decline quickly. With

significant variation in delays from exposure to euthanasia it is possible to have a wider range of peak CO values. The incremental impact of delay when harvesting animals during the recovery time is less critical.

- The effectiveness of irrigation in removing blood and COHb. Although every effort was made to blanch tissues during irrigation, all were not assessed for residual [Hb] and the possibility of residual COHb contamination must be recognized.

- The similarity/dissimilarity of tissue- and tissue structures sampled from the respective animals. Vascular tissue contains greater quantities of CO and accordingly histological differences may impact CO concentrations.

- Effectiveness of homogenization (sonication).

- Heating of tissue homogenate during sonication. Heating may result in premature denaturation of tissue protein with the release of CO and a consequent reduction in tissue [CO].

- Effect of microcentrifugation with stratification of tissue within homogenate prior to measurement. Although microcentrifugation was followed by vortexing / inverting the Microcentrifuge tubes containing homogenate prior to measurement to avoid clumping or stratification of contents, the possibility (although highly unlikely) does exist.

- Possible 'skimming' of tissue during transfer to the Hamilton syringes. Heart and muscle tissue is particularly viscous and a lower concentration may ultimately be preferred.

- Delay from the addition of the homogenate to the reaction vials until completion of the RGA measurement. At 0 °C (i.e., on ice) 5 minutes is adequate to release CO into the headspace after which a plateau is achieved and maintained for more than 90 minutes.

- Calibration drift on the RGA.

- Matching / appropriateness of 'bunch' and 'sense' settings on the RGA in relation to the concentration of CO (peak area).

- Impact of spontaneous CO production by the silicon septa.

The various procedures and techniques described in this thesis were developed and chosen to minimize the impact of the abovementioned variables. Nevertheless, these need to be considered in any work of this nature.

In conclusion, this study measured, and compared the changes in blood and tissue CO levels following acute exposure to 2500 ppm CO. The results of the study support the alternative hypothesis (H_1) that, following exposure to CO, changes in blood and tissue CO levels are different over time. This implies that COHb levels are unable to predict tissue [CO] at a given time point following CO exposure. It also documents the time and tissue-related variability of CO concentration following exposure.

CHAPTER 7. RECOMMENDATIONS

Much more is going on in CO poisoning than meets the eye. Yet COHb – an overt manifestation of exposure – has possibly been afforded too much biological significance in CO toxicity in lieu of considering the impact of elevated blood pCO and tissue pO2 and CO values. Of course, measuring the latter is complicated and impractical for *in vivo* CO-exposure models. Nevertheless, we should strive towards direct measurement for which the technique outlined in this study provides a practicable solution.

This study has also emphasized the importance of eliminating COHb from tissue in an effort to isolate tissue values from background COHb contamination. Unfortunately, for practical reasons, it was not possible to measure the residual quantities of hemoglobin in each tissue sample used in this analysis. While some animals were monitored for residual COHb -- and here the removal was found to be greater than 95% -- there remains an inevitable level of uncertainty about the residual COHb quantities that could have remained. This should be addressed more comprehensively in future studies.

The respective contributions of endogenous production within tissue vs. exogenous delivery to tissue remain undefined variables at present. Endogenously produced CO may vary with heme degradation, photo-oxidation, lipid peroxidation and/or mitochondrial consumption of CO. Exogenous delivery of blood CO to tissue may also be affected by a number of factors including, but not limited to, alveolar and arterial pCO; hemoglobin concentration; percentage COHb; tissue and cellular hypoxia; metabolic activity; acidosis; vascular (capillary) density; perfusion; and vasoreactivity in response to intravascular CO concentrations; and the type and concentration of various intracellular heme compounds (e.g., myoglobin, cytochromes and other mixed-function oxidizes). The latter, either as a CO 'sink' (i.e. a CO trap) or as a source of endogenous CO production linked to HO-1 activity – may increase intracellular [CO] significantly. Blocking HO-1

activity and measuring intracellular heme may assist in delineating these factors [112].

While understated in recent research, CO – like nitric oxide – is a biologically active molecule involved in many physiological processes. The study of its toxicity has also stimulated research in unraveling the intricacies of its physiological functions.

The study has revealed several promising areas of future research that would benefit from further emphasis on, and application of, both the methods described in this study as well as some of the findings. These include:

1. Determining the effect of increased pO_2 on changes in tissue [CO] concentrations (this has already been performed and published [112]).
2. Confirming or developing the equivalent of Warburg Coefficients for different tissue homogenates based on actual measurement of O_2 and CO. This would need to be performed while respectively blocking HO-1 and detecting products of lipid peroxidation to exclude endogenous production, and either blocking or attempting to measure CO to CO_2 conversion by cytochrome a-a3.
3. Correlating levels or changes in tissue [CO] with ultimate histological damage – particularly in the brain – to determine clinical relevance.

The ability to measure tissue [CO] at this level of resolution represents a powerful and versatile research tool. It is hoped that this manuscript may assist in advancing its application.

CHAPTER 8. REFERENCES

1. Vreman HJ, Kwong LK, Stevenson DK. Carbon monoxide in blood: an improved microliter blood-sample collection system, with rapid analysis by gas chromatography. *Clin Chem* 1984;**30**(8)**:**1382-6.

2. Raub JA, Benignus VA. Carbon monoxide and the nervous system. *Neurosci Biobehav Rev* 2002;**26**(8)**:**925-40.

3. Grant WJ. Helium, Nitrogen and some Other Gases. Medical Gases. Buckinghamshire: HM+M Publishers, 1978: 159-160.

4. Raub JA. The setting of health-based standards forambient carbon monoxide and their impact on atmospheric levels. In: Penney DG, ed. Carbon Monoxide Toxicity. New York: CRC Press, 2000: 84-99.

5. Raub JA, Mathieu-Nolf M, Hampson NB, Thom SR. Carbon monoxide poisoning--a public health perspective. *Toxicology* 2000;**145**(1)**:**1-14.

6. Sokal JA, Pach J. Acute carbon monoxide poisonings in Poland -- research and clinical experience. In: Penney DG, ed. Carbon Monoxide Toxicity. New York: CRC Press, 2000: 310-329.

7. AIRS data: monitor values report. Washington, DC: Office of Air & Radiation: US Environmental Protection Agency, 1999.

8. Health effects of exposure to low levels of regulated air pollutants. Discussion papers. *J Air Pollut Control Assoc* 1978;**28**(9)**:**883-94.

9. Peng WX, Ledingham KW, Singhal RP, McCanny T. Urban air pollution monitoring: laser-based procedure for the detection of carbon monoxide gas. *Analyst* 1998;**123**(5)**:**1035-9.

10. Atzori L, Caramori G, Lim S, et al. Effect of cigarette smoking on haem-oxygenase expression in alveolar macrophages. *Respir Med* 2004;**98**(6)**:**530-5.

11. Jaffe LS. Sources, characteristics, and fate of atmospheric carbon monoxide. *Ann N Y Acad Sci* 1970;**174**(1)**:**76-88.

12. Varon J, Marik P. Carbon monoxide poisoning and gas powered equipment. *J Emerg Med* 2001;**21**(3)**:**283-4.

13. Kwor R. Carbon Monoxide Detectors. In: Penney DG, ed. Carbon Monoxide Toxicity. New York: CRC Press, 2000: 61-82.

14. The Merck Index. 11th ed. Rahway, N.J.: Merck Research Laboratories, 2000.

15. Dodge MC, Richter HG. Properties and principles of formation of carbon monoxide, in EPA 600/8-90/045F: Air quality criteria for carbon monoxide. Research Triangle Park, NC: Environmental Criteria and Assessment Office, Office of Health and Environmental Assessment, Office of Research and Development, US Environmental Protection Agency, 1991: 3-1 to 3-17.

16. AIRSData: monitor values report. Washington, DC: Office of Air & Radiation: U.S. Environmental Protection Agency, 1999.

17. Iablochkin VD, Rodionova VS, Mishchikhin VA, Kirillova TI. [Gas chromatographic method of quantitative determination of carbon monoxide in cadaver blood]. *Sud Med Ekspert* 2001;**44**(6)**:**33-5.

18. Johansson MB, Wollmer P. Measurement of carboxyhaemoglobin by spectrophotometry and gas chromatography. *Clin Physiol* 1989;**9**(6)**:**581-6.

19. Mahoney JJ, Vreman HJ, Stevenson DK, Van Kessel AL. Measurement of carboxyhemoglobin and total hemoglobin by five specialized spectrophotometers (CO-oximeters) in comparison with reference methods. *Clin Chem* 1993;**39**(8)**:**1693-700.

20. Marks GS, Vreman HJ, McLaughlin BE, Brien JF, Nakatsu K. Measurement of endogenous carbon monoxide formation in biological systems. *Antioxid Redox Signal* 2002;**4**(2)**:**271-7.

21. Vreman HJ, Mahoney JJ, Van Kessel AL, Stevenson DK. Carboxyhemoglobin as measured by gas chromatography and with the IL 282 and 482 CO-Oximeters. *Clin Chem* 1988;**34**(12)**:**2562-6.

22. Vreman HJ, Stevenson DK, Zwart A. Analysis for carboxyhemoglobin by gas chromatography and multicomponent spectrophotometry compared. *Clin Chem* 1987;**33**(5)**:**694-7.

23. Small KA, Radford EP, Frazier JM, Rodkey FL, Collison HA. A rapid method for simultaneous measurement of carboxy- and methemoglobin in blood. *J Appl Physiol* 1971;**31**(1)**:**154-60.

24. Widdop B. Analysis of carbon monoxide. *Ann Clin Biochem* 2002;**39**(Pt 4)**:**378-91.

25. Fukui M, Shigemi K. Determination of single and repeated red cell volumes by the indicator dilution method using carbon monoxide as the indicator. *Crit Care Med* 1989;**17**(11)**:**1199-202.

26. Glass HI, Brant A, Clark JC, De Garetta AC, Day LG. Measurement of blood volume using red cells labeled with radioactive carbon monoxide. *J Nucl Med* 1968;**9**(11)**:**571-5.

27. Glass HI, De Garreta AC, Lewis SM, Grammaticos P, Szur L. Measurement of splenic red-blood-cell mass with radioactive carbon monoxide. *Lancet* 1968;**1**(7544)**:**669-70.

28. Lapostolle F, Gourlain H, Pizagalli MN, et al. Measurement of carbon monoxide in simulated expired breath. *Resuscitation* 2005;**64**(2)**:**201-4.

29. Franck P, Nabet P, Dousset B. Applications of infrared spectroscopy to medical biology. *Cell Mol Biol (Noisy-le-grand)* 1998;**44**(2)**:**273-5.

30. Rodkey FL, Hill TA, Pitts LL, Robertson RF. Spectrophotometric measurement of carboxyhemoglobin and methemoglobin in blood. *Clin Chem* 1979;**25**(8)**:**1388-93.

31. Dubowski KM, Luke JL. Measurement of carboxyhemoglobin and carbon monoxide in blood. *Ann Clin Lab Sci* 1973;**3**(1)**:**53-65.

32. Tietz NW, Fiereck EA. The spectrophotometric measurement of carboxyhemoglobin. *Ann Clin Lab Sci* 1973;**3**(1)**:**36-42.

33. Lily RE, Cole PV, Hawkins LH. Spectrophotometric measurement of carboxyhaemoglobin. An evaluation of the method of Commins and Lawther. *Br J Ind Med* 1972;**29**(4)**:**454-7.

34. Engelbrecht R. A compact NIR fiber-optic diode laser spectrometer for CO and CO(2): analysis of observed 2f wavelength modulation spectroscopy line shapes. *Spectrochim Acta A Mol Biomol Spectrosc* 2004;**60**(14)**:**3291-8.

35. Kiger L, Stetzkowski-Marden F, Poyart C, Marden MC. Correlation of carbon monoxide association rates and the position of absorption band III in hemoproteins. *Eur J Biochem* 1995;**228**(3)**:**665-8.

36. Potter WT, Hazzard JH, Kawanishi S, Caughey WS. Direct measurement of carbon monoxide bound to different subunits of hemoglobin A in solution and in red cells by infrared spectroscopy. *Biochem Biophys Res Commun* 1983;**116**(2)**:**719-25.

37. Guillot JG, Weber JP, Savoie JY. Quantitative determination of carbon monoxide in blood by head-space gas chromatography. *J Anal Toxicol* 1981;**5**(6)**:**264-6.

38. Juntarawijit C, Poovey HG, Rando RJ. Determination of carbon monoxide with a modified zeolite sorbent and methanization-gas chromatography. *Aihaj* 2000;**61**(3)**:**410-4.

39. Kaminski M, Kartanowicz R, Jastrzebski D, Kaminski MM. Determination of carbon monoxide, methane and carbon dioxide in refinery hydrogen gases and air by gas chromatography. *J Chromatogr A* 2003;**989**(2)**:**277-83.

40. Mueller W, Schubert J, Benzing A, Geiger K. Method for analysis of exhaled air by microwave energy desorption coupled with gas chromatography-flame ionization detection-mass spectrometry. *J Chromatogr B Biomed Sci Appl* 1998;**716**(1-2)**:**27-38.

41. Theis DE, Saurer M, Blum H, Frossard E, Siegwolf RT. A portable automated system for trace gas sampling in the field and stable isotope analysis in the laboratory. *Rapid Commun Mass Spectrom* 2004;**18**(18)**:**2106-12.

42. Tsunogai U, Nakagawa F, Komatsu DD, Gamo T. Stable carbon and oxygen isotopic analysis of atmospheric carbon monoxide using continuous-flow isotope ratio MS by isotope ratio monitoring of CO. *Anal Chem* 2002;**74**(22)**:**5695-700.

43. Tsunogai U, Nakagawa F, Hachisu Y, Yoshida N. Stable carbon and oxygen isotopic analysis of carbon monoxide in natural waters. *Rapid Commun Mass Spectrom* 2000;**14**(16)**:**1507-12.

44. Thom SR, Keim LW. Carbon monoxide poisoning: a review epidemiology, pathophysiology, clinical findings, and treatment options including hyperbaric oxygen therapy. *J Toxicol Clin Toxicol* 1989;**27**(3)**:**141-56.

45. Girman JR, Chang YL, Hayward SB, Liu KS. Causes of unintentional deaths from carbon monoxide poisonings in California. *West J Med* 1998;**168**(3)**:**158-65.

46. Marks GS. Heme oxygenase: the physiological role of one of its metabolites, carbon monoxide and interactions with zinc protoporphyrin, cobalt protoporphyrin and other metalloporphyrins. *Cell Mol Biol (Noisy-le-grand)* 1994;**40**(7)**:**863-70.

47. Marks GS, Brien JF, Nakatsu K, McLaughlin BE. Does carbon monoxide have a physiological function? *Trends Pharmacol Sci* 1991;**12**(5)**:**185-8.

48. Barrowcliff DF, Knell AJ. Cerebral damage due to endogenous chronic carbon monoxide poisoning caused by exposure to methylene chloride. *J Soc Occup Med* 1979;**29**(1)**:**12-4.

49. Tariot PN. Delirium resulting from methylene chloride exposure: case report. *J Clin Psychiatry* 1983;**44**(9)**:**340-2.

50. Piantadosi CA. Biological chemistry of carbon monoxide. *Antioxid Redox Signal* 2002;**4**(2)**:**259-70.

51. Gunsalus IC, Sligar SG, Nordlund T, Frauenfelder H. Oxygen sensing heme proteins: monoxygenases, myoglobin and hemoglobin. *Adv Exp Med Biol* 1977;**78:**37-50.

52. Coburn RF. The carbon monoxide body stores. *Ann N Y Acad Sci* 1970;**174**(1)**:**11-22.

53. Caughey WS. Carbon monoxide bonding in hemeproteins. *Ann N Y Acad Sci* 1970;**174**(1)**:**148-53.

54. Jaffe FA. Pathogenicity of carbon monoxide. *Am J Forensic Med Pathol* 1997;**18**(4)**:**406-10.

55. Mims MP, Porras AG, Olson JS, Noble RW, Peterson JA. Ligand binding to heme proteins. An evaluation of distal effects. *J Biol Chem* 1983;**258**(23)**:**14219-32.

56. Ponka P. Cell biology of heme. *Am J Med Sci* 1999;**318**(4)**:**241-56.

57. Keilin D, Hartree EF. Cytochrome and cytochrome oxidase. *Proc Roy Soc (London) Ser B* 1939;**127:**167-191.

58. Keilin D. Inhibition of cell respiration by carbon monoxide. History of cell respiration and cytochrome. Cambridge: Cambridge Press, 1966: 252-268.

59. Widdop B. Analysis of carbon monoxide. *Ann Clin Biochem* 2002;**39**(4)**:**378-91.

60. Cunnington AJ, Hormbrey P. Breath analysis to detect recent exposure to carbon monoxide. *Postgrad Med J* 2002;**78**(918)**:**233-7.

61. Andersson JA, Uddman R, Cardell LO. Carbon monoxide is endogenously produced in the human nose and paranasal sinuses. *J Allergy Clin Immunol* 2000;**105**(2 Pt 1)**:**269-73.

62. Madany IM. Carboxyhemoglobin levels in blood donors in Bahrain. *Sci Total Environ* 1992;**116**(1-2)**:**53-8.

63. Bureau MA, Shapcott D, Berthiaume Y, et al. Maternal cigarette smoking and fetal oxygen transport: a study of P50, 2,3-diphosphoglycerate, total hemoglobin, hematocrit, and type F hemoglobin in fetal blood. *Pediatrics* 1983;**72**(1)**:**22-6.

64. Benignus VA, Kafer ER, Muller KE, Case MW. Absence of symptoms with carboxyhemoglobin levels of 16-23%. *Neurotoxicol Teratol* 1987;**9**(5)**:**345-8.

65. Longo LD, Hill EP. Carbon monoxide uptake and elimination in fetal and maternal sheep. *Am J Physiol* 1977;**232**(3)**:**H324-30.

66. Gottlieb SO. Cardiovascular benefits of smoking cessation. *Heart Dis Stroke* 1992;**1**(4)**:**173-5.

67. Olson KR. Carbon monoxide poisoning: mechanisms, presentation, and controversies in management. *J Emerg Med* 1984;**1**(3)**:**233-43.

68. Thom SR. Carbon monoxide-induced deficits in cognitive performance of mice and lack of effect of hyperbaric oxygen treatment. *Acad Emerg Med* 2002;**9**(1)**:**75-7.

69. Gorman DF, Runciman WB. Carbon monoxide poisoning. *Anaesth Intensive Care* 1991;**19**(4)**:**506-11.

70. Flanagan RJ, Rooney C. Recording acute poisoning deaths. *Forensic Sci Int* 2002;**128**(1-2)**:**3-19.

71. Risser D, Schneider B. Carbon monoxide-related deaths from 1984 to 1993 in Vienna, Austria. *J Forensic Sci* 1995;**40**(3)**:**368-71.

72. Moolenaar RL, Etzel RA, Parrish RG. Unintentional deaths from carbon monoxide poisoning in New Mexico, 1980 to 1988. A comparison of medical examiner and national mortality data. *West J Med* 1995;**163**(5)**:**431-4.

73. Piantadosi CA. Carbon monoxide poisoning. *N Engl J Med* 2002;**347**(14)**:**1054-5.

74. Weaver LK. Carbon monoxide poisoning. *Crit Care Clin* 1999;**15**(2)**:**297-317, viii.

75. Turnbull TL, Hart RG, Strange GR, et al. Emergency department screening for unsuspected carbon monoxide exposure. *Ann Emerg Med* 1988;**17**(5)**:**478-83.

76. Selvakumar S, Sharan M, Singh MP. A mathematical model for the elimination of carbon monoxide in humans. *J Theor Biol* 1993;**162**(3)**:**321-36.

77. Wazawa H, Yamamoto K, Yamamoto Y, Matsumoto H, Fukui Y. Elimination of CO from the body: an experimental study on the rabbit. *Nippon Hoigaku Zasshi* 1996;**50**(4)**:**258-62.

78. Coburn RF, Forster RE, Kane PB. Considerations of the physiological variables that determine the blood carboxyhemoglobin concentration in man. *J Clin Invest* 1965;**44**(11)**:**1899-910.

79. Pace NS, E. Walker, EL. Acceleration of carbon monoxide elimination in man by high pressure oxygen. *Science* 1950;**111:**652-654.

80. Myers RA, Thom SR. Carbon Monoxide and Cyanide Poisoning. Second ed. Flagstaff: Best Publishing, 1999.

81. Weaver LK, Hopkins RO, Chan KJ, et al. Hyperbaric oxygen for acute carbon monoxide poisoning. *N Engl J Med* 2002;**347**(14)**:**1057-67.

82. Scheinkestel CD, Bailey M, Myles PS, et al. Hyperbaric or normobaric oxygen for acute carbon monoxide poisoning: a randomized controlled clinical trial. *Undersea Hyperb Med* 2000;**27**(3)**:**163-4.

83. Thom SR, Ischiropoulos H. Mechanism of oxidative stress from low levels of carbon monoxide. *Res Rep Health Eff Inst* 1997(80)**:**1-19; discussion 21-7.

84. Sokal JA, Majka J, Palus J. The content of carbon monoxide in the tissues of rats intoxicated with carbon monoxide in various conditions of acute exposure. *Arch Toxicol* 1984;**56**(2)**:**106-8.

85. Haldane JS. The relation of the action of carbonic oxide to oxygen tension. *J Physiol (London)* 1895;**18:**201-217.

86. Haldane JS, Smith JL. The oxygen tension of arterial blood. *J Physiol* 1896;**20:**497-520.

87. Warburg O. The enzyme problem and biological oxidations. Johns Hopkins Bull, 1930: 341-358.

88. Sedlacek M, Halpern NA, Uribarri J. Carboxyhemoglobin and lactate levels do not correlate in critically ill patients. *Am J Ther* 1999;**6**(5)**:**241-4.

89. Shusterman D, Alexeeff G, Hargis C, et al. Predictors of carbon monoxide and hydrogen cyanide exposure in smoke inhalation patients. *J Toxicol Clin Toxicol* 1996;**34**(1)**:**61-71.

90. Farber JP, Schwartz PJ, Vanoli E, Stramba-Badiale M, De Ferrari GM. Carbon monoxide and lethal arrhythmias. *Res Rep Health Eff Inst* 1990(36)**:**1-17; discussion 19-27.

91. Goldbaum LR, Orellano T, Dergal E. Mechanism of the toxic action of carbon monoxide. *Ann Clin Lab Sci* 1976;**6**(4)**:**372-6.

92. Blackmore DJ. The determination of carbon monoxide in blood and tissue. *Analyst* 1970;**95**(130)**:**439-58.

93. Shinomiya K, Orimoto C, Shinomiya T. [Experimental exposure to carbon monoxide in rats (I)--Relation between the degree of carboxyhemoglobin saturation and the amount of carbon monoxide in the organ tissues of rats]. *Nippon Hoigaku Zasshi* 1994;**48**(1)**:**19-25.

94. Bernard C. Lecons sur les effects des substance toxiques et medicamenteuses. Pairs: Bailliere, 1857.

95. Allen TA, Root WS. Partition of carbon monoxide and oxygen between air and whole blood of rats, dogs and men as affected by plasma pH. *J Appl Physiol* 1957;**10**(2)**:**186-90.

96. Rodkey FL, O'Neal JD, Collison HA, Uddin DE. Relative affinity of hemoglobin S and hemoglobin A for carbon monoxide and oxygen. *Clin Chem* 1974;**20**(1)**:**83-4.

97. Sladen RN. The oxyhemoglobin dissociation curve. *Int Anesthesiol Clin* 1981;**19**(3)**:**39-70.

98. Astrup P, Garby L, de Verdier CH. Displacements of the oxyhemoglobin dissociation curve. *Scand J Clin Lab Invest* 1968;**22**(3)**:**171-6.

99. Buehler JH, Berns AS, Webster JR, Addington WW, Cugell DW. Lactic acidosis from carboxyhemoglobinemia after smoke inhalation. *Ann Intern Med* 1975;**82**(6)**:**803-5.

100. Mansley GE, Stanbury JT, Lemberg R. Cytochrome oxidase and its derivatives. VI. The CO combining capacity of cytochrome C oxidase. *Biochim Biophys Acta* 1966;**113**(1)**:**33-40.

101. Davison AJ, Wainio WW. Reactions of oxygenated cytochrome oxidase. *J Biol Chem* 1968;**243**(19)**:**5023-7.

102. Landaw SA, Winchell HS. Endogenous production of carbon-14 labeled carbon monoxide: an in vivo technique for the study of heme catabolism. *J Nucl Med* 1966;**7**(9)**:**696-707.

103. Coburn RF. Endogenous carbon monoxide production. *N Engl J Med* 1970;**282**(4)**:**207-9.

104. Coceani F. Carbon monoxide in vasoregulation: the promise and the challenge. *Circ Res* 2000;**86**(12)**:**1184-6.

105. Turcanu V, Dhouib M, Gendrault JL, Poindron P. Carbon monoxide induces murine thymocyte apoptosis by a free radical-mediated mechanism. *Cell Biol Toxicol* 1998;**14**(1)**:**47-54.

106. Verma A, Hirsch DJ, Glatt CE, Ronnett GV, Snyder SH. Carbon monoxide: a putative neural messenger. *Science* 1993;**259**(5093)**:**381-4.

107. Vreman HJ, Mahoney JJ, Stevenson DK. Carbon monoxide and carboxyhemoglobin. *Adv Pediatr* 1995;**42:**303-34.

108. Avogadro A. *Essai d'une manière de déterminer les masses relatives des molecules élémentaires des corps, et les proportions selon lesquelles elles entrent dans ces combinaisons. Journal de Physique, de Chemie et d'Histoire naturelle* 1809.

109. Luomanmaki K, Coburn RF. Effects of metabolism and distribution of carbon monoxide on blood and body stores. *Am J Physiol* 1969;**217**(2)**:**354-63.

110. Vreman HJ, Wong RJ, Kadotani T, Stevenson DK. Determination of carbon monoxide (CO) in rodent tissue: Effect of heme administration and environmental CO exposure. *Anal Biochem* 2005;**341**(2)**:**280-9.

111. Sjostrand T. The formation of carbon monoxide by the decomposition of haemoglobin in vivo. *Acta Physiol Scand* 1952;**26:**338.

112. Cronje FJ, Carraway MS, Freiberger JJ, Suliman HB, Piantadosi CA. Carbon monoxide actuates O(2)-limited heme degradation in the rat brain. *Free Radic Biol Med* 2004;**37**(11)**:**1802-12.

113. Coburn RF. Endogenous carbon monoxide production and body CO stores. *Acta Med Scand Suppl* 1967;**472:**269-82.

114. Coburn RF. Carbon monoxide uptake in the gut. *Ann N Y Acad Sci* 1968;**150**(1)**:**13-21.

115. Coburn RF. Endogenous carbon monoxide metabolism. *Annu Rev Med* 1973;**24:**241-50.

116. Coburn RF. Oxygen tension sensors in vascular smooth muscle. *Adv Exp Med Biol* 1977;**78:**101-15.

117. Coburn RF. Mechanisms of carbon monoxide toxicity. *Prev Med* 1979;**8**(3)**:**310-22.

118. Coburn RF, Clark BJ. Mean myoglobin oxygen tension during exercise at maximal oxygen uptake. *Adv Exp Med Biol* 1976;**75:**675-83.

119. Coburn RF, Kane PB. Maximal erythrocyte and hemoglobin catabolism. *J Clin Invest* 1968;**47**(6)**:**1435-46.

120. Coburn RF, Mayers LB. Myoglobin O2 tension determined from measurement of carboxymyoglobin in skeletal muscle. *Am J Physiol* 1971;**220**(1)**:**66-74.

121. Coburn RF, Wallace HW, Abboud R. Redistribution of body carbon monoxide after hemorrhage. *Am J Physiol* 1971;**220**(4)**:**868-73.

122. Coburn RF, Williams WJ, Forster RE. Effect of Erythrocyte Destruction on Carbon Monoxide Production in Man. *J Clin Invest* 1964;**43:**1098-103.

123. Coburn RF, Williams WJ, Kahn SB. Endogenous carbon monoxide production in patients with hemolytic anemia. *J Clin Invest* 1966;**45**(4)**:**460-8.

124. Coburn RF, Williams WJ, White P, Kahn SB. The production of carbon monoxide from hemoglobin in vivo. *J Clin Invest* 1967;**46**(3)**:**346-56.

125. Hill EP, Hill JR, Power GG, Longo LD. Carbon monoxide exchanges between the human fetus and mother: a mathematical model. *Am J Physiol* 1977;**232**(3)**:**H311-23.

126. Warburg O. Heavy metal prosthetic groups and enzyme action. Oxford: Clarendon Press, 1949.

127. Coburn RF, Forman HJ. Carbon monoxide toxicity. *Handbook Physiol* 1987;**4:**439-456.

128. Fenn WO, Cobb DM. The burning of carbon monoxide by heart and skeletal muscle. *Am J Physiol* 1932;**102:**393-401.

129. Young LJ, Caughey WS. Mitochondrial oxygenation of carbon monoxide. *Biochem J* 1986;**239**(1)**:**225-7.

130. Young LJ, Caughey WS. Pathobiochemistry of CO poisoning. *FEBS Lett* 1990;**272**(1-2)**:**1-6.

131. Young LJ, Choc MG, Caughhey WS. Role of oxygen and cytochrome c oxidase in the detoxification of carbon monoxide by oxidation to carbon dioxide. Biochemical and clinical aspects of oxygen: proceedings of a symposium 1979, Ft Colins, CO: 355.

132. Young LJ, Einarsdottir O, Vossbrink CR, Caughey WS. Infrared spectra of carbon monoxide bound to mitochondria from diverse species and tissues reveal structurally similar cytochrome c oxidase dioxygen reaction sites. *Biochem Biophys Res Commun* 1984;**123**(1)**:**247-53.

133. Ramos KS, Lin H, McGrath JJ. Modulation of cyclic guanosine monophosphate levels in cultured aortic smooth muscle cells by carbon monoxide. *Biochem Pharmacol* 1989;**38**(8)**:**1368-70.

134. Brune B, Ullrich V. Inhibition of platelet aggregation by carbon monoxide is mediated by activation of guanylate cyclase. *Mol Pharmacol* 1987;**32**(4)**:**497-504.

135. Thom SR. Leukocytes in carbon monoxide-mediated brain oxidative injury. *Toxicol Appl Pharmacol* 1993;**123**(2)**:**234-47.

136. Hardy KR, Thom SR. Pathophysiology and treatment of carbon monoxide poisoning. *J Toxicol Clin Toxicol* 1994;**32**(6)**:**613-29.

137. Thom SR, Ohnishi ST, Fisher D, Xu YA, Ischiropoulos H. Pulmonary vascular stress from carbon monoxide. *Toxicol Appl Pharmacol* 1999;**154**(1)**:**12-9.

138. Zhang J, Piantadosi CA. Mitochondrial oxidative stress after carbon monoxide hypoxia in the rat brain. *J Clin Invest* 1992;**90**(4)**:**1193-9.

139. Ischiropoulos H, Beers MF, Ohnishi ST, Fisher D, Garner SE, Thom SR. Nitric oxide production and perivascular nitration in brain after carbon monoxide poisoning in the rat. *J Clin Invest* 1996;**97**(10)**:**2260-7.

140. Maulik N, Engelman DT, Watanabe M, et al. Nitric oxide/carbon monoxide. A molecular switch for myocardial preservation during ischemia. *Circulation* 1996;**94**(9 Suppl)**:**II398-406.

141. Piantadosi CA, Zhang J, Demchenko IT. Production of hydroxyl radical in the hippocampus after CO hypoxia or hypoxic hypoxia in the rat. *Free Radic Biol Med* 1997;**22**(4)**:**725-32.

142. Christova T, Diankova Z, Setchenska M. Heme oxygenase--carbon monoxide signalling pathway as a physiological regulator of vascular smooth muscle cells. *Acta Physiol Pharmacol Bulg* 2000;**25**(1)**:**9-17.

143. Wang R, Wang Z, Wu L. Carbon monoxide-induced vasorelaxation and the underlying mechanisms. *Br J Pharmacol* 1997;**121**(5)**:**927-34.

144. Wang R, Wu L, Wang Z. The direct effect of carbon monoxide on KCa channels in vascular smooth muscle cells. *Pflugers Arch* 1997;**434**(3)**:**285-91.

145. Herman ZS. Carbon monoxide: a novel neural messenger or putative neurotransmitter? *Pol J Pharmacol* 1997;**49**(1)**:**1-4.

146. Piantadosi CA, Zhang J, Levin ED, Folz RJ, Schmechel DE. Apoptosis and delayed neuronal damage after carbon monoxide poisoning in the rat. *Exp Neurol* 1997;**147**(1)**:**103-14.

147. Dulak J, Jozkowicz A. Carbon monoxide -- a "new" gaseous modulator of gene expression. *Acta Biochim Pol* 2003;**50**(1)**:**31-47.

148. Furchgott RF, Vanhoutte PM. Endothelium-derived relaxing and contracting factors. *Faseb J* 1989;**3**(9)**:**2007-18.

149. Moore EG, Gibson QH. Cooperativity in the dissociation of nitric oxide from hemoglobin. *J Biol Chem* 1976;**251**(9)**:**2788-94.

150. Hawkins RD, Zhuo M, Arancio O. Nitric oxide and carbon monoxide as possible retrograde messengers in hippocampal long-term potentiation. *J Neurobiol* 1994;**25**(6)**:**652-65.

151. Ingi T, Cheng J, Ronnett GV. Carbon monoxide: an endogenous modulator of the nitric oxide-cyclic GMP signaling system. *Neuron* 1996;**16**(4)**:**835-42.

152. Maines M. Carbon monoxide and nitric oxide homology: differential modulation of heme oxygenases in brain and detection of protein and activity. *Methods Enzymol* 1996;**268:**473-88.

153. Meilin S, Rogatsky GG, Thom SR, Zarchin N, Guggenheimer-Furman E, Mayevsky A. Effects of carbon monoxide on the brain may be mediated by nitric oxide. *J Appl Physiol* 1996;**81**(3)**:**1078-83.

154. Tetreau C, Tourbez M, Gorren A, Mayer B, Lavalette D. Dynamics of carbon monoxide binding with neuronal nitric oxide synthase. *Biochemistry* 1999;**38**(22)**:**7210-8.

155. Xue L, Farrugia G, Miller SM, Ferris CD, Snyder SH, Szurszewski JH. Carbon monoxide and nitric oxide as coneurotransmitters in the enteric nervous system: evidence from genomic deletion of biosynthetic enzymes. *Proc Natl Acad Sci U S A* 2000;**97**(4)**:**1851-5.

156. Hartsfield CL. Cross talk between carbon monoxide and nitric oxide. *Antioxid Redox Signal* 2002;**4**(2)**:**301-7.

157. Yang ZX, Qin J. Interaction between endogenous nitric oxide and carbon monoxide in the pathogenesis of recurrent febrile seizures. *Biochem Biophys Res Commun* 2004;**315**(2)**:**349-55.

158. Omaye S. Metabolic modulation of carbon monoxide toxicity. *Toxicology* 2002;**180**(2)**:**139.

159. Kozma F, Johnson RA, Nasjletti A. Role of carbon monoxide in heme-induced vasodilation. *Eur J Pharmacol* 1997;**323**(2-3)**:**R1-2.

160. Thorup C, Jones CL, Gross SS, Moore LC, Goligorsky MS. Carbon monoxide induces vasodilation and nitric oxide release but suppresses endothelial NOS. *Am J Physiol* 1999;**277**(6 Pt 2)**:**F882-9.

161. Vedernikov YP, Graser T, Vanin AF. Similar endothelium-independent arterial relaxation by carbon monoxide and nitric oxide. *Biomed Biochim Acta* 1989;**48**(8)**:**601-3.

162. Wong RJ, Vreman HJ, Kadotani DK, Stevenson DK. Concentration of carbon monoxide in tissue. *J. Invest. Med.* 2000;**48:**23A.

163. Gothert M, Malorny G. [On the distribution of carbon monoxide between blood and tissue]. *Arch Toxikol* 1969;**24**(4)**:**260-70.

164. Aleksandrov NP, Korobov RN, Filippov VG. [Poison content in the blood and tissues of mammals after the inhalational uptake of carbon monoxide and benzene and cyanide vapors]. *Farmakol Toksikol* 1979;**42**(6)**:**670-4.

165. Roth RA, Rubin RJ. Comparison of the effect of carbon monoxide and of hypoxic hypoxia. I. In vivo metabolism, distribution and action of hexobarbital. *J Pharmacol Exp Ther* 1976;**199**(1)**:**53-60.

166. Raub JA. Carbon monoxide. Geneva: World Health Organization, 1999.

167. Vreman HJ, Stevenson DK, Henton D, Rosenthal P. Correlation of carbon monoxide and bilirubin production by tissue homogenates. *J Chromatogr* 1988;**427**(2)**:**315-9.

168. Vreman HJ, Stevenson DK. Carbon monoxide generation from tin- and zinc-protoporphyrin by tissue homogenates. *Biochem Biophys Res Commun* 1987;**148**(1)**:**417-21.

169. Vreman HJ, Wong RJ, Stevenson DK. Carbon monoxide in breath, blood, and other tissues. In: Penney DG, ed. Carbon monoxide toxicity. Boca Raton: CRC Press, 2000: 19-60.

170. Vreman HJ, Wong RJ, Stevenson DK. Sources, sinks and measurement of carbon monoxide. In: (eds) WR, ed. Carbon monoxide in cardiovascular functions. Boca Raton, Florida: CRC Press, 2001: 273-307.

171. Wong RJ, Vreman HJ, Kadotani T, Stevenson DK. Concentration of carbon monoxide (CO) in tissue. *J Invest Med* 2000;**48:**23A(#123).

172. Wong RJ, Vreman HJ, Stevenson DK. Carbon monoxide concentrations in tissues. *Acta Haematol* 2000;**103**(78)**:**A310.

173. Carraway MS, Ghio AJ, Suliman HB, Carter JD, Whorton AR, Piantadosi CA. Carbon monoxide promotes hypoxic pulmonary vascular remodeling. *Am J Physiol Lung Cell Mol Physiol* 2002;**282**(4)**:**L693-702.

174. Clayton CE, Carraway MS, Suliman HB, et al. Inhaled carbon monoxide and hyperoxic lung injury in rats. *Am J Physiol Lung Cell Mol Physiol* 2001;**281**(4)**:**L949-57.

175. Carraway MS, Ghio AJ, Carter JD, Piantadosi CA. Expression of heme oxygenase-1 in the lung in chronic hypoxia. *Am J Physiol Lung Cell Mol Physiol* 2000;**278**(4)**:**L806-12.

176. Brown SD, Piantadosi CA. Recovery of energy metabolism in rat brain after carbon monoxide hypoxia. *J Clin Invest* 1992;**89**(2)**:**666-72.

177. Brown SD, Piantadosi CA. In vivo binding of carbon monoxide to cytochrome c oxidase in rat brain. *J Appl Physiol* 1990;**68**(2)**:**604-10.

178. Piantadosi CA. Spectrophotometry of b-type cytochromes in rat brain in vivo and in vitro. *Am J Physiol* 1989;**256**(4 Pt 1)**:**C840-8.

179. Brown SD, Piantadosi CA. Reversal of carbon monoxide-cytochrome c oxidase binding by hyperbaric oxygen in vivo. *Adv Exp Med Biol* 1989;**248:**747-54.

180. Piantadosi CA, Lee PA, Sylvia AL. Direct effects of CO on cerebral energy metabolism in bloodless rats. *J Appl Physiol* 1988;**65**(2)**:**878-87.

181. Jobsis-VanderVliet FF, Piantadosi CA, Sylvia AL, Lucas SK, Keizer HH. Near-infrared monitoring of cerebral oxygen sufficiency. I. Spectra of cytochrome c oxidase. *Neurol Res* 1988;**10**(1)**:**7-17.

182. Piantadosi CA, Sylvia AL, Jobsis-Vandervliet FF. Differences in brain cytochrome responses to carbon monoxide and cyanide in vivo. *J Appl Physiol* 1987;**62**(3)**:**1277-84.

183. Piantadosi CA, Sylvia AL. Cerebral cytochrome a,a3 inhibition by cyanide in bloodless rats. *Toxicology* 1984;**33**(1)**:**67-79.

184. Piantadosi CA, Sylvia AL, Saltzman HA, Jobsis-Vandervliet FF. Carbon monoxide-cytochrome interactions in the brain of the fluorocarbon-perfused rat. *J Appl Physiol* 1985;**58**(2)**:**665-72.

185. Piantadosi CA, Tatro L, Zhang J. Hydroxyl radical production in the brain after CO hypoxia in rats. *Free Radic Biol Med* 1995;**18**(3)**:**603-9.

186. Kubic VL, Anders MW. Metabolism of dihalomethanes to carbon monoxide. II. In vitro studies. *Drug Metab Dispos* 1975;**3**(2)**:**104-12.

187. Kubic VL, Anders MW, Engel RR, Barlow CH, Caughey WS. Metabolism of dihalomethanes to carbon monoxide. I. In vivo studies. *Drug Metab Dispos* 1974;**2**(1)**:**53-7.

188. Vreman HJ. General accuracy and rounding of values. in RGA Personal communication; Stanford, CA, 2002.

189. Coburn RF, Forman HJ. Carbon monoxide toxicity. Handbook Physiol, 1987: 439-456.

APPENDIX A: EQUIPMENT & SUPPLIERS

CO-Oximeter

IL Model 482 CO-oximeter; Instrumentation Laboratory; 101 Hartwell Avenue; Lexington, MA 02421-3125

Gas Chromatograph

RGA5 Process Gas Analyzer; Trace Analytical; 3517A Edison Way; Menlo Park; California 94025-1815

Centrifuge

Model DW-41N-115 Micro Centrifuge; Qualitron, Inc. / Witz Scientific; 7556 Hill Ave.; Holland, OH, 43528, USA; Phone : 419-861-2111 / Fax : 419-861-2219

Sonifier

Branson-Sonifier Model 450; Branson Ultrasonics ; 41 Eagle Road; Danbury, CT; 06813-1961

Cell Culture Tray

24 Well Cell Culture Cluster #3524; flat bottom with lid, tissue culture treated, non-pyrogenic, polystyrene, sterile; Corning Incorporated; One Riverfront Plaza Corning, NY 14831-0001; http://www.scienceproducts.corning.com

Pipettes

Pipetman P-20 and P-1000; Rainin Instrument Company, Inc.; Rainin Road; Woburn, MA 01888-4026; 1-800-472-4646;

Microcentrifuge Tubes

Catalog #05-408-25J flat top, 2.0 mL ; Fisher Scientific; 585 Alpha Drive; Pittsburgh, PA 15238; (412) 963-8098

Mettler Balance

Mettler Model AE100 Balance; Mettler-Toledo, Inc.; 1900 Polaris Parkway; Columbus, OH 43240; 614-438-4511

Detergent

PCC-54 Detergent Concentrate; Pierce Biotechnology Inc.; PO Box 117; Rockford, IL 61105; 800-874-3723; http://www.piercenet.com

Syringes

1.0 mL , 50 μl, 100 μl Hamilton Syringe; Hamilton Company; P.O. Box 10030; Reno, NV 89520-0012; 800-648-5950

0.25 mL VICI Precision Pressurelok Gastight Syringe; Valco Instruments Co. Inc. 8275 W. El Cajon Drive; Baton Rouge, LA 70815; 800-828-1653

Repeating Mechanism

Hamilton Syringe Repeater; Hamilton Company; P.O. Box 10030; Reno, NV 89520-0012; 800-648-5950

Reaction Vials

12 x 32 mm screw thread 2 mL clear type 1 borosilicate glass vial; part # 95191; Alltech Associates, Inc. 2701 Carolean Industrial Drive; State College, PA 16801; 800-437-3784; http://www.alltechWEB.com

Caps

Open hole screw thread caps unlined, 10/425; (part # 98143); Alltech Associates, Inc. 2701 Carolean Industrial Drive; State College, PA 16801; 800-437-3784; http://www.alltechWEB.com

Septa

HT-X Blue Septa, 5/16" (part # 15491); Alltech Associates, Inc.; 2701 Carolean Industrial Drive; State College, PA 16801; 800-437-3784; http://www.alltechWEB.com

Test tube rack

Full-view polypropylene test tube rack 10-13 mm (part # 60983-007). Note: peg length must be shortened to 20 mm to permit trouble free handling of the reaction vials; VWR Scientific Products; 1050 Satellite Blvd.; Suwannee, GA; 800-932-5000; http://www.vwr.com

Gases

5 ppm CO, Balance Nitrogen; Scott Specialty Gases; 6141 Easton Road Box 310; Plumsteadville, PA 18949; 800-331-4953; http://www.scottgas.com/

Getter

PS11-MC1 Ambient Temperature Gas Purifier (Getter Stabilized Zeolite); SAES Getters USA Inc.; 1122 East Cheyenne Mountain Blvd.; Colorado Springs, CO; 80906; 719-576-5025; http://www.saesgetters.com/

APPENDIX B: COMPLETE DATA SET

The first four pages in this section contain the complete data set of the experimental sessions. They contain animals A1-24. Note that Animal 6 was deleted because of a technical difficulty that arose during the tissue irrigation. The organs were incompletely irrigated and accordingly the tissues had to be discarded and could not be included in the study. However these tissues were not wasted but were used to determine the impact of homogenization (see Figure 32).

The subsequent two pages contain all the control animal data. Animals C1-9.

The labels of the various sections are clearly defined in Section 4.7.1.

WEIGHT	SAMPLE	g TISSUE	Weight: T+H2C	R	V Sample	Sample 1	Sample 2	Sample 3	Mean	R	Mean Blank	CO-pmol	CO-pmol/mg	[Hb] / Predicted CO (pmol/mg)
290	A1-B	0.080	0.80	0.0194	20	138	152	120	137	0.0194	16	2	1.17	[Hb] 14.5
TIME OFF CO	A1-H	0.089	0.89	MEAN BLANK	10	2354	2268	2300	2307	0.0194	16	44	44.46	
0	A1-M	0.139	1.39	15.670	40	1719	1582	1626	1642	0.0194	16	32	7.89	Predicted CO (pmol/mg) 3664
	A1-BG	0.020	2.00	CO-Hb	5	12349	10161	9696	10735	0.0194	16	208	4159.23	
	A1-BC			40.700 / BG-SYRINGE										
273	A2-B	0.089	0.89	0.0194	10	435	440	393	423	0.0194	16	8	7.90	[Hb] 14.4
TIME OFF CO	A2-H	0.066	0.66	MEAN BLANK	20	1480	1472	1447	1466	0.0194	16	28	14.07	
30	A2-M	0.072	0.72	15.670	20	560	401	403	455	0.0194	16	9	4.26	Predicted CO (pmol/mg) 2341
	A2-BG	0.020	2.00	CO-Hb	20	25591	26333	26000	25975	0.0194	16	504	2518.02	
	A2-BC			26.200 / BG-SYRINGE										
307	A3-B	0.053	0.53	0.0194	40	408	335	344	362	0.0194	16	7	1.68	[Hb] 13.8
TIME OFF CO	A3-H	0.067	0.67	MEAN BLANK	40	1359	1185	1200	1248	0.0194	16	24	5.98	
60	A3-M	0.083	0.83	15.670	40	994	982	926	967	0.0194	16	18	4.62	Predicted CO (pmol/mg) 1387
	A3-BG	0.020	2.00	CO-Hb 16.200	40	23048	22741	22900	22896	0.0194	16	444	1109.71	
	A3-BC			BG-SYRINGE										
276	A4-B	0.052	0.52	0.0194	40	523	544	506	524	0.0194	16	10	2.47	[Hb] 15.9
TIME OFF CO	A4-H	0.060	0.60	MEAN BLANK	40	2800	2741	2915	2819	0.0194	16	54	13.59	
90	A4-M	0.075	0.75	15.670	40	696	790	763	750	0.0194	16	14	3.56	Predicted CO (pmol/mg) 1283
	A4-BG	0.020	2.00	CO-Hb 13.000	40	20868	19352	20000	20073	0.0194	16	389	972.80	
	A4-BC			BG-SYRINGE										
319	A5-B	0.064	0.64	0.0194	40	808	676	722	735	0.0194	16	14	3.49	[Hb] 14.1
TIME OFF CO	A5-H	0.098	0.98	MEAN BLANK	40	5449	5472	5352	5424	0.0194	16	105	26.23	
120	A5-M	0.075	0.75	15.670	40	1728	1759	1713	1733	0.0194	16	33	8.33	Predicted CO (pmol/mg) 744
	A5-BG	0.020	2.00	CO-Hb 8.500	40	5883	5500	5200	5528	0.0194	16	107	267.33	
	A5-BC			BG-SYRINGE										
	A6-B		0.00	0.0194	40				0	0.0194	0	0	0.00	[Hb]
TIME OFF CO	A6-H		0.00	MEAN BLANK	40				0	0.0194	0	0	0.00	
150	A6-M		0.00	15.670	40				0	0.0194	0	0	0.00	Predicted CO (pmol/mg) 0
	A6-BG		0.00	CO-Hb	40				0	0.0194	0	0	0.00	
	A6-BC			BG-SYRINGE										

WEIGHT	SAMPLE	g TISSUE	Weight: T+H2C	R	V Sample	Sample 1	Sample 2	Sample 3	Mean	R	Mean Blank	CO-pmol	CO-pmol/mg	[Hb]	Predicted CO (pmol/mg)
323	A7-B	0.136	1.36	0.0194	40	2644	2653	2549	2615	0.0194	43	50	12.47	13.9	
TIME OFF CO	A7-H	0.103	1.03	MEAN BLANK	40	24946	23901	24208	24352	0.0194	43	472	117.90		Predicted CO (pmol/mg)
0	A7-M	0.097	0.97	43.330	40	4952	5692	5220	5288	0.0194	43	102	25.44		
	A7-BG	0.020	2.00	CO-Hb	5	21707	21977	18917	20867	0.0194	43	404	8079.58		5979
	A7-BC		BG-SYRINGE	69.300											
343	A8-B	0.114	1.14	0.0194	40	3194	3140	3142	3159	0.0194	43	60	15.11	14.5	
TIME OFF CO	A8-H	0.104	1.04	MEAN BLANK	40	19716	18461	19789	19322	0.0194	43	374	93.50		Predicted CO (pmol/mg)
30	A8-M	0.107	1.07	43.330	40	2704	3008	3103	2938	0.0194	43	56	14.04		
	A8-BG	0.020	2.00	CO-Hb	10	14959	14950	14091	14667	0.0194	43	284	2836.93		3023
	A8-BC		BG-SYRINGE	33.600											
350	A9-B	0.084	0.84	0.0194	40	1634	1399	1307	1447	0.0194	43	27	6.81	14	
TIME OFF CO	A9-H	0.103	1.03	MEAN BLANK	40	5536	5545	4828	5303	0.0194	43	102	25.51		Predicted CO (pmol/mg)
60	A9-M	0.079	0.79	43.330	40	547	1009	666	741	0.0194	43	14	3.38		
	A9-BG	0.020	2.00	CO-Hb	10	7672	7027	7461	7387	0.0194	43	142	1424.61		1416
	A9-BC		BG-SYRINGE	16.300											
330	A10-B	0.150	1.50	0.0194	40	3746	3570	3987	3768	0.0194	43	72	18.06	14.6	
TIME OFF CO	A10-H	0.104	1.04	MEAN BLANK	40	19143	19389	19916	19483	0.0194	43	377	94.28		Predicted CO (pmol/mg)
90	A10-M	0.085	0.85	43.330	40	5994	6033	5480	5836	0.0194	43	112	28.09		
	A10-BG	0.020	2.00	CO-Hb	10	4800	4815	4492	4702	0.0194	43	90	903.85		1006
	A10-BC		BG-SYRINGE	11.100											
339	A11-B	0.103	1.03	0.0194	40	1597	2215	2049	1954	0.0194	16	38	9.40	13.8	
TIME OFF CO	A11-H	0.096	0.96	MEAN BLANK	40	19359	17291	19407	18686	0.0194	16	362	90.55		Predicted CO (pmol/mg)
120	A11-M	0.114	1.14	15.670	40	485	574	493	517	0.0194	16	10	2.43		
	A11-BG	0.020	2.00	CO-Hb	10	2810	2678	2641	2710	0.0194	16	52	522.64		565
	A11-BC		BG-SYRINGE	6.600											
347	A12-B	0.143	1.43	0.0194	40	5111	4841	4980	4977	0.0194	16	96	24.06	14	
TIME OFF CO	A12-H	0.054	0.54	MEAN BLANK	40	4521	4425	4141	4362	0.0194	16	84	21.08		Predicted CO (pmol/mg)
150	A12-M	0.107	1.07	15.670	40	1148	1208	1161	1172	0.0194	16	22	5.61		
	A12-BG	0.020	2.00	CO-Hb	10	1846	1856	1766	1823	0.0194	16	35	350.56		417
	A12-BC		BG-SYRINGE	4.800											

WEIGHT	SAMPLE	g TISSUE	Weight: T+H2C	R	V Sample	Sample 1	Sample 2	Sample 3	Mean	R	Mean Blank	CO-pmol	CO-pmol/mg	[Hb] / Predicted CO (pmol/mg)
308	A13-B	0.112	1.12	0.0208	40	2479	2907	2860	2749	0.0208	20	57	14.19	[Hb] 14
	A13-H	0.108	1.08	MEAN BLANK	4	6155	6469	6945	6523	0.0208	20	135	338.16	Predicted CO (pmol/mg)
0	A13-M	0.076	0.76	20.000	40	3151	3221	3465	3279	0.0208	20	68	16.95	6292
	A13-BG	0.010	2.04	CO-Hb	1	2691	2649	2714	2685	0.0208	20	55	542.51	
	A13-BC		BG-SYRINGE	72.400										
302	A14-B	0.078	0.78	0.0208	40	1713	1482	1576	1590	0.0208	20	33	8.17	[Hb] 14.6
	A14-H	0.087	0.87	MEAN BLANK	4	3353	3480	3569	3467	0.0208	20	72	179.26	Predicted CO (pmol/mg)
30	A14-M	0.079	0.79	20.000	40	2597	2888	2641	2709	0.0208	20	56	13.98	2636
	A14-BG	0.010	2.06	CO-Hb	1	1133	1158	1180	1157	0.0208	20	24	2364.96	
	A14-BC		BG-SYRINGE	29.100										
294	A15-B	0.064	0.64	0.0208	40	1157	1171	1121	1150	0.0208	20	23	5.87	[Hb] 14.5
	A15-H	0.075	0.75	MEAN BLANK	4	20162	22689	22476	21776	0.0208	20	453	113.13	Predicted CO (pmol/mg)
60	A15-M	0.103	1.03	20.000	40	1235	1270	1204	1236	0.0208	20	25	6.32	1665
	A15-BG	0.010	2.04	CO-Hb	1	892	822	813	842	0.0208	20	17	1710.45	
	A15-BC		BG-SYRINGE	18.500										
294	A16-B	0.086	0.86	0.0208	40	3118	3666	3627	3470	0.0208	20	72	17.94	[Hb] 13.7
	A16-H	0.097	0.97	MEAN BLANK	4	17593	17308	17433	17445	0.0208	20	362	90.61	Predicted CO (pmol/mg)
90	A16-M	0.112	1.12	20.000	40	895	863	850	869	0.0208	20	18	4.42	1199
	A16-BG	0.011	2.10	CO-Hb	1	636	545	535	572	0.0208	20	11	1148.16	
	A16-BC		BG-SYRINGE	14.100										
314	A17-B	0.068	0.68	0.0208	40	2779	2452	2617	2616	0.0208	20	54	13.50	[Hb] 14.2
	A17-H	0.078	0.78	MEAN BLANK	4	14276	13826	12615	13572	0.0208	20	282	70.47	Predicted CO (pmol/mg)
120	A17-M	0.098	0.98	20.000	40	4955	5412	4869	5079	0.0208	20	105	26.31	652
	A17-BG	0.011	2.24	CO-Hb	1	607	577	502	562	0.0208	20	11	1127.36	
	A17-BC		BG-SYRINGE	7.400										
310	A18-B	0.078	0.78	0.0208	40	8492	8257	8256	8335	0.0208	20	173	43.24	[Hb] 13.7
	A18-H	0.087	0.87	MEAN BLANK	4	12412	12585	12430	12476	0.0208	20	259	64.77	Predicted CO (pmol/mg)
150	A18-M	0.097	0.97	20.000	40	2905	2909	3054	2956	0.0208	20	61	15.27	298
	A18-BG	0.010	2.04	CO-Hb	1	286	302	269	286	0.0208	20	6	552.59	
	A18-BC		BG-SYRINGE	3.500										

WEIGHT / TIME OFF CO	SAMPLE	g TISSUE	Weight: T+H2C	R	V Sample	Sample 1	Sample 2	Sample 3	Mean	R	Mean Blank	CO-pmol	CO-pmol/mg	[Hb] / Predicted CO (pmol/mg)
WEIGHT 272	A19-B	0.064	0.64	0.0208	40	1078	1058	957	1031	0.0208	37	21	5.17	[Hb] 14.7
	A19-H	0.066	0.66	MEAN BLANK	5	668	699	622	663	0.0208	37	13	26.05	
	A19-M	0.062	0.62	36.830	40	1201	1207	1032	1147	0.0208	37	23	5.77	Predicted CO 6634
	A19-BG	0.010	2.00	CO-Hb	0.5	1446	1434	1562	1481	0.0208	37	30	6006.36	
TIME OFF CO 0	A19-BC		BG-SYRINGE	72.700										
WEIGHT 281	A20-B	0.065	0.65	0.0207	40	3588	3134	3581	3434	0.0207	37	70	17.58	[Hb] 15.3
	A20-H	0.067	0.67	MEAN BLANK	10	7550	6869	6091	6837	0.0207	37	141	140.76	
	A20-M	0.065	0.65	36.830	40	2547	3153	3987	3229	0.0207	37	66	16.52	Predicted CO 2801
	A20-BG	0.010	2.00	CO-Hb	0.5	787	666	716	723	0.0207	37	14	2840.74	
TIME OFF CO 30	A20-BC		BG-SYRINGE	29.500										
WEIGHT 292	A21-B	0.079	0.79	0.0207	40	3118	3150	3436	3235	0.0207	37	66	16.55	[Hb] 15
	A21-H	0.073	0.73	MEAN BLANK	40	20479	20306	20161	20315	0.0207	37	420	104.94	
	A21-M	0.065	0.65	36.830	40	5467	4561	5152	5060	0.0207	37	104	25.99	Predicted CO 1620
	A21-BG	0.010	2.00	CO-Hb	0.5	613	507	430	517	0.0207	37	10	1986.52	
TIME OFF CO 60	A21-BC		BG-SYRINGE	17.400										
WEIGHT 281	A22-B	0.067	0.67	0.0207	40	900	903	903	902	0.0207	37	18	4.48	[Hb] 15.2
	A22-H	0.082	0.82	MEAN BLANK	20	5793	5366	4678	5279	0.0207	37	109	54.26	
	A22-M	0.088	0.88	36.830	40	5175	6453	6537	6055	0.0207	37	125	31.14	Predicted CO 1160
	A22-BG	0.010	2.00	CO-Hb	0.5	389	308	318	338	0.0207	37	6	1248.22	
TIME OFF CO 90	A22-BC		BG-SYRINGE	12.300										
WEIGHT 274	A23-B	0.084	0.84	0.0207	40	6008	6001	6016	6008	0.0207	37	124	30.90	[Hb] 13.8
	A23-H	0.071	0.71	MEAN BLANK	40	5421	5314	5436	5390	0.0207	37	111	27.70	
	A23-M	0.082	0.82	36.830	40	4015	3378	2994	3462	0.0207	37	71	17.73	Predicted CO 642
	A23-BG	0.010	2.00	CO-Hb	1	392	377	377	382	0.0207	37	7	714.50	
TIME OFF CO 120	A23-BC		BG-SYRINGE	7.500										
WEIGHT 283	A24-B	0.059	0.59	0.0207	40	2283	2372	2182	2279	0.0207	37	46	11.60	[Hb] 14.3
	A24-H	0.060	0.60	MEAN BLANK	40	1936	1460	1924	1773	0.0207	37	36	8.99	
	A24-M	0.099	0.99	36.830	40	6953	7173	7319	7148	0.0207	37	147	36.80	Predicted CO 373
	A24-BG	0.010	2.00	CO-Hb	1	224	183	218	208	0.0207	37	4	355.01	
TIME OFF CO 150	A24-BC		BG-SYRINGE	4.200										

WEIGHT		R	V Sample	Sample 1	Sample 2	Sample 3	Mean	R	Mean Blank	CO-pmol	CO-pmol/mg	[Hb] / Predicted CO (pmol/mg)
274	C1-B	0.0208	40	5279	4684	4473	4812	0.0208	37	99	24.83	[Hb] 14.9
	C1-H	MEAN BLANK	40	5247	4917	4936	5033	0.0208	37	104	25.98	Predicted CO (pmol/mg)(pmol/mg) 92
	C1-M	36.500	40	132	152	144	143	0.0208	37	2	0.55	
	C1-BG	CO-Hb	2	353	274	280	302	0.0208	37	6	276.47	
	C1-BC	1.000										
275	C2-B	0.0208	40	2165	2410	2335	2303	0.0208	37	47	11.79	[Hb] 14.5
	C2-H	MEAN BLANK	40	6739	6649	6504	6631	0.0208	37	137	34.29	Predicted CO (pmol/mg) 81
	C2-M	36.500	40	1210	1214	1196	1207	0.0208	37	24	6.08	
	C2-BG	CO-Hb	2	236	178	258	224	0.0208	37	4	195.00	
	C2-BC	0.900										
279	C3-B	0.0208	40	5445	5219	4892	5185	0.0208	37	107	26.77	[Hb] 14.4
	C3-H	MEAN BLANK	40	15799	15643	15675	15706	0.0208	37	326	81.48	Predicted CO (pmol/mg) 80
	C3-M	36.500	40	373	457	399	410	0.0208	37	8	1.94	
	C3-BG	CO-Hb	2	208	201	167	192	0.0208	37	3	161.72	
	C3-BC	0.900										
279	C4-B	0.0208	40	1638	1650	1649	1646	0.0208	37	33	8.37	[Hb] 15.1
	C4-H	MEAN BLANK	40	17314	17006	17098	17139	0.0208	37	356	88.93	Predicted CO (pmol/mg) 112
	C4-M	36.500	40	201	193	199	198	0.0208	37	3	0.84	
	C4-BG	CO-Hb	2	337	235	288	287	0.0208	37	5	260.17	
	C4-BC	1.200										
274	C5-B	0.0208	40	4820	4580	4769	4723	0.0208	37	97	24.37	[Hb] 15.5
	C5-H	MEAN BLANK	40	5344	5107	4600	5017	0.0208	37	104	25.90	Predicted CO (pmol/mg) 77
	C5-M	36.500	40	779	697	708	728	0.0208	37	14	3.60	
	C5-BG	CO-Hb	2	322	218	216	252	0.0208	37	4	224.12	
	C5-BC	0.800										
282	C6-B	0.0208	40	503	451	459	471	0.0208	37	9	2.26	[Hb] 15.3
	C6-H	MEAN BLANK	40	6611	7586	9058	7752	0.0208	37	160	40.12	Predicted CO (pmol/mg) 95
	C6-M	36.500	40	1848	1790	1778	1805	0.0208	37	37	9.20	
	C6-BG	CO-Hb	2	250	190	193	211	0.0208	37	4	181.48	
	C6-BC	1.000										

WEIGHT	SAMPLE	R	V Sample	Sample 1	Sample 2	Sample 3	Mean	R	Mean Blank	CO-pmol	CO-pmol/mg	[Hb]
286	C7-B	0.0217	40	474	466	608	516	0.0217	24	11	2.67	14.6
	C7-H		40	9309	9295	9284	9296	0.0217	24	201	50.30	
	C7-M	24.300	40	3650	3487	3607	3581	0.0217	24	77	19.30	Predicted CO (pmol/mg)
	C7-BG	CO-Hb	10	961	962	1023	982	0.0217	24	21	207.82	45
	C7-BC	0.500										

WEIGHT	SAMPLE	R	V Sample	Sample 1	Sample 2	Sample 3	Mean	R	Mean Blank	CO-pmol	CO-pmol/mg	[Hb]
286	C8-B	0.0217	40	484	497	490	490	0.0217	24	10	2.53	14.1
	C8-H	MEAN BLANK	40	11103	11225	11113	11147	0.0217	24	241	60.34	
	C8-M	24.300	40	5054	4841	4628	4841	0.0217	24	105	26.13	Predicted CO (pmol/mg)
	C8-BG	CO-Hb	10	782	865	816	821	0.0217	24	17	172.88	35
	C8-BC	0.400										

WEIGHT	SAMPLE	R	V Sample	Sample 1	Sample 2	Sample 3	Mean	R	Mean Blank	CO-pmol	CO-pmol/mg	[Hb]
298	C9-B	0.0217	40	468	526	592	529	0.0217	24	11	2.74	14.5
	C9-H	MEAN BLANK	40	4481	4601	4799	4627	0.0217	24	100	24.97	
	C9-M	24.300	40	1026	1179	1145	1117	0.0217	24	24	5.93	Predicted CO (pmol/mg)
	C9-BG	CO-Hb	10	790	874	765	810	0.0217	24	17	170.42	27
	C9-BC	0.300										

APPENDIX C: APPROVALS BY DUKE INSTITUTIONAL ANIMAL CARE AND USE COMMITTEE & UNIV. PRETORIA ONDERSTEPOORT

C-1 APPROVAL FROM DUKE UNIVERSITY INSTITUTIONAL ANIMAL CARE AND USE COMMITTEE

Jan-22-2003 05:22pm   From-GRANTS & CONTRACTS   +9196846278   T-079 P.002/003 F-531

Frans J Cronje
01/21/2003 03:31 PM

To: Michelle J Keys/Grants/MCAdmin/mc/Duke@mc, Frans J Cronje/Anesthesiology/mc/Duke@mc, Marti
       Hanes/LabAnimal/mc/Duke@mc
cc: jfreib@acpub.duke.edu

Subject: Re: IACUC Protocol entitled, "Carbon Monoxide Elimination from Brain, Heart and Skeletal Muscle..."
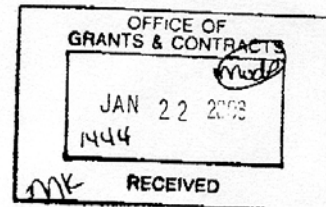
Dear All,

Subsequent to the humane endpoint concern from L Tyrey, sent by fax on 1/17/03, please note the
appropriate changes to the protocol on pages 8 & 10.

Regards,

Frans Cronje, MD

IACUC PROTOCOL-CO-ELIMINATION1.!

OFFICE OF
GRANTS & CONTRACTS

JAN 2 2 2003

1444

RECEIVED

Approved 1/22/03
L. Tyrey

E. LEE TYREY, CHAIRMAN
DUKE UNIVERSITY INSTITUTIONAL ANIMAL
CARE AND USE COMMITTEE

Duke University Institutional Animal Care & Use Committee (IACUC)

The appended protocol has been deferred for additional information that must be reviewed by Designated Review or Full Committee Method. Studies MUST NOT BE ACTIVATED until response to the IACUC questions and concerns has been received and approved by the method specified below.

Designated Reviewer ■

Full Committee Review ☐

Signature below indicates Final Approval

MEETING DATE. 12/19/2002
REGISTRY # ASSIGNED A368-02-12

19N

h ⟨ypry 1/22/03

E. Lee Tyrey, Chairman
Duke University Institutional Animal Care and
Use Committee

■Signature(s) required from:

☐ Co-PI's/Department Chairman
■ **Occupational & Environmental Safety Office**
☐ CCIF Director
☐ Primate Center Director
☐ VA Research & Development Office
■ **DLAR Veterinary Oversight**

☐ The facility requires inspection by the IACUC. You will be contacted by a DLAR veterinarian to arrange for an inspection of Room   Building   for housing/surgery.

☐ Please list the name(s) and phone number(s) of person(s) to contact in case of an emergency.

☐ Please clarify and justify the number of animals on the basis of experimental design.

☐ (Renewals) Please specify the number of animals used during the past year.

☐ Please describe the method of euthanasia.

☐ Please describe the preoperative or postoperative routine and note who will be responsible.

☐ Please complete Section VII (A,B,C) addressing alternatives to potentially painful procedures

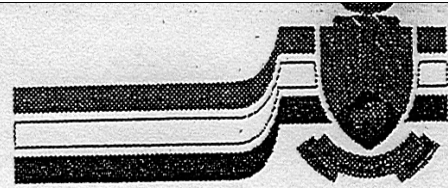☐ Please specify animal handling roles for all personnel (Section XIII)

Other Changes:

1. **Please clarify the humane endpoints to be used that would lead to animals being withdrawn prematurally from the study for humane reasons.**

- 137 -

C-2   APPROVAL FROM UNIVERSITY OF PRETORIA – ONDERSTEPOORT

University of Pretoria

Enq.   : Mario Smuts
Tel.   : 012-529 8388
Fax.   : 012-529 8321
E-mail : mario.smuts@up.ac.za

University of Pretoria Biomedical
Research Centre (UPBRC)
Private Bag X04
Onderstepoort 0110

Dr. Chris le Roux
Faculty of Health Sciences
School of Medicine
Aerospace Medicine
P.O. Box 667
Pretoria
0001

Dear Dr. Le Roux,

RE: AUCC APPROVAL – PROJECT 09/2003 – CARBONMONOXIDE ELIMINATION FROM BRAIN, HEART AND SKELETAL MUSCLE IN AIR, 100% OXYGEN AND HYPERBARIC OXYGEN - DR. FRANS JOHANNES CRONJE

Please find herewith notification that the Chairman of the Animal Use and Care Committee (AUCC) approved and signed off the above-mentioned protocol submitted for approval on July 28, 2003. The AUCC approved the protocol in principle, but would like to request the researcher to reconsider the use of Methoxyflurane as it is no longer available in South Africa. However, if all the research is to be conducted in the USA as specified in the application, this may not be an issue.

Please contact us for any further information.

Sincerely,

MR. M.P. SMUTS
MANAGER: LABORATORY ANIMALS
2003/09/26

- 138 -

APPENDIX D: CALCULATORS & RESEARCH TOOLS[♠]

D-1   CALCULATORS

PREDICTED CO VALUES IN BLOOD AND CO CONCENTRATIONS VIA RGA

Determination of CO Content in Blood (Hb and Dissolved)

COHb	Hüfner	[Hb] in g/dL
0.7	1.39	15.1

ppm CO	fiCO	pAmbient (ATA)	ppCO (ATA)
2500	0.0025	0.992	0.00248

Sol.CO (mL/dL/ATA)
1.83

Hb bound CO	[Dissolved CO]
14.6923	0.0045

TOTAL CO (mL CO/ dL blood)	14.697
mL CO / mole @ STP	22400
moles / dL blood	6.56E-04
pmoles /dL blood	6.56E+08
pmoles/mg blood assuming 1uL /mg density	6561

Determination of moles of CO / mg Blood via RGA

Standard Concentration for Blood: 20uL/2mL	1 % solution	
PA (Modified & Rounded)	287	
R-value	0.0208	
pmoles CO detected in Sample	5.97	
pmoles CO in average Blank	0.76	**MEAN BLANK**
pmoles from Homogenate (blank value subtracted)	5.21	36.5
uL Tissue Homogenate from which CO was derived	2	
pmoles / ul	2.6052	
Concentration of Homogenate % (w/w)	1%	
pmoles/mg blood assuming a 1uL /mg density	260.52	

Determination of moles of CO / mg Tissue via RGA

Standard Concentration for Tissue: 0.1g/1g	10 % solution	
PA (Modified & Rounded)	5033	
R-value	0.0208	
pmoles CO detected in Sample	104.69	
pmoles CO in average Blank	0.77	**MEAN BLANK**
pmoles from Homogenate (blank value subtracted)	103.92	37
uL Tissue Homogenate from which CO was derived	40	
pmoles / ul	2.60	
Concentration of Homogenate % (w/w)	10%	
pmoles/mg tissue assuming a 1uL /mg density	25.98	

[♠] All calculators and spreadsheets were created independently by the author. Refer to the Resource CD-ROM in Appendix D-2.

This spreadsheet was used to determine the quantity of CO in blood as predicted by CO-Oximetry as well as the respective quantities of CO in blood and tissue using the RGA. The shaded cells accept variables and then generate the quantities of CO based upon them.

VAN DER WAALS VS. IDEAL GAS MOLAR VOLUME CALCULATOR

n	P	V	T	a	b	V2	an2	nb	R
1	1	22.4	273.15	1.39	0.03913	501.76	1.39	0.03913	0.08206

22.42282   Molar Volume (VD Waals)

22.4   Molar Volume (Ideal)

0.99898 Fraction (VdWaals / Ideal)

$$\left[P + \frac{an^2}{V^2}\right](V - nb) = nRT$$

Van Der Waals Equation

D-2   RESEARCH RESOURCE CD:

This CD ROM Contains:

- ➤ Final Version of the Manuscript as MS Word and Adobe 6 PDF.

- ➤ Compete DATA Set (MS Excel)

- ➤ All Converters & Calculators

- ➤ Endnote® Library of CO References

- ➤ All PDF References on CO

D-3 SUMMARISED RESEARCH PROTOCOL

ANIMAL EXPOSURE

1. Prepare a 6 port manifold with 0-10 Lpm span flow meters and a 2500 ppm CO in compressed air and a CO-free compressed air source in a fume hood.

2. Transfer 6 male Sprague Dawley rats respectively into six 2 L transparent containers; seal them in; open the compressed air source and adjust flow meters to maintain a flow rate of 5 to 6 Lpm per container of CO free air to eliminate exhaled carbon dioxide.

3. Record zero-time and switch the animals to the 2500 ppm CO in air source for 45 minutes.

4. At time = 45 minutes change the gas supply to CO-free air and remove the first animal and sacrifice it in a killing jar with Halothane.

5. Remove the subsequent animals at 30, 60, 90, 120 and 150 minutes respectively.

ANIMAL DISSECTION & TISSUE HARVESTING

1. After 4 minutes, remove the animal from Halothane jar and weigh the animal.

2. Using straight scissors, open the peritoneal cavity and cut through the anterior attachments of the diaphragm to expose the thoracic cavity.

3. Withdraw 2 mL of blood from the inferior vena cava using a heparinized syringe for co-oximetry and RGA analysis.

4. Prepare an infusion of 60 mL of 0.9% saline in a 100 mL syringe and attach it to a 14 G hypodermic needle via flexible tubing.

5. Puncture the left ventricle with the needle; transect the pulmonary artery using straight scissors; and perfuse the tissues gently with 60 mL of 0.9% saline making sure that the tissues blanch during irrigation and the excess blood and fluid flows from the transected pulmonary artery until the liquid runs clear. Repeat if needed.

6. Prepare a 24-cell tissue culture (24-CTC) try with cells $2/3^{rd}$ filled with 0.9% saline on a bed of crushed ice.

7. Resect the heart and store in a prepared 24-CTC cell for later processing.

8. Decapitate the animal and incise the skin over the calvarium to expose the skull. Using lateral incisions unroof the brain, remove it with a flat spatula and store it in a prepared 24-CTC cell.

9. Resect a midsection of pectoralis major muscle and transfer to the prepared 24-CTC cell.

TISSUE PROCESSING

1. Place an empty Microcentrifuge tube upright in the Mettler Balance and zero the scale.

2. Dissect between 0.06 and 0.12 g of tissue from the harvested heart, brain and muscle tissue and add to the Microcentrifuge tube on the scale and record the weight.

3. Prepare the suspensions: <u>For tissue</u>: Add dd-H_2O so that the weight of the water and tissue is exactly 10 times the weight of the tissue alone – thus making a 10% w/w solution. <u>For blood</u>: Add 100 μL blood to the Microcentrifuge tube and add dd-H_2O so that the weight of the blood and dd-H_2O is exactly 20 times the weight of the blood alone – thus making a 5% w/w solution.

4. Pre-homogenization preparation: <u>For heart and muscle tissue</u>: Dice the tissue with straight scissors inside the Microcentrifuge tube to shorten the subsequent ultrasonic homogenization (sonication). <u>For brain tissue and blood</u>: No special preparation is required as both homogenize easily.

5. Close the caps and place the Microcentrifuge tubes in a container with crushed ice and store for 5 minutes prior to homogenization to pre-cool the tissue.

6. Open the Microcentrifuge tube caps carefully so as not to lose any solution thereby altering the concentration of the homogenate. Then, using a Branson sonicator at a setting of 50% Duty Cycle and an intensity of 40% (#4), homogenize (sonicate) the tissue in the bed of crushed ice for 1 minute making sure not to allow any of the liquid to spill and directing the energy at suspended tissue particles until the suspension appears homogenous. If this has not been achieved in one minute, commence with fresh tissue sample. Close the caps again and slowly invert and revert the Microcentrifuge tube five times to ensure complete admixture of the dd-H2O and tissue homogenate[℘]. This should be repeated just prior to RGA measurement being careful not to form bubbles or froth.

7. The Microcentrifuge tubes can then stored in a bed of crushed ice for up to 6 hours for RGA analysis.

[℘] For the purpose of the actual experiment, the initial admixture was achieved by a more elaborate method of microcentrifuging the suspension for 20 seconds and then vortexing the homogenate. Although this ensured admixture and prevented stratification of tissue within the homogenate this has been deemed unnecessary by Vreman.

REACTION VIAL PREPARATION

1. Pack the test tube rack with 80 cleaned and dried GC reaction vials.

2. Add 2 μL of 60% w/v sulfosalicylic acid (SSA) with a 100 μL Hamilton Syringe.

3. Add 20 μL dd-H_2O with a 1000 μL Hamilton syringe.

4. Seal the reaction vials with a cap and silicon septum.

5. Store the vials in a bed of crushed ice making sure to also cover the septa.

6. Purge all the reaction vials with CO free nitrogen at a flow rate of 300-400 Lpm for 3 to 5 seconds. Repeat just prior to the addition of tissue homogenate.

7. Depending on the anticipated CO in tissue homogenate add between 1 and 40 μL of homogenate to sets of three reaction vials for each tissue sample; shake each vigorously to mix the SSA with the tissue homogenate.

8. Place the reaction vials with homogenate back into the bed of ice.

9. Allowing at least 5 minutes for reaction time, commence measurement of the tissue samples headspace using the RGA.

RGA PREPARATION AND MEASUREMENT

1. The RGA should be set up as detailed in Chapter 4.3. and the Sampling and Detection Sequence selected as detailed in Fig. 7.

2. The RGA should be calibrated as detailed in Chapter 4.4 with derivation of a Standard curve as described in section 4.4.5. and Table 5.

3. Once linearity of measurement within the range of anticipated CO readings has been confirmed the RGA measurements can be made.

4. Commence the measurement of 3 blank reaction vials to determine a baseline CO headspace reading.

5. Continue measuring the sets of three tissue samples ensuring that measurements do not deviate by more than 10%. Where one sample deviates from the other two, but the latter have a tolerance of less than 10%, the third measurement may be ignored. If the tolerance between each of the three measurements is greater than 10% this should be repeated with fresh homogenate until at least two of the three measurements have a tolerance of less than 10%.

6. Continue measurements until all the reaction vials containing tissue have been measured.

7. Conclude by measuring a final three blanks to determine the baseline CO drift as a function of CO-production by the septa and / or RGA calibration drift.

8. Convert all measurements from uV.sec to mV.sec and round the values.

9. Using the CO calculator provided in the Resource CD, calculate the tissue CO in pmol/g wet weight tissue.

D-4 CHEMICAL CHARACTERISTICS OF CO [14,15]

Formula		CO
Molecular Weight		28.01
Density (Gas), 1 atm. 0 °C		1.250 kg/m^3
Density (Gas), 1 atm. 15 °C		1.165 kg/m^3
Density (Gas), 1 atm. 25 °C		1.145 kg/m^3
Specific Volume		0.86 m^3/kg
Specific Gravity (relative to air)		0.967
Boiling point, 1 bar		- 192°C
Freezing point		- 207°C
Critical Temperature		- 139°C
Critical Pressure		35.5 atm
Critical Density		311 kg/m^3
Heat of Vaporization (1 bar)		216 J.g^{-1}
Specific Heat (gas) 25 ° C		0.99 J.g^{-1}.K^{-1}
Specific Heat Ratio Cp / Cv		1.404
Viscosity (gas):	0°C	0.0162 mPa.s
	25°C	0.0172 mPa.s
	100°C	0.0205 mPa.s
Thermal Conductivity (gas):	0°C	0.0215 W m^{-1} K^{-1}
	25°C	0.0229 W m^{-1} K^{-1}
	100°C	0.0274 W m^{-1} K^{-1}
Solubility in Water:	0°C	3.3 mL/100 mL H_2O/ATA
	20°C	2.3 mL /100 mL H_2O/ATA
	37°C	1.83 mL /100 mL H_2O/ATA
Ostwald coefficient (0°C)		0.0354

D-4 IL-482 MANUAL CONTAINING INFORMATION ON CO-OXIMETRY SETTINGS AND COEFFICIENTS FOR THE MEASUREMENT OF HUMAN VS RAT BLOOD

This section includes a general description of the Instrumentation Laboratory 482^{TM} CO-Oximeter System*. The material covered in this section includes product use, features, methodology, and procedural limitations. Personnel responsible for operating and maintaining this instrument should read and understand this material prior to use. This manual should be kept near the instrument or in a suitable location for reference as required.

1.1 PRODUCT USE

The IL 482 CO-Oximeter System is an automated instrument which analyzes a whole blood sample for Total Hemoglobin (THb), percent Oxyhemoglobin (%O_2Hb), percent Carboxyhemoglobin (%COHb), percent Methemoglobin (%MetHb), and percent Reduced Hemoglobin (%RHb). Correction for %O_2Hb ad %COHb in the presence of Fetal Hemoglobin is available if required.

In addition, the system calculates Oxygen Content (O_2Ct), Oxygen Capacity (O_2Cap), and percent Measured Oxygen Saturation (%SO_2M).

The CO-Oximeter can be interfaced with the IL 13XX pH/Blood Gas Systems (excluding the IL 1304 System). Analyzed data for both instruments can be displayed on the blood gas instrument and/or printed on the blood gas instrument thermal printer or optional ticket printer.

When interfaced with the IL 1312 (BGM) or 1306 pH/Blood Gas Systems, the following special parameters can be calculated:

- Capillary Oxygen Content (CcO_2)
- Arterial Oxygen Content (CaO_2)
- Mixed Venous Oxygen Content ($C\bar{v}O_2$)
- Arterial Venous Oxygen Gradient ($a\bar{v}DO_2$)
- Physiologic Shunt ($\dot{Q}_{sp}/\dot{Q}_{st}$)
- P_{50}

* IL 482 is a trademark of Instrumentation Laboratory.

Rev. 1   1-1

1.2 FEATURES

The IL 482 System features the following specific advantages:

1. **MICROPROCESSOR CONTROLLED** – The sampling and measurement cycles are fully automated. An auto zero cycle is automatically initiated after each sample or every 30 minutes if no samples are analyzed.

2. **EASY OPERATION** – An alphanumeric display guides the operator through the use of the sytem and indicates the system status at all times.

3. **RAPID AND SIMPLE CALIBRATION** – The only user-adjustable calibration is the THb value which is calibrated with IL CalDye or whole blood.

4. **EASE OF MAINTENANCE** – Tubing and pump windings are highly visible and readily accessible.

5. **WARNING DETECTION** – The system automatically monitors for faults to ensure accuracy of sample data and proper system response. Diagnostics are available to aid in troubleshooting.

6. **SERIAL COMMUNICATION INTERFACE** – Two RS-232C outputs allow the system to transfer results to a computer, compatible line printer or ticket printer.

7. **BLOOD GAS INTERFACE** – The CO-Oximeter can be interfaced to a pH/blood gas system to form a complete blood gas analysis laboratory.

8. **MICRO SAMPLE SIZE OF 85 μL**

9. **SAMPLING VERSATILITY** –

   - Macro Sampling

   - Micro Sampling

   - Fetal Hb correction capability for $\%O_2Hb$ and %COHb.

   - Analysis of animal blood.

10. **BATTERY STORAGE** – Provides a back up power source for data retrieval (e.g. Cal Factor, Date/Time, RS-232C Communication Setup, etc.) if a power failure occurs.

1.3 METHODOLOGY

● ELECTRO OPTICAL DESIGN

An anticoagulated whole blood sample is aspirated into the instrument, mixed with diluent, hemolyzed, and brought to a constant temperature in the cuvette. Monochromatic light at four specific wavelengths (Figure 1-1) passes through the cuvette to a photo-detector, whose output is used to generate absorbances. A dedicated microcomputer measures Total Hemoglobin (THb), percent Oxyhemoglobin ($\%O_2Hb$), percent Carboxyhemoglobin ($\%COHb$), percent Methemoglobin ($\%MetHb$), and percent Reduced Hemoglobin ($\%RHb$). Percent measured Oxygen Saturation ($\%SO_2M$), Oxygen Content (O_2Ct), and Oxygen Capacity (O_2Cap) are calculated.
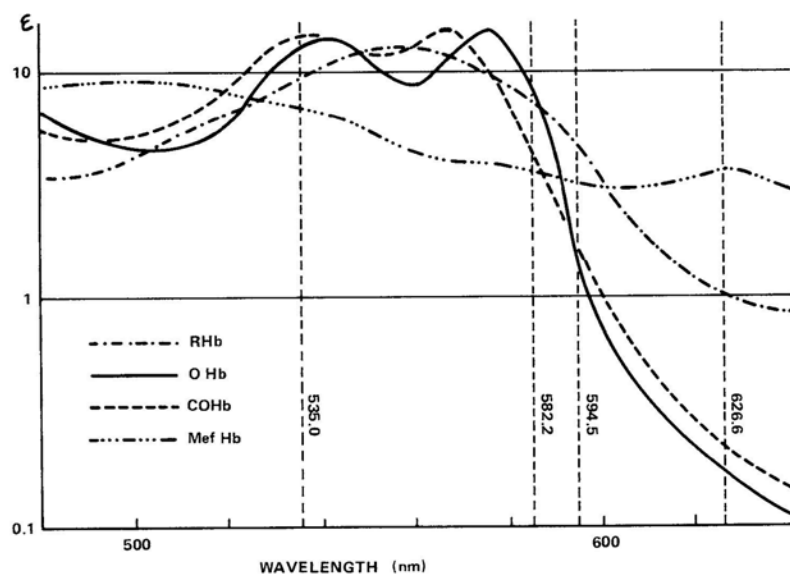

Figure 1-1. Hemoglobin Spectra

A thallium/neon hollow cathode lamp (HCL) emits light at the desired
wavelengths. Four spectral lines (535.0, 585.2, 594.5 and 626.6 nm) are
isolated using interference filters mounted on a motor-driven filter wheel.
The light beam emerging from the reflective isolator is beamsplit; one beam
is imaged onto the reference detector and the other beam is imaged through
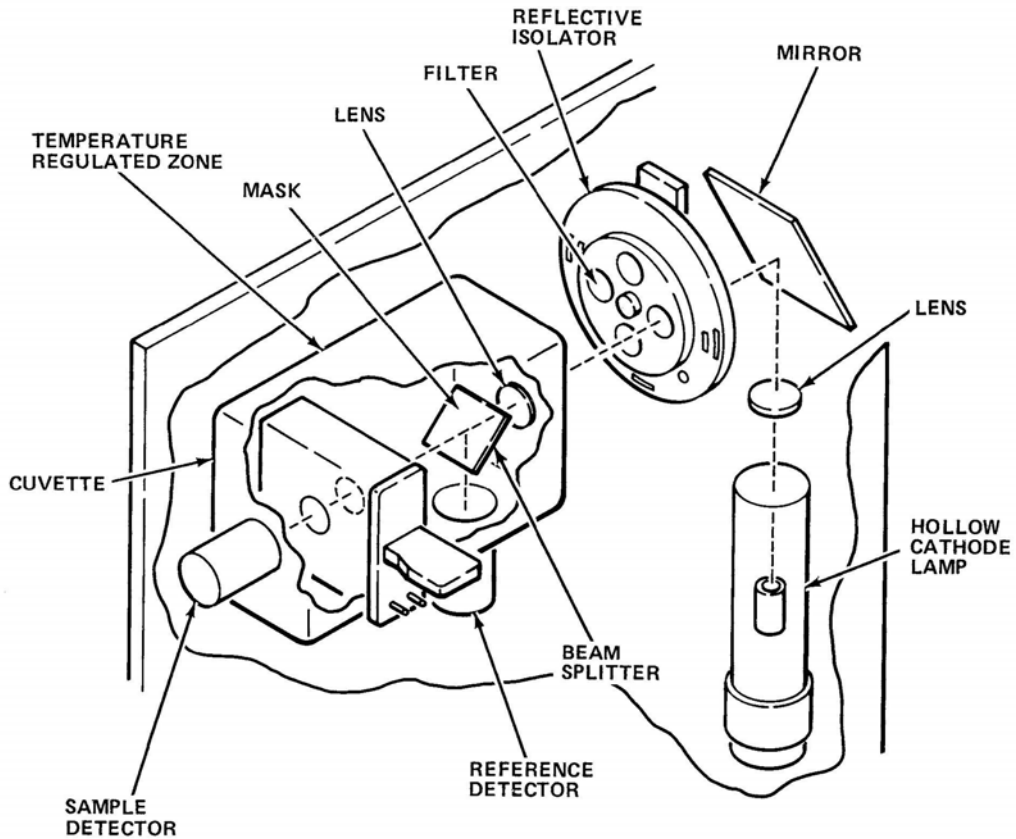the cuvette onto the sample detector (see Figure 1-2).

Figure 1-2. Electro-Optical System

● COMPUTATION OF ABSORBANCES

1. Four successive absorbance measurements are made at each wavelength, averaged and stored as the absorbance values in temporary memory. With zeroing solution in the cuvette, four "blank" absorbances (one for each wavelength) are obtained in this way, as part of the Blank Update function. Then, when a diluted, hemolyzed sample is analyzed, four "sample" absorbances are similarly obtained (one for each wavelength) from which the four "blank" absorbances are subtracted to derive the actual absorbance òf the blood sample at each wavelength.

   A (sample) − A (blank) = A (blood)
   Where A = the absorbance at each wavelength.

2. The four absorbance values (A) are then multiplied by the coefficients matrix stored in permanent memory. The matrix is based on the analysis of 100% content for each of the four Hemoglobin species measured by the IL 482 (i.e., %RHb, %O$_2$Hb, %COHb and %MetHb) at each of the four wavelengths. The computer uses this matrix to solve the following set of equations for the concentrations (C) of the four measured Hb species in the blood sample.

$$C_{(RHb)} = K(\epsilon_{535RHb}A_{535} + \epsilon_{585RHb}A_{585}$$
$$+ \epsilon_{594RHb}A_{594} + \epsilon_{626RHb}A_{626})$$

$$C_{(O_2Hb)} = K(\epsilon_{535O_2Hb}A_{535} + \epsilon_{585O_2Hb}A_{585}$$
$$+ \epsilon_{594O_2Hb}A_{594} + \epsilon_{626O_2Hb}A_{626})$$

$$C_{(COHb)} = K(\epsilon_{535COHb}A_{535} + \epsilon_{585COHb}A_{585}$$
$$+ \epsilon_{594COHb}A_{594} + \epsilon_{626COHb}A_{626})$$

$$C_{(MetHb)} = K(\epsilon_{535MetHb}A_{535} + \epsilon_{585MetHb}A_{585}$$
$$+ \epsilon_{594MetHb}A_{594} + \epsilon_{626MetHb}A_{626})$$

where

   C = concentration of each Hb species
   K = a scalar constant set by the THb calibration procedure
   ϵ = each coefficient in the matrix (4 Hb species at 4 wavelengths)
   A = the absorbance value of the blood at each wavelength

3. The THb value (g/dL) is the sum of the four concentrations:

   $THb = C_{(RHb)} + C_{(O_2Hb)} + C_{(COHb)} + C_{(MetHb)}.$

Rev. 1

4. The percentage concentration values are derived for O_2Hb, $COHb$, $MetHb$ and RHb:

$$\%O_2Hb = \frac{C_{(O_2Hb)}}{THb} \times 100$$

$$\%COHb = \frac{C_{(COHb)}}{THb} \times 100$$

$$\%MetHb = \frac{C_{(MetHb)}}{THb} \times 100$$

$$\%RHb = 100 - (\%O_2Hb + \%COHb + \%MetHb)$$

5. The O_2 content (Vol% O_2) is derived by the equation:

$$Vol\ \%\ O_2 = 1.39^* \times THb \times \frac{\%\ O_2Hb}{100}$$

6. The O_2 Capacity (O_2Cap) is derived by the equation:

$$O_2Cap = 1.39^* \times THb \times 1 - \left(\frac{\%COHb + \%MetHb}{100}\right)$$

NOTE: The IL 482 may be adjusted to employ any factor from 1.00 to 2.00 if the user so desires. Otherwise, the 1.39 factor is customer adjustable through Mode 4.

THb is displayed automatically. The operator can press each of the data keys (in any order) to display $\%O_2Hb$, $\%COHb$, $\%MetHb$ and $\%RHb$. Pressing the Calc key will display O_2 Content, measured O_2 Saturation and O_2 Capacity. The data may be recalled until another sample is analyzed or an Auto Zero is performed.

* Based on the molecular weight of Hb established at the Annual Meeting of the International Committee for Standardization in Hematology, 1966, and discussed in: Eilers, R.J., "Notification of Final Adoption of an International Method and Standard Solution for Hemoglobinometry - Specifications for Preparation of Standard Solution," Am. J. Clin. Path., 47: 1967, p. 212.

● SAMPLING OF ANIMAL BLOOD

The IL 482 has been set at the factory for use with human coefficients only. The system can be activated for analysis of animal blood by contacting an authorized IL field service engineer.

When activated, the following coefficients are available:

- Dog
- Rat
- Baboon - Investigational Use Only
- Bovine - Investigational Use Only
- Investigational Coefficients - Call IL for further information.

If other than human coefficients are activated, the following precautions should be observed:

1. Do not analyze human blood. A non-flashing asterisk appears on the display to alert the operator the system is set for blood specimens other than human.

2. Whenever the system is changed from human to animal or from animal to human, the system will require recalibration as prompted by the display of "Press Cal".

Information on sampling of animal blood is available from Instrumentation Laboratory. Call IL for further information.
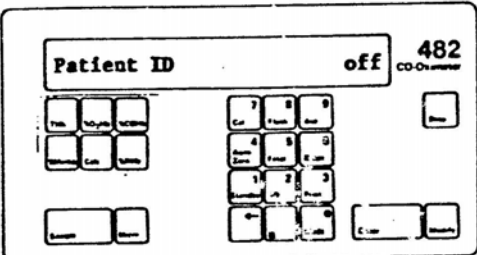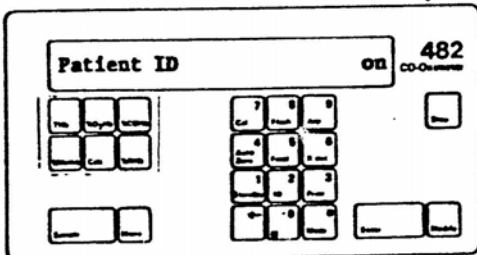
✓ MODE 5: SELECT COEFFICIENT SET

If other than human coefficients are desired, contact an authorized IL Field
Service Engineer.

[handwritten notes] MODE 5 ENTER
MODIFY — HUMAN BLOOD
DOG BLOOD
RAT BLOOD
BOVINE
BABOON
EXP ENTER

● MODE 6: SAMPLE ID ON/OFF

This program is used to select the automatic request for patient identifica-
tion number during sample analysis. If SAMPLE ID is not selected and a
patient ID is desired, pressing the ID key during or after sampling will allow
entry of an ID number.

OPERATOR ACTION	SYSTEM RESPONSE
1. Press Mode, 6, Enter.	Current ID request is displayed. Patient ID off 482
Note: Press Enter or ← to exit program.	
2. Press Modify to select ON/OFF request for patient identification.	Current status is displayed. Patient ID on 482
3. Press Enter or ← to return to previous system status.	Ready for Sample

---